Dissertation

submitted to the
Combined Faculty of Natural Sciences and Mathematics
of the Ruperto Carola University Heidelberg, Germany
for the degree of

Doctor of Natural Sciences

Presented by

M. Sc. Marlene Alice Vierthaler

born in: Karlsruhe, Germany

Oral-examination: 28.02.2022

The influence of ADCK2 on melanoma cells and during the development to melanocytic progenitors (NCCs)

Referees: Prof. Dr. Viktor Umansky

Prof. Dr. Jochen Utikal

Declarations according to §8 (3) b) and c) of the doctoral degree regulations:

b) I hereby declare that I have written the submitted dissertation myself and, in this process, have used no other sources or materials than those expressly indicated.

c) I hereby declare that I have not applied to be examined at any other institutions, nor have I used the dissertation in this or any other form at any other institution as an examination paper, nor submitted it to any other faculty as a dissertation.

Heidelberg, November 2021

(Marlene Alice Vierthaler)

"Knowledge is an unending adventure at the edge of uncertainty."

Jacob Bronowski

Parts of this thesis have been published/presented in:

Conferences and workshop presentations:

- Marlene Vierthaler. Online Scheme your Project presentation: "The role of ADCK2 in melanoma cells and during the development to melanocytic progenitors"

DKFZ PhD Retreat, July 2021, online (Heidelberg), Germany

- Marlene Vierthaler, Juliane Poelchen, Jennifer Dworacek, Katrin Schrenk-Siemens, Daniel Novak and Jochen Utikal. Online Poster presentation: "KD of specific kinases leads to a more efficient differentiation of human induced pluripotent stem cells to neural crest cells"

ISSCR Annual Meeting Virtual, June 2021, Online, USA

- Marlene Vierthaler and Jochen Utikal. Oral presentations: "Biomat for iPS & Hep"

ZIM Meetings, December 2017, Karlsruhe, Germany, June 2018, Konstanz, Germany, December 2018, Heidelberg, Germany, August 2019, Hannover, Germany, July 2020, Online

- Marlene Vierthaler, Lionel Larribere and Jochen Utikal. Poster presentation: "Molecular mechanisms in the development of melanocytic progenitors"

DKFZ PhD poster session, November 2019, Heidelberg, Germany

Table of Contents

Abstract

Melanoma is a devastating disease with a growing incidence, which represents a challenge for scientists and physicians worldwide. Due to its high metastatic potential and the rapid development of resistances to established therapies, this cancer still accounts for the majority of skin cancer-related deaths. In my thesis, I could show that ADCK2 plays a role in melanoma cells, especially affecting their metastatic capacity. After knocking down ADCK2 I observed a lower cell viability, but better migration and invasion of melanoma cells. Moreover, I noticed a reduced pigmentation of the pellets of melanoma cell lines, which could be explained by lower expression of melanocyte and higher expression of neural crest cell (NCC) markers. These results indicate a phenotype switch of melanoma cells to a more de-differentiated state, which is often associated with a higher metastatic potential. Additional analyses revealed a positive correlation between ADCK2 and Sox5, FoxD3, MYL6 and RAB2A expression in melanoma cells. Since the ADCK2 knockdown (KD) most significantly affected the migrative capacity of melanoma cells, I continued investigating the connection with MYL6, a protein involved in cell motility. I could demonstrate that overexpression (OE) of ADCK2 in melanoma cells had the opposite effect on cell viability and motility compared to the KD. The effect of ADCK2 OE on cell viability and migration could be reversed by a KD of MYL6, which suggests that MYL6 could be a downstream effector of ADCK2. Immunofluorescence stainings of ADCK2 KD cells revealed that these cells showed an altered actin cytoskeleton compared to control cells. One can assume that MYL6 could influence the cell motility of melanoma cells due to its function within non-muscle myosin 2, a known binding partner of actin filaments. Since ADCK2 negatively affected the metastatic potential of melanoma cells, it could be considered a tumor suppressor. As tumorigenesis and development share many similarities, I further investigated the role of ADCK2 (and other kinases) in the differentiation process of human induced pluripotent stem cells (hiPSCs) towards neural crest cells (NCCs). First to mention, I generated and validated two hiPSC lines that were stably maintained on Matrigel, one by reprogramming fibroblasts and another one by subcloning an existing cell line. Both cell lines were then successfully differentiated into NCCs in a xeno-free environment in ten days. Moreover, I could detect a downregulation of stem cell and upregulation of NCC marker expression upon KD of ADCK2 and DBF4 on day 0 followed by ten days of differentiation. Due to this result, one can speculate, that a KD of ADCK2 and DBF4 could lead to a more efficient differentiation of hiPSCs into NCCs. However, additional experiments are necessary to test this hypothesis. Moreover, it needs to be examined if these NCCs are functional and resemble naturally occurring NCCs. Additionally, I could demonstrate that a KD of TYK2 or EPHA4 resulted in increased stem cell marker and decreased NCC marker expression, which indicates that these kinases might be necessary for NCC development. Further experiments are needed to clarify this assumption. To conclude, I found that ADCK2 plays a role in melanoma cell behavior, but no strong role in the development of NCCs. A KD of ADCK2 induced a phenotype switch of melanoma cells to a more NC-like identity, validated by an upregulation of NCC markers and an increased motility. It would be interesting to further study the involvement of ADCK2 in melanoma and NCC development, which could yield more insights into melanoma development and thereby could open up new possibilities for melanoma therapy or diagnosis.

Zusammenfassung

Das Melanom ist eine verheerende Erkrankung mit einer steigenden Inzidenz. Aufgrund seiner ausgeprägten Tendenz zur Metastasierung und der schnellen Ausbildung von Resistenzen gegen etablierte Therapien, ist diese Krebserkrankung nach wie vor verantwortlich für die Mehrheit hautkrebsbedingter Todesfälle. In meiner Arbeit konnte ich zeigen, dass ADCK2 eine Rolle in Melanomzellen spielt und insbesondere deren Metastasierungspotential beeinflusst. Ich konnte zeigen, dass die Runterregulierung von ADCK2 zu einer geringeren Zellviabilität, aber dafür zu einer höheren Migrations- und Invasionsfähigkeit führte. Zudem beobachtete ich eine verringerte Pigmentierung von Melanomzellpellets, die durch eine geringere Expression von Melanozytenmarkern und eine höhere Expression von Neuralleistenzellmarkern erklärt werden kann. Diese Ergebnisse deuten darauf hin, dass die Melanomzellen einen Phänotypwechsel hin zu einem stärker dedifferenzierten Status durchlaufen, der häufig mit einer höheren Wahrscheinlichkeit zu metastasieren assoziiert ist. Weitere Analysen offenbarten eine positive Korrelation zwischen den Expressionen von ADCK2 und Sox5, FoxD3, MYL6 als auch RAB2A. Da die Runterregulierung von ADCK2 das Migrationsverhalten der Melanomzellen am stärksten beeinflusste, fokussierte ich mich im Anschluss auf die Verbindung zwischen ADCK2 und MYL6, da MYL6 ein Protein ist, welches bei der Zellmotilität eine Rolle spielt. Ich konnte nachweisen, dass die Überexpression von ADCK2 einen entgegengesetzten Effekt auf die Zellviabilität und -motilität der Zellen hatte im Vergleich zur Runterregulierung. Durch eine Runterregulierung von MYL6 konnte der durch Überexpression von ADCK2 auf die Zellviabilität und -migration ausgelöste Effekt umgekehrt werden. Dies ist ein Hinweis darauf, dass MYL6 als nachgeschalteter Effektor von ADCK2 fungieren könnte. Immunfluoreszenzfärbungen von ADCK2-runterregulierten Melanomzellen zeigten, dass diese Zellen im Vergleich zu den Kontrollzellen ein verändertes Aktinskelett aufwiesen. Aus dieser Beobachtung kann man ableiten, dass MYL6 die Zellmobilität über seine Funktion im nicht-Muskel Myosin 2 beeinflusst, welches ein bekannter Bindungspartner von Aktinfilamenten ist. Da ADCK2 das metastatische Potential von Melanomzellen negativ beeinflusste, könnte man folgern, dass es sich bei ADCK2 um einen Tumorsuppressor handeln könnte. Da Tumorentstehung und normale Entwicklungsprozesse viele Ähnlichkeiten aufweisen, habe ich auch die Rolle von ADCK2 (und anderen Kinasen) bei der Differenzierung von humanen induzierten Stammzellen (hiPS) zu Neuralleistenzellen untersucht. Als erstes habe ich dafür zwei auf Matrigel-wachsende hiPS-Zelllinien generiert, eine durch Reprogrammierung von Fibroblasten sowie eine weitere durch Subklonierung einer anderen hiPS-Zelllinie. Beide Linien wurden anschließend in einer xeno-freien Umgebung innerhalb von zehn Tagen erfolgreich zu Neuralleistenzellen differenziert. Die Runterregulierung von ADCK2 und DBF4 an Tag 0 gefolgt von einer zehntägigen Differenzierung resultierte in einer Runterregulierung von Stammzell- und einer Hochregulierung von Neuralleistenmarkern. Anhand dieses Ergebnisses kann man die Hypothese aufstellen, dass die Runterregulierung von ADCK2 und DBF4 die Effizienz der Differenzierung zu Neuralleistenzellen erhöhen könnte. Zusätzliche Experimente sind nötig, um diese Hypothese zu überprüfen. Darüber hinaus muss noch geprüft werden, ob diese Neuralleistenzellen funktional sind und ob sie Ähnlichkeit mit natürlich vorkommenden Neuralleistenzellen aufweisen. Des Weiteren, konnte ich sehen, dass eine Runterregulierung von TYK2 und EPHA4 zu einer Hochregulierung der Stammzellmarker und einer Runterregulierung von Neuralleistenmarkern führte. Daraus ergibt sich die Vermutung, dass diese Kinasen eine Rolle in der Entwicklung von Neuralleistenzellen spielen könnten. Zusammenfassend habe ich herausgefunden, dass ADCK2 eine Rolle im

Melanom, besonders dessen Metastasierung, aber nicht in der Differenzierung zu Neuralleistenzellen spielt. Eine Runterregulierung von ADCK2 in Melanomzellen führt dazu, dass diese einen Neuralleistenzellen-ähnlichen Phänotyp annehmen, was sich in der Hochregulierung von Neuralleistenmarkern und einer erhöhten Motilität äußert. Es wäre durchaus interessant, die Rolle von ADCK2 in Melanomzellen und während der Entwicklung von Neuralleistenzellen genauer zu untersuchen. Dies könnte neue Erkenntnisse hinsichtlich der Melanomentwicklung liefern und neue Optionen für die Therapie und Diagnose von Melanomen schaffen.

List of Figures

List of Supplementary Figures

List of Tables

List of Supplementary Tables

Abbreviations

%	percent
(h)iPSCLs	(human) induced pluripotent stem cell lines
(h)iPSCs	(human) induced pluripotent stem cells
°C	degree celsius
µ	micro
18S	18S ribosomal RNA
A	
aarF	probable protein kinase, locus required for ubiquinone production
ADCK2	aarF-domain containing kinase 2
AKT	Serine/Threonine Kinase, v-akt murine thymoma viral oncogene
AP	Alkaline Phosphatase
ARAF	A-Raf Proto-Oncogene, Serine/Threonine Kinase
ATCC	American type culture collection
ATP	Adenosine triphosphate
AXL	AXL Receptor Tyrosine Kinase
B	
BCA	Bichinonic Acid Protein Assay
BCL2L1	Apoptosis regulator BCL2 like 1
bFGF	Basic Fibroblast Growth Factor (also: FGF2)
BME	Basement Membrane Extract
bp	base pair
BRAF	B-Raf Proto-Oncogene, Serine/Threonine kinase
BSA	Bovine Serum Albumin
C	
Cdc7	Cell Division Cycle 7
CDK	cyclin-dependent kinase
c-Myc	Proto-Oncogene c-Myc
CSPG4	Chondroitin sulfate proteoglycan 4
CT	cycle threshold
Cxcr4	C-X-C Motif Chemokine Receptor 4
D	
DNA	Deoxyribonucleic Acid
DBF4	Dumbell Faktor 4, (also: ASK or MEKK5/6)
DCT	Dopachrome Tautomerase
DKFZ	Deutsches Krebsforschungszentrum
DMEM	Dulbeccos modified eagle´s medium
DMSO	Dimethylsulfoxide
E	
E	Glutamic Acid
EB	embryonic body
E-Cadherin	CDH1, Cadherin 1
EDTA	Ethylenediaminetetraacetic acid
ELC	essential light chain
EMT	Epithelial-to-Mesenchymal Transition
EPHA4	Ephrin type-A receptor 4
ER	endoplasmic reticulum
ER+(ve)	estrogen receptor positive
ERK	Extracellular Signal regulated Kinase
ES-cells	embryonic stem cells
et al.	et alteri
EV	empty vector

F	
FACS	fluorescence-activated cell sorting
FC	fold change
FCS	fetal calf serum
FGF	Fibroblast Growth Factor
Fibro	Fibronectin
FoxD3	Forkhead Box D1
G	
g	gram
G1/G2-phase	cell cycle phase, Gap1/2
GAPDH	Glyceraldehyde 3-phosphate dehydrogenase
GLUT1	Glucose Transporter Type 1
GP100	Premelanosome Protein (also: PMEL)
H	
h	hour
H&E staining	Hematoxylin and eosin staining
HER	Erb-B2 Receptor Tyrosine Kinase (also:ERBB)
HIF1α	Hypoxia Inducible Factor 1 Subunit Alpha
HMGS	human melanocyte growth supplement
HNK1	Beta-1,3-Glucuronyltransferase 1 (also: CD57 or B3GAT1)
HRP	Horseradish peroxidase
I	
IF	Immunofluorescence
IL2	Interleukin 2
J	
JNK	c-Jun N-terminal kinase (also: MAPK8)
K	
K	Lysine
KD	knockdown
kDa	kilo Dalton
KLF	Kruppel Like Factor
KOS	acronym for the genes Klf4, Oct3/4 and Sox2
KSR	Knockout serum replacement
L	
L	liter
Lam	Laminin
LB	lysogeny broth
Lin28	Lin-28 Homolog A
log	logarithm
log2	binary logarithm
M	
M	molar
m	milli
MAP2K3	Mitogen-Activated Protein Kinase 3 (also: MKK3 or MEK3 or MAPKK3)
MAPK	Mitogen-Activated Protein Kinase
MCAM	Melanoma adhesion-molecule
min	minutes
MITF	Microphthalmia-Associated Transcription Factor
MLANA	Melan-A, Melanoma Antigen Recognized By T-Cells 1 (also: MART1)
MMP	metalloproteinase
MMT1-MMP	membrane type 1 metalloproteinase
M-phase	cell cycle phase, Mitotic phase
mRNA	Messenger Ribonucleic Acid
MSX1	Msh Homeobox 1
MTS1	metastasin 1 (also: S100A4)

MYH	myosin heavy chain
MYL	myosin light chain
MYL6	myosin light chain 6
N	
n	nano
Nanog	Nanog Homeobox
N-Cadherin	CDH2, Cadherin 2
NCCs	neural crest cells
NEAA	non-essential amino acids
NFκB	Nuclear Factor Kappa B subunit 1
NHM	normal human melanocytes
NIH 3T3	cell line established from primary mouse embryonic fibroblasts from NIH Swiss mouse embryo
NM2	non-muscle myosin 2
NOD/SCID	Nonobese Diabetic/Severe Combined Immunodeficient
NRAS	Neuroblastoma RAS viral Oncogene Homolog
ns	non-significant
NUMBL	NUMB Like Endocytic Adaptor Protein
O	
ON	over night
Oct4	Octamer-Binding Protein 4
OE	overexpression
OS	overall survival
OSCC	oral squamous cell carcinoma
P	
p	p-value
P/O	Polyornithine
p38	Mitogen-Activated Protein Kinase
p75	Nerve Growth Factor Receptor (also: CD271 or NGFR)
Pax3	Paired Box 3
PBS	Phosphate buffered saline
PCBP1	Poly (RC) Binding Protein 1
PFA	Paraformaldehyde
PLEKHA7	Pleckstrin Homology Domain Containing A7
PTEN	Phosphatase And Tensin Homolog
PTTG1	PTTG1 Regulator of Sister Chromatid Separation, Securin
PVDF	Polyvinylidenfluorid
Q	
Q	Glutamine
qPCR	quantitative real-time Polymerase Chain Reaction
R	
R	Arginine
RAB	Ras oncogene family
RIPA	radioimmunoprecipitation assay buffer
RLC	regulatory light chain
RT	room temperature
S	
SAPK	Stress Activated Protein Kinases
SDS	sodium dodecyl sulfate
SERTAD1	SERTA Domain Containing 1
siRNA	small interfering RNA
SLUG	Snail Family Transcriptional Repressor 2
SNAIL	Snail Family Transcriptional Repressor
Sox	SRY (sex determined region Y)-box
S-phase	cell cycle phase, synthesis phase

T	
TF	transcription factor
TGFβ	Transforming Growth Factor Beta 1
TNF	Tumor Necrosis Factor
TRP1	Tyrosinase related protein 1
TRP2	Tyrosinase-related protein 2
TWIST1	Twist Family BHLH Transcription Factor 1
TYK2	Tyrosinase Kinase 2
TYR	Tyrosinase
U	
UMM	Universitätsklinikum Mannheim
UV	ultraviolet
V	
V	Valine
vs	Versus
W	
WB	Western Blot
Wnt	Wingless/Integrated
WT	Wild Type
Z	
ZEB	Zinc Finger E-Box Binding Homeobox
ZGA	zygotic genome activation
ZIM	Zentrales Innovationsprogramm Mittelstand (Germany´s largest innovation programme for small and medium-sized enterprises)
ZNF275	Zinc Finger Protein 275

1 Introduction

1.1 Melanoma

The human body is exposed to diverse environmental factors of whom some can be harmful for the organism and cause diseases. The skin is the first barrier of the body, protecting it against these factors and contributing to the preservation of homeostasis. Due to its shielding function the skin is also exposed to sunlight and thereby the harming UV and ionizing radiation [1]. In the 21st century skin diseases have become a major health problem with increasing skin cancer numbers being as high as all cases from all other cancer types together [1], [2]. At this time, melanoma is one of the deadliest skin cancers with more than 55,500 cases worldwide per year [3]. Although there are many therapies available, including surgery, radio-, chemo- and immunotherapy the 5-year survival rate is still less than 12% [4]. Along with extensive sun exposure, a high number of melanocytic nevi, a family history of melanoma as well as previous melanomas are the most common risk factors [5]. Melanoma is a cancer with high heterogeneity which makes the treatment very difficult [6]. This heterogeneity enables it to establish mechanisms to evade from an efficient treatment easily, mostly by mutations in common signaling pathways [3]. The BRAF and NRAS genes are the most commonly mutated ones and approximately 75% of melanoma patients carry a mutation in one of these genes [5]. These mechanisms by which melanoma cells evade therapy often lead to resistance and relapse of the disease. Furthermore, melanoma is known to metastasize very early, which still makes the early detection and dissection to the most effective treatment [3], [7]. There is evidence that the aggressive behavior of metastasizing melanoma cells is due to a higher similarity with melanocytic progenitors or even stem-cell like gene expression. Both promote survival, growth and migration [8]. Further, this also goes along with a phenotype switching which is commonly observed in metastasizing tumors as they switch from a proliferative to an invasive gene expression and behavior [6].

How melanoma arises is not yet fully understood. Among others, there is still a debate on which cells give rise to melanoma. Two different scenarios are discussed at this time, one which proposes a direct descent from degenerated melanocytes and the other one which suggests that melanocytic progenitors are the source of melanoma [9]–[11]. The possible ways of evolution of melanoma are schematically depicted in **Figure 1**. Melanocytes are the pigmented cells of the skin which are located between the keratinocytes in the basal layer of the epidermis [6]. Due to their ability to produce melanin (eumelanin and pheomelanin) they are responsible for skin, hair and eye color [12]. These melanocytes arise from neural crest cells (NCCs) early in development [9], [11], [13], [14]. A mutation in NCCs or aberrant regulation during their development could alter these cells to become melanoma progenitors [15].

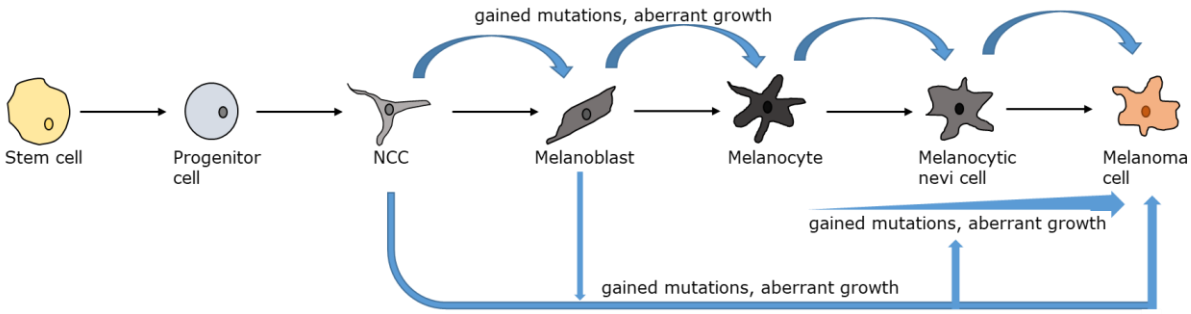

Figure 1: Putative mechanisms of melanoma development.
Schematic development of melanocytes and melanoma from left to right. The blue arrows indicate different possible ways how cells develop to melanoma and which cells could be the starting point of melanoma development. Partially adapted from [14]

1.1.1 Phenotype switching in melanoma

In cancer progression, the occurrence of metastases is correlated with the worst outcome, especially in melanoma [3], [7]. There has been intensive research on how melanoma cells can metastasize. One important incident in this process is the switch from a proliferative to an invasive phenotype, a mechanism known as phenotype switching, which also leads to a more heterogeneous cell population within the tumor and thereby giving it advantages to resist therapy [16]. The mechanism of phenotype switching has originally been discovered in epithelial cells, that undergo epithelial to mesenchymal transition (EMT) to form the epithelium [17]. To metastasize, melanoma cells switch from the proliferative into the invasive state, which goes along with the downregulation of melanocyte differentiation and pigment-associated genes and upregulation of precursor cell markers, like NCC or stem cell markers, leading to a more dedifferentiated melanoma cell [16], [18], [19]. An overview on phenotype switching in melanoma is depicted in **Figure 2**. It has been shown that a cultivation of melanoma cells in specific NCC medium leads to a more migrative and invasive phenotype of these cells [18]. One of the most studied factors involved in phenotype switching is the microphthalmia-associated transcription factor (MITF), which has been shown to have tumor-suppressive as well as tumor-promoting functions [3]. MITF is highly expressed in the proliferative phenotype, along with the melanocyte-specific genes DCT and TYR, but the expression is downregulated when melanoma cells switch to an invasive phenotype. MITF regulates various other genes which have been associated with phenotype switching, for example MLANA and GP100 [16], [19]. A downregulation of MITF has been shown sufficient enough for the increase of migrative behavior in mouse and human cells, giving evidence that MITF is the key driver of this phenotypic switch [16]. Interestingly, MITF also plays a key role in melanocyte differentiation and is known as differentiation marker [20]. During the switch to the invasive phenotype, cells often adopt a more dedifferentiated state as shown by the downregulation of melanocyte differentiation markers like MITF, TYR and MLANA and the upregulation of melanoma stem cell or precursor cell markers like p75, ZEB1 and SNAIL [19], [21], [22]. Further, also Msh homeobox 1 (MSX1) plays an important role in phenotype switching of melanoma, as it has been shown that an overexpression (OE) of MSX1 leads to more migration of melanoma cells. Interestingly, MSX1 has also been shown to reprogram melanocytes into their precursors (NCCs), which leads to a depletion of MITF [3]. Another gene known to promote the invasive phenotype of melanoma cells is metastasin 1 (MTS1) (also known as S100A4). Extracellular MTS1 induces the downregulation of MITF and the switching of melanoma

cells to a more invasive phenotype. In this case, the effect is regulated by metabolic alterations, enhancing glycolysis and reducing mitochondrial oxidation [19]. An enhanced glycolysis has also been connected with a high expression of Wnt5a, which together with TGFß and FGF is often used as a marker for the invasive phenotype [3], [19]. Other known factors for the different phenotypes in melanoma are E- and N-Cadherins which also show differential expression during epithelial-to-mesenchymal transition (EMT) [17], [22]. Highly proliferative cells often express E-Cadherin together with MITF, whereas the invasive cells are more likely to express N-Cadherin often together with AXL [17]. Also the expression of ZEB2 and SLUG is associated with a proliferative phenotype while the expression of the EMT-associated markers ZEB1 and TWIST correlates with an invasive phenotype [21]. Moreover, it has been observed that there are different levels of oxygen within a tumor. Usually, the hypoxic regions are more in the middle of tumors and are associated with a gene expression characteristic for a more invasive phenotype [3]. The hypoxic regions express specific markers like GLUT1 and HIF1α. HIF1α is further known to decrease MITF and MLANA, thereby dedifferentiating these cells and resulting in a more invasive phenotype [3], [16], [22].

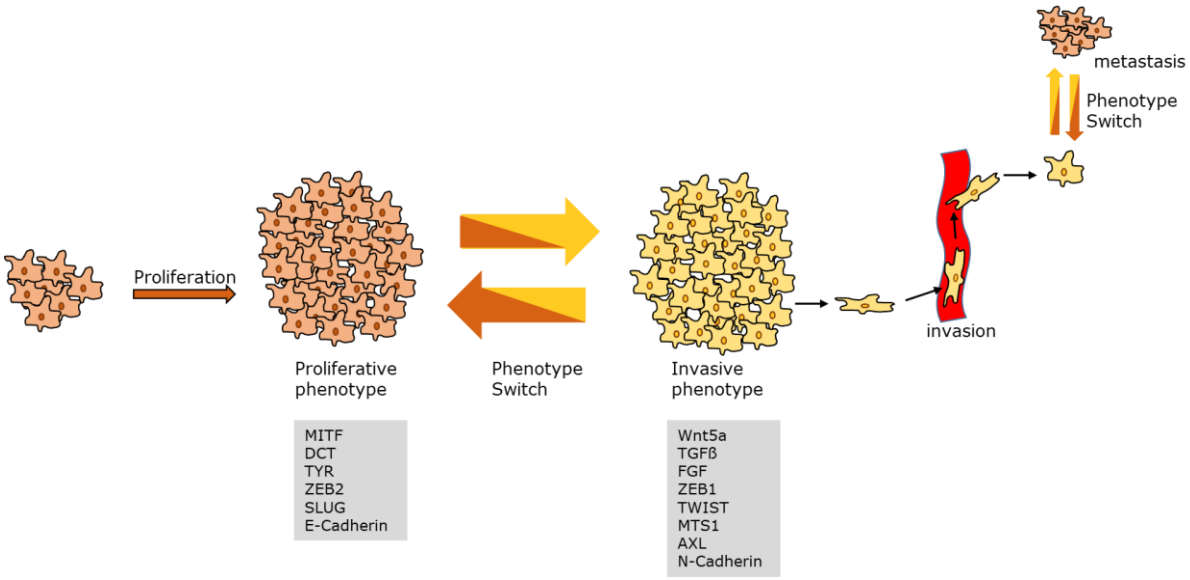

Figure 2: Phenotype switching in melanoma
Schematic representation of the two distinct phenotypes of melanoma cells: proliferative and invasive phenotype, together with typical marker expression. Figure adapted from [3]

1.2 Neural crest cells

NCCs were first described in 1868 and represent a cell population that only occurs in vertebrates and that has the potential to differentiate into various cell types with distinct functions [15], [23]. Because of this feature along with their ability to self-renew they are also referred to as the "adult counterpart of embryonic stem cells" [15]. NCCs evolve very early in development in a multistep process involving signals from the mesenchym and the notochord. At about 4 weeks after fertilization (in humans) they appear in the embryo. The NCCs emerge from the edges of the neural plate which folds to the neural tube, that later gives rise to the brain and the spinal cord. The NCCs represent an independent, multipotent cell population which is located between the neural tube and the surface ectoderm [24], [25]. Due to this position they were also first described as "the layer in between" [15]. From this location they migrate along different routes, splitting up into trunk, cranial, vagal

and sacral NCCs. During their migration they differentiate to diverse cell types depending on their final location [25]. They can form cornea cells, cells from the craniofacial skeleton e.g., osteocytes and chondrocytes, as well as cells from the peripheral nervous system including neurons, Schwann cells and adrenal medulla. Further, they can also give rise to smooth muscle cells and contribute to skin pigmentation. Melanocytes of the head emerge from cranial and melanocytes of the body from trunk NCCs [24], [25]. The emergence of the NCCs as well as differentiation into melanocytes are depicted in **Figure 3**.

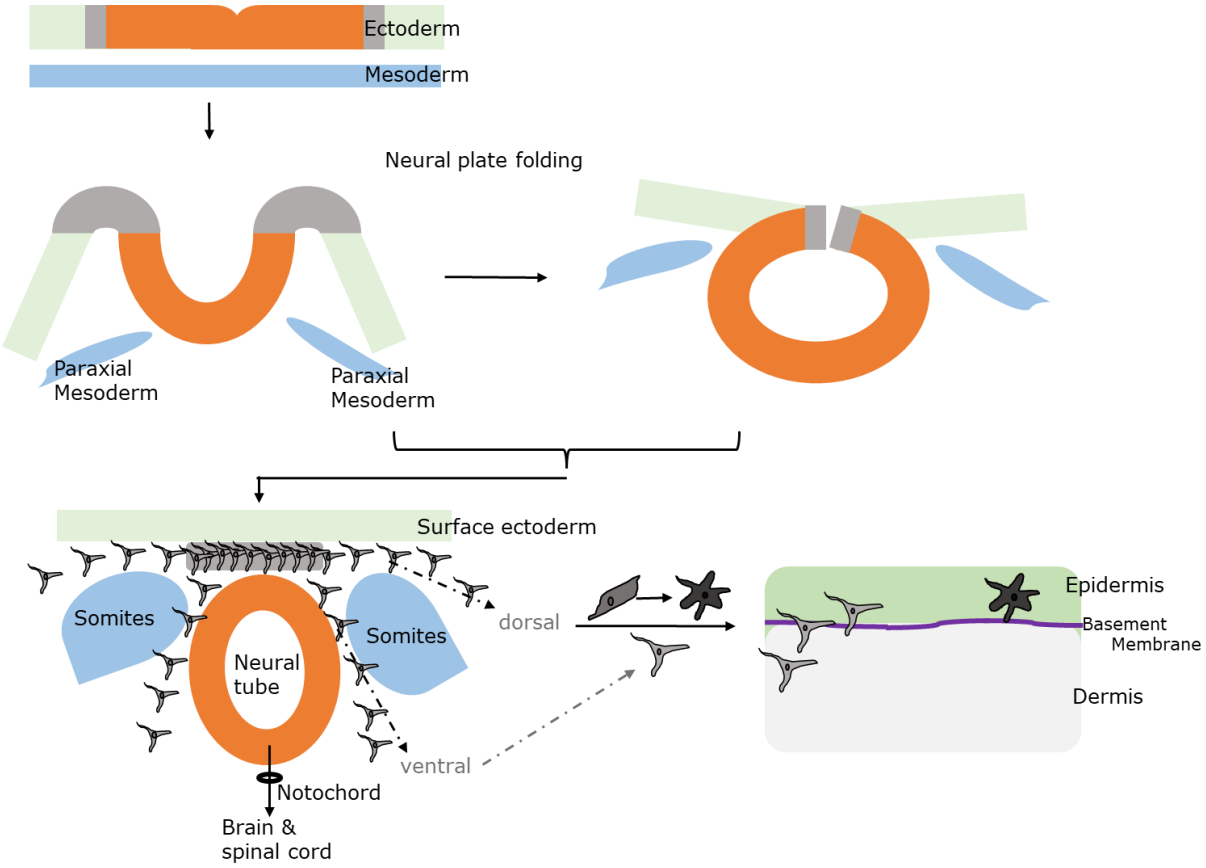

Figure 3: The emergence and migration of NCCs
NCCs arise early in development upon the folding of the neural plate and are a layer of independent, multipotent cells located in between the surface ectoderm and the neural tube. By migrating mostly by the dorsal pathway, NCCs integrate into the dermis. Here, they differentiate to melanoblasts and further to melanocytes. In this graph, the NCCs are highlighted in dark grey, the neural tube in orange, the surface ectoderm in light green, the somites in blue and the epidermis in green. Figure adapted from [3], [25]

Abnormal NCC differentiation or migration can lead to diseases including severe developmental defects [26]–[28]. Because of their developmental potential NCCs are of particular interest for regenerative medicine. Since the embryo itself is the direct source of NCCs, their extraction brings along ethical problems. Also, the amount of NCCs that can be extracted from an embryo is quite small in the undifferentiated stage which is another hurdle for research [15]. Although several alternative methods for generating NCCs have been developed, producing sufficient amounts of these cells for therapeutic purposes is still challenging. A more recent approach is the differentiation of induced pluripotent stem cells (iPSCs) to NCCs. iPSCs can self-renew indefinitely under controlled conditions and are able to differentiate into all cell types of the three germ layers and hence represent a possible new source for generating substantial quantities of NCCs for research and therapeutic purposes [15], [26].

1.3 Stem cells and induced pluripotent stem cells

Stem cells have the unique ability to undergo either a symmetric or an asymmetric cell division. The symmetric cell division yields two identical pluripotent daughter cells and allows "endless" self-renewal while the asymmetric cell division yields one cell that retains the pluripotent phenotype and another cell that differentiates into one of the many cell types of the body [29]. Directly after fertilization, cells are totipotent and have the potential to generate a complete organism including extraembryonic tissue, like the placenta. As soon as the embryo reaches the morula stage, the cells become pluripotent. These cells can develop into any cell type of the three germ layers, which are mesoderm, endoderm and ectoderm, but cannot form extraembryonic tissue anymore. During further development the cells than reach a multipotent stage, where they can only differentiate into predetermined cells of a specific tissue [29]–[31]. In the adult, only oligo- or unipotent, adult stem cells persist, which bring forth only one or a few different types of somatic cells. Examples are mesenchymal stem cells in the bone marrow, which give rise to different blood cells or epithelial stem cells in the hair follicles, which give rise to various cell types that form a pigmented hair [29], [31], [32]. The different developmental potencies of cells are due to epigenetic changes that selectively lead to the inactivation of specific genes without changing the DNA sequence. Epigenetic changes include different modifications, e.g. methylation/acetylation of chromatin, changes of the chromatin constituents or the chromatin structure [33]. Interestingly, the totipotent stage of the cells after fertilization can be reconstituted by reprogramming somatic germ cells, involving demethylation and other epigenetic reprogramming to activate the zygotic gene (ZGA) [33]–[35]. **Figure 4** depicts the different stages of developmental potency and their underlying epigenetic changes.

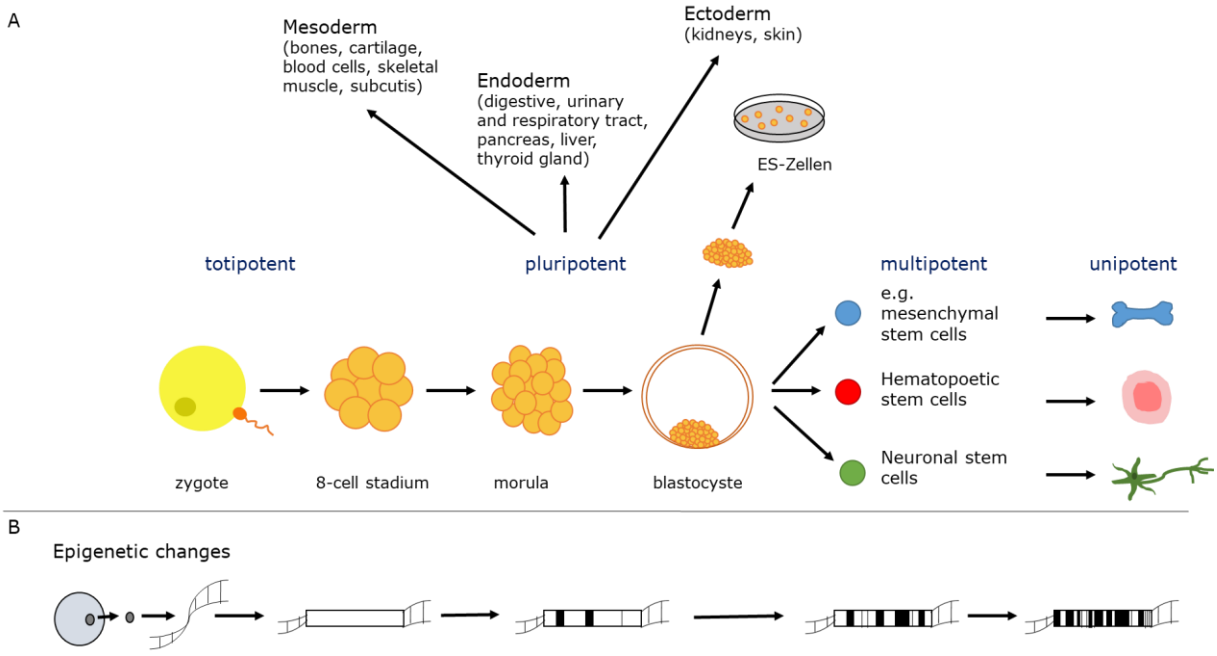

Figure 4: Stages of developmental potency and epigenetic changes during development ***A:*** *During development the differentiation potential of cells changes from totipotent to unipotent.* ***B:*** *Schematic depiction of epigenetic changes during development. The DNA is modified by different mechanisms leading to gene silencing (black bars). This specific gene silencing is responsible for the decreasing potency of cells during development. Figure adapted from* [36]

Nowadays there are several methods available to reprogram somatic cells to stem-like cells *ex vivo*. The first evolved one was the somatic nuclear transfer, which enabled the cloning of organisms. In this approach, the nucleus of a somatic cell is transferred into an enucleated oocyte. After this cell starts to divide, it is implanted into the uterus of a surrogate mother, where the embryo than develops until birth. Alternatively, in therapeutic cloning the blastocyst obtained after nuclear transfer is not implanted into a uterus, but the embryonal stem cells are extracted and expanded *in vitro* in order to be differentiated and used for tissue replacement therapy. According to the embryo protection law therapeutic cloning is forbidden in most countries [30], [37]. Another method to generate cells of a specific type for research or therapeutic purposes is called transdifferentiation. With this approach somatic cells are directly converted into another differentiated cell type without going back completely to the dedifferentiated stem cell level [37]. In 2006, Kazutoshi Takahashi and Shinya Yamanaka successfully reprogrammed somatic cells to pluripotent stem cells by ectopically overexpressing four specific transcription factors, Oct4, Sox2, Klf4 and c-Myc. This approach was a breakthrough in modern regenerative medicine and the four factors were later termed Yamanaka factors [37], [38]. Up to date a successful reprogramming has also been performed with other factors like Nanog, Lin28 or small molecules. To ectopically overexpress these proteins, cells can be transduced with viral vectors carrying the genes for the reprogramming factors. Although viral transduction is one of the most efficient methods for gene transfer, the actual reprogramming efficiency only ranges from 0.0002 to 1% [36], [39], [40]. The disadvantage of conventional viruses is that their genome integrates into the host genome. To avoid integration of viral DNA into the host genome Sendai viruses can be used. The Sendai virus does not integrate its genome into the host genome, but securely delivers the reprogramming factors to the nucleus for overexpression (OE). Besides viral transduction of the genes of reprogramming factors, other methods for reprogramming somatic cells, like mRNA transfection, miRNA infection or transfection, PiggyBac systems, minicircle vectors or episomal plasmids have been studied. However, all these methods either show an even lower efficiency than the reprogramming with viruses, have not been established with human cells or result in unwanted integration of foreign genetic elements into the host genome [40]. Successful reprogramming yields iPSCs, which are a great tool for regenerative medicine as they share many functions with embryonal stem cells but can be generated in a way that does not constitute an ethical problem. Until today, iPSCs have successfully been generated from mouse, rat, swine, sheep, dog, horse, ape and human somatic cells [36], [41], [42]. These iPSCs can be used to study basic questions of developmental biology, for drug testing, disease modelling and in regenerative medicine [36], [37]. Since iPSCs give rise to tumors upon transplantation into an organism, for medical applications somatic cells derived from iPSCs will be used. Some examples for the use of iPSC-derived somatic cells for tissue replacement therapy include the transplantation of differentiated pigment cells into the eyes of patients with macular degeneration or the injection of cells of the central nervous system into patients with spinal cord injury. So far, the prognosis is promising even though long term studies still remain to be done [30], [43]. Different possible areas of application for hiPSCs in research and medical therapy are depicted in **Figure 5**.

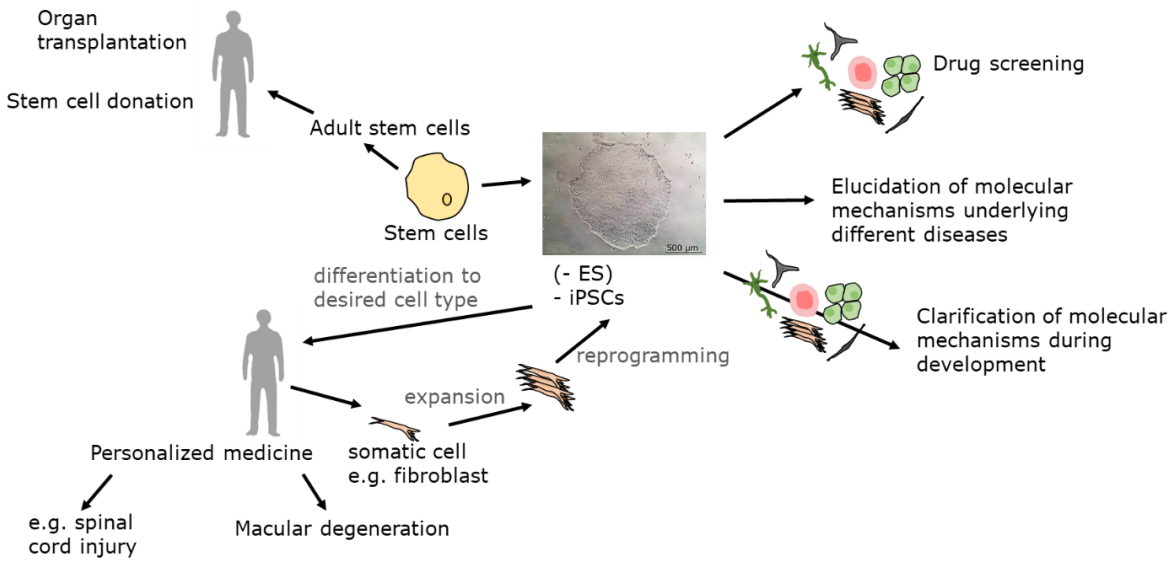

Figure 5: Possible applications for hiPSCs in research and therapy
Figure adapted from [36]

1.4 Similarities between tumorigenesis and development (focusing on NCC and melanocyte development)

As mentioned in 1.1 and 1.2 melanocytes evolve from NCCs during embryogenesis and are sometimes even termed as "a product of embryonic epithelial to mesenchymal transition (EMT)" [21], [25]. The development and migration of neural crest cells has been widely used as a developmental study model, for example for pluripotency, EMT, cell fate determination and migration [44]. Further, it is known that during embryogenesis cells undergo many processes which can be also found in cancer development These are for example cell invasion or EMT [25]. As an example, EMT reactivation in epithelial cells features an oncogenic transformation and propagation [21]. In addition, it has been shown that metastatic melanoma cells start anew to express NCC markers, which are involved in EMT or migration. These include epinephrins, which have been shown to be upregulated in migrative melanoma cells upon insertion into chick NC areas, but have not been expressed in non-invasive melanoma cells and melanocytes [44]. Similarly, it has been reported that malignant melanoma cells hijack specific functions of NC migration during development [44] and especially in aggressive melanoma the developmental migration mechanisms of NCCs are used in an abnormal way [45]. Moreover, it has been shown that highly invasive melanoma cells, when transplanted into chick embryonic NC environment, migrate along NC-specific routes and also highly respond to signals from the NC environment which is typical for NC induction, EMT and migration [44]. During the development and further differentiation of NCCs, specific factors are necessary to prime the NCCs into a specific NCC type for further development. Among these factors are Wnt and BMP4 which are thought to be antagonistic, thereby a continuous Wnt signaling is important for melanocyte differentiation, where BMP4 in high concentrations is necessary for neural and glial differentiation [44]. Especially BMP4 signaling plays a key role in the differentiation process to NCCs, favoring either a differentiation into keratinocytes (higher concentration) or NCCs (lower concentration) [46]. Nevertheless, it has been shown that BMP4 is necessary for the differentiation of stem cells to melanocytes because it induces the expression of MITF. However, EDN3 is then needed to facilitate the complete differentiation to melanocytes

[47]. BMPs in general have a promoting effect on cell migration, including the migration of NCCs [48]. In melanoma cells BMP4 (together with BMP7) has been shown to be upregulated and to play an important role in promoting migration and invasion [44], [48]. Together with the promoted migration high BMP expression also induces the switch to a more neuronal-like phenotype that helps melanoma cells to form brain metastases [44].

Furthermore, NCCs itself also share several functions with cancer cells, including their migration ability, the signaling pathways they utilize and their heterogeneity [13], [49]. Especially for NC-derived tumors (melanoma and neuroblastoma) the development of NCCs is a great model. For example, NCC-derived Schwann cell precursors migrate along developing neurons to their final destination. Likewise, a process called perineural invasion is often seen in metastasizing cancer where the cancer cells migrate along nerves to spread [13]. During development NCCs first develop to melanoblasts and then further to melanocytes. Just like NCCs, also melanoblasts show a highly migrative behavior. This ability as well as diverse further functions and gene expression during their development have been also seen in metastasizing cancer cells. So, the hypothesis is, that when melanoma cells switch to a metastatic phenotype, they reactivate some of the same signaling pathways that are active in melanoblasts during development [45], [50].

As already described in 1.1.1 a higher expression of NC-related genes in melanomas has been associated with a phenotype switch in melanoma to a more migrative phenotype. This phenotype switching of melanoma cells not only goes along with the expression of NCC markers but also melanocyte as well as stem cell markers. As an example, MSX1 is highly expressed in early NCCs and can lead to a phenotype switch in melanoma cells which results in a more migrative phenotype. A second example is the pigmentation marker MITF, whose expression is dysregulated in about 20% of melanomas and which also has an important function in melanoma phenotype switching [3]. This divergent expression of NC, melanocyte and stem cell markers reflects the high plasticity and heterogeneity of melanoma, which can also be seen in different stages during development [18], [21]. A higher degree of heterogeneity of melanomas is due to the existence of so-called cancer stem cells. These cells are dedifferentiated cancer cells, which show stem cell marker expression and behavior. Cancer stem cells contribute to slow tumor growth, tumor spread and resistance, while the majority of the mass of a tumor is differentiated to various extents and is responsible for fast tumor growth. As mentioned before, cancer stem cells are often linked to therapy resistance due to several reasons, one of them being their slow proliferation rate by which they can escape many chemotherapeutic drugs [21].

It is also worth mentioning that stem cells show similarities with cancer cells, especially melanoma cells. The most prominent feature here is their self-renewing capability making them theoretically immortal [18]. Moreover, both cell types benefit from a depletion of p53. This depletion facilitates the reprogramming of somatic cells to a pluripotent state and p53 is further known to be a tumor suppressor in many cancers [18], [51]. Also, the morphologies of stem cells and melanoma cells show similarities, as some melanoma cells, especially in the proliferative state, show a more round phenotype resembling the small and round phenotype of stem cells [18]. Also, HIF1α, a known marker for hypoxia, has been shown to be beneficial for the survival of melanoma and stem cells [52], [53]. An overview of the above-mentioned similarities between tumorigenesis and development with the focus on NCCs and melanoma can be seen in **Figure 6**.

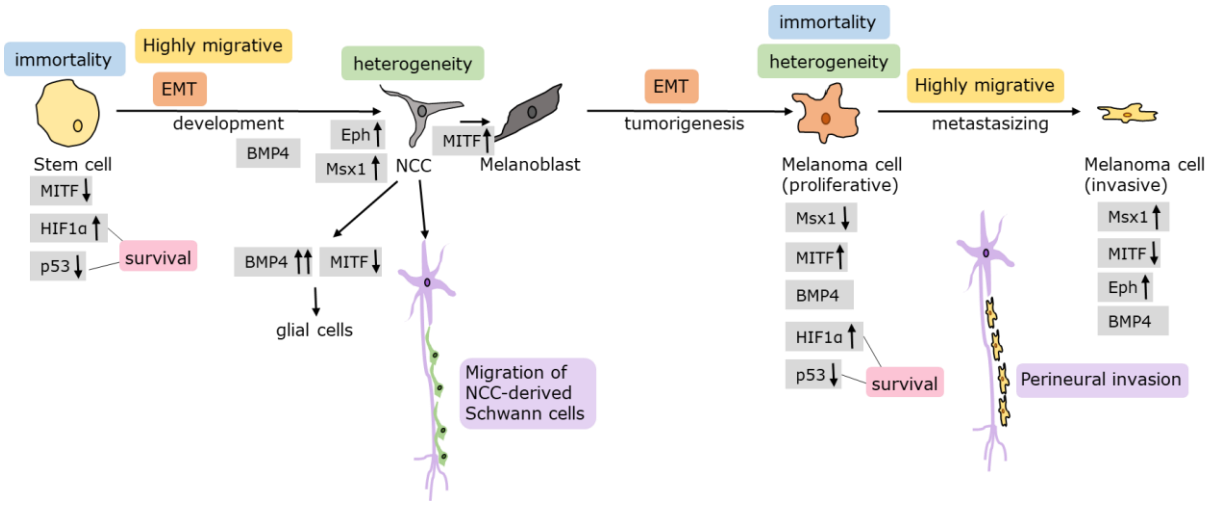

Figure 6: Similarities between development and tumorigenesis
Schematic overview of similar mechanisms and factors that play a role in normal development of NCC and in melanomagenesis. Comparable mechanisms are highlighted in the same color . Arrows indicate up- or downregulation of gene expression in the respective cell types.

All the above-mentioned similarities between development and tumorigenesis leads at first separated research fields closely together. And by this, NCCs are an excellent model for cancer development and metastasis, specifically for melanoma. Therefore, the investigation of melanoma cell behavior and of the mechanism from stem cells to melanocytes via neural crest cells could help together to understand the mechanism of developing melanoma and thereby could help to find an efficient treatment for melanoma patients.

1.5 ADCK2

ADCK2 belongs to a highly conserved aarF-domain containing protein family [54], which has five members (ADCK1-5). This family was first described in 1998 and belongs to an atypical kinase family, more specific the ABC1 family [55]–[57]. Interestingly, this family is thought to have been transferred via horizontal gene transfer from bacteria to eukaryotes [55]. The functions and substrates of the ADCK kinases are mostly unknown, but there is evidence that they are mitochondrial kinases. Also, they harbor specific protein-kinase motifs which are involved in ATP binding and phosphotransferase reactions and from ADCK5 it is known that this kinase contains about half of the motifs known for canonical kinases [56], [57]. Some family members (ADCK2, ADCK3, ADCK4) have been shown to play a role in CoQ_{10}/ubiquinone biosynthesis [58]–[61] and there is also evidence that the ADCK proteins affect cancer survival and migration as well as inflammatory processes [52], [54], [57], [62], [63]. In skin cancer, ADCK4 and NUMBL form a complex specifically in sun-exposed areas, which slightly improves cell proliferation [63] and the expression of ADCK5 is upregulated in diverse cancers [57]. Also ADCK4 as well as ADCK1 have been shown to have a negative effect on epithelial cell migration [64]. Regarding ADCK2, there is some evidence that it plays a role in tumor survival, especially when upregulated [62]. An effect on cell viability and proliferation was shown in ER+ve breast cancer and glioblastoma cells [54], [65]. Interestingly, a long-term NAET treatment in breast cancer resulted in improved tumor shrinkage when ADCK2 expression was high [59].

1.6 MYL6

Myosins are small nanomachines, which have major functions in cytoskeletal arrangement due to their interaction with actin filaments. Other cytoskeletal components are intermediate filaments and microtubules, which are bound by kinesins and dyneins [66]. The cytoskeleton is an important element in various cell processes including cell division, embryogenesis and cell motility [66], [67]. Myosins either bind cargoes and transport them along the actin skeletal network or simultaneously bind to each other and actins to assert movement. They have been described approximately four decades ago, but their exact functional performance is still not understood completely [67]. Typically, myosins consists of a head, a neck and a tail domain with specific functions. The head directly binds to actin and contributes the most to building up mechanical force. The neck region has arms to bind essential (ELCs) and regulatory light chains (RLCs) as well as calmodulin family members and the C-terminal tail either binds a cargo or assembles with other myosin molecules [66], [68]. To date, 135 myosins have been detected in eukaryotes and have been categorized into 35 classes [67]. Myosin II forms a hexamer, consisting of two heavy chains, two ELCs and two RLCs [69]. According to the heavy chain (MYH11, MYH9, MYH10 or MYH14) they are called smooth muscle myosin, non-muscle myosin (NM) 2A, NM2B or NM2C, respectively. In every cell at least one of the four myosin IIs is expressed [67]. All myosin IIs share 60-80% homology, where NM2C is more related to smooth muscle myosin than to NM2A and NM2B regarding the phylogenetic level [70]. The RLCs of NM2C are MYL (Myosin light chain) 9, MYL12A or MYL12B and can be phosphorylated and dephosphorylated. Phosphorylation converts the myosin molecule into an active state and a conformational change upon ATP hydrolysis promotes mechanical movement relative to the actin filaments [71]. The ELCs are MYL6 and MYL6B, whose functions are still not clear, but most probably they play a stabilizing role in myosin complexes. The structure of NM2C and its function in cell motility are depicted in **Figure 7**. Alternative splicing of MYL6 and MYL9 contributes to an additional diversity of myosin IIs [66], [72]. Interestingly, NM2C and smooth muscle myosin exclusively bind MYL6 as ELC, the mechanism and influence behind this is still unknown [66]. However, it has been reported that different splicing variants of MYL6 might bind to smooth muscle myosin and NM2s and that these different splicing variants might also play a role in the development of breast cancer [72].

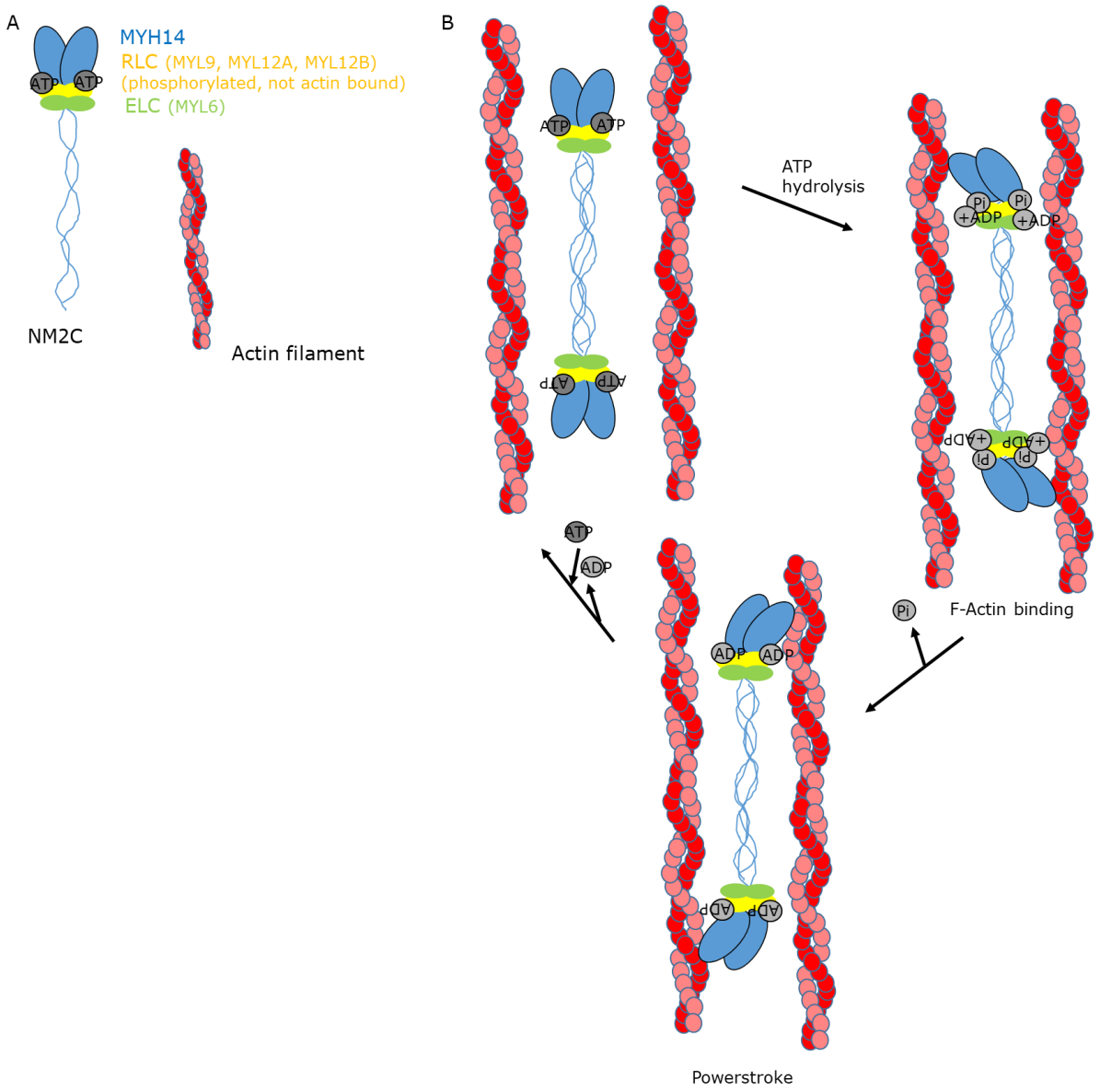

Figure 7: The structure and function of NM2C
A: *Structure of a hexameric NM2C with two MYL6 essential light chains (green), two regulatory light chains (yellow) and two MYH14 chains (blue). The two actin filaments consisting of many actin monomers are highlighted in red and pink, respectively.* ***B:*** *The mechanism of the interaction of NM2C and actin filaments to create movement. ATP-bound NM2C is released from actin filaments (top left), ATP hydrolysis to ADP and phosphate (Pi) by the myosin head leads to binding of NM2C to actin filaments (top right). As soon as the Pi is released the conformation of NM2C changes, which leads to a power stroke (contraction of actin filaments) (bottom). An exchange of ADP with ATP again releases NM2C from the actin filaments (top left). Figure adapted from* [66]

Aberrations in myosin molecules are often connected with diseases including cancer and especially myosin II is known to be a target for pathogens [67]. In skin cells, NM2A has been shown to limit cell division to a necessary level and thereby acts as a tumor-suppressor. The downregulation of NM2A (through either disassembling or mutations) correlates with skin cancer with a higher ability to metastasize [66], [69]. Furthermore, NM2A reduction by siRNA leads to more migrative cells due to less stress fibers and focal adhesions but more stable microtubules at the leading edge. A reduction of NM2C expression leads to decreased proliferation in lung cancer cells [70]. Moreover, a connection between NM2B mutations and lung diseases as well as between mutations in NM2C and cancer, deafness and muscle atrophy has been shown [69]. Interestingly, in

migrating melanoma cells only NM2C has been found which implicates that also this variant of non-muscle myosins is capable to form a front-back polarization [70]. An aorta smooth muscle myosin construct was constitutively active after deletion of RLCs [73]. In NIH 3T3 fibroblasts a downregulation of MYL6, MYH9 and MYH10 was seen after a siRNA mediated knockdown (KD) of MYL12A and MYL12B which also led to altered cell dynamics [74]. A similar effect could be also seen in cells that harbored a mutant NM2A gene expressing, a constitutively active NM2A protein [70].

Interestingly, myosin II has also been shown to provide the mechanotransduction involved in regulatory processes of stem cell proliferation and their differentiation [67]. However, NM2C has been shown to be less expressed in human fetal tissue and could not be detected in mouse embryonic stem cells [75]. This leads to the assumption that NM2A and NM2B play a more prominent role in stem cell development and NM2C is more functional in adult tissues and differentiated cells. This hypothesis was also confirmed by the fact that NM2C knockout in mice is not lethal and does not go along with obvious phenotype changes, whereas NM2A and NM2B knockout mice were not viable [70].

2 Aims of this thesis

In this thesis, I aimed at learning more about the role of ADCK2 in melanoma cells and in normal development, with a particular emphasis on the relevance of ADCK2 for the differentiation of hiPSCs to NCCs.

In more detail, my aims were to:

- Evaluate the correlation of ADCK2 expression in melanomas to the survival of melanoma patients.
- Investigate the role of ADCK2 on melanoma cell behavior, focusing on the cell motility to determine the effect of ADCK2 on the metastatic capacity of melanoma cells. Furthermore, I wanted to gain more insights into how ADCK2 possibly affects functional characteristics of melanoma cells.
- Generate hiPSCs and establish an efficient protocol for their differentiation into NCCs in a xeno-free environment.
- Examine the involvement of ADCK2 (and other kinases) on the differentiation of hiPSCs into NCCs.

3 Materials and Methods

3.1 Materials

Table 1: Reagents and Kits used in this thesis

Product	Company	Catalog No.
ActinRed 555	Life Technologies	R37112
Alamar Blue	Invitrogen	DAL1025
Albumin Fraction V (BSA)	Carl Roth	T844.4
AP Staining Kit	StemGent	00-0055
Aphidicolin	Sigma Aldrich	A4487
cOmplete Mini Protease Inhibitor Cocktail	Roche Diagnostics	11836145001
Cultrex Basement Membrane Extract Cell Invasion Assay, 24-Well	R&D Systems	3455-024-K
DAPI	Roche Diagnostics	10236276001
DH5α Competent Cells	Thermo Fisher Scientific	18265017
Endofree Plasmid Maxi Kit	Qiagen	12391
Immobilon Forte Western HRP Substrate	Merck Millipore	WBLUF0100
Immobilon PVDF membrane, 0.45µM	Merck Millipore	IPVH00010
LB Medium	Carl Roth	X965.2
Methanol	Sigma Aldrich	CAS: 67-56-1
Fluoromount Aqueous Mounting Medium	Sigma Aldrich	F4680
NuPAGE Bis Tris MiniGels (4-12%)	Invitrogen	NP0321BOX
NuPAGE LDS Sample Buffer (4x)	Thermo Fisher Scientific	NP0007
NuPAGE MOPS SDS Running buffer (20x)	Invitrogen	NP0001
NuPAGE Sample Reducing Agent (10x)	Thermo Fisher Scientific	NP0009
PageRuler Plus Prestained Protein Ladder	Life Technologies	26619
Paraformaldehyde	Sigma Aldrich	P6148-1KG
PhosSTOP Phosphatase inhibitor Cocktail	Roche Diagnostics	4906845001
Pierce BCA Protein Assay Kit	Thermo Fisher Scientific	23225
Qiaprep Spin Miniprep Kit	Qiagen	27106
QuantiNova SYBR Green Kit	Qiagen	208154
RevertAid First strand cDNA Synthesis Kit	Thermo Fisher Scientific	K1621
Rnase-Free Dnase Set	Qiagen	79256
Rneasy Plus Mini Kit	Qiagen	74136
Sendai2.0 Kit	Invitrogen	A34546
Skim milk powder	Gerbu Biotechnik	68514-61-4
TritonX-100	Carl Roth	3051.1
Tween 20	Applichem	A4974
Venor Gem Classic Myco PCR Kit	Minerva Biolabs	11-1025
X-treme GENE 9 DNA Transfection Reagent	Roche Diagnostics	6365787001

Table 2: Reagents for cell culture used in this thesis

Product	Company	Catalog No.
adenin	Sigma Aldrich	A2786
Apo human transferrin	Sigma Aldrich	T1147
ascorbic acid	Carl Roth	NC00.1
B27 supplement	Gibco Life Technologies	17504044
Bambanker	nippon genetics	BB02
bFGF = FGF2	Peprotech or Promokine	100-18B
BMP4	Promokine	C-67314
cAMP	Sigma Aldrich	A3262
CHIR99021	Axon Medchem	HY-10182

cholera toxin	Sigma Aldrich	C9903
Dexamethasone	Sigma Aldrich	D2915
DMEM	Gibco Life Technologies	11965092
DMEM/F-12	Gibco Life Technologies	11330032
DMEM/F-12 powder	Thermo Fisher Scientific	12500096
DMEM+GlutaMAXX	Gibco Life Technologies	10566016
DMSO	Carl Roth	A994.2
EDN-3	Sigma Aldrich	E9137
EGF	PromoCell	C-60169A
Fetal Calf Serum (FCS)	Biochrom	S0115
Fibronectin (bovine)	Thermo Fisher Scientific	#33010-018
Glucose	Sigma Aldrich	G7021
HAM/F12	Gibco Life Technologies	11765054
Human melanocyte growth supplement (HMGS) 100x	Gibco Life Technologies	S0025
hydrocortison	Sigma Aldrich	H0888
insulin	CS Bio	CS9212
ITS+	Corning (Fisher Scientific)	354351
Knockout-DMEM	Gibco Life Technologies	10829018
KSR (knockout serum replacement)	Thermo Fisher Scientific	10828028
Laminin	StemCell Technologies	# 77003
LDN193189	StemCell Technologies	#72147
L-Glutamine	Sigma Aldrich	G7513
Lipofectamine RNAiMAX Transfection Reagent	Thermo Fisher Scientific	13778030
Low-glucose DMEM	Thermo Fisher Scientific	31885049
Matrigel	Corning	354277
MCDB201	Sigma Aldrich	M6770
Medium 254	Gibco Life Technologies	M254500
mTeSR	StemCell Technologies	#85850
N2	Gibco Life Technologies	A1370701
Neurobasal medium	Gibco Life Technologies	10888022
Non-essential amino acids (NEAA or MEM)	Sigma Aldrich	M7145
Normocin	InvivoGen	ant-nr-1
PageRuler Plus prestained Protein Ladder	Thermo Fisher Scientific	#26619
PBS	Gibco Life Technologies	20012027
Penicillin/Streptomycin	Sigma Aldrich	P4333
Polybrene Infection/Transfection Reagent	Sigma Aldrich	TR-1003
Polyornithine	Sigma Aldrich	P4957
Progesterone	Sigma Aldrich	P8783
Puromycin	Carl Roth	0240.1
Putrescine dihydrochloride	Sigma Aldrich	P5780
Rock inhibitor (Y27632)	Merck	SCM075
SB431542	StemCell Technologies	#72234
Sodium bicarbonate	ChemCruz (Santa Cruz Biotechnology)	sc-203271A
Sodium pyruvate	Gibco Life Technologies	11360070
Sodium selenite	Sigma Aldrich	S5261
ß-mercaptoethanol	Gibco Life Technologies	31350010
Stem cell factor	Sigma Aldrich	H8416
StemFit Basic 02 (A+B)	nippon genetics	Basic02
StemPro Accutase Cell Dissociation Reagent	Gibco Life Technologies	A1110501
triiodothyronine	Sigma Aldrich	T6397
Triton X100	Carl Roth	2367.3
Trypan blue solution	Sigma Aldrich	T8154
Trypsin-EDTA solution	Gibco Life Technologies	25300054

Wnt3A	abcam	ab153563

Table 3: All cell lines used in this thesis

Cell Line	Source	Cell type	Mutation
A375	ATCC	Melanoma cell line	BRAF V600E
C32	ATCC	Melanoma cell line	BRAF V600E
HT144	ATCC	Melanoma cell line	BRAF V600E
MeWo	ATCC	Melanoma cell line	WT
SkMel103	ATCC	Melanoma cell line	Q61R
SkMel173	ATCC	Melanoma cell line	Q61R
SkMel28	ATCC	Melanoma cell line	BRAF V600E
SkMel30	ATCC	Melanoma cell line	Q61K
WM2664	ATCC	Melanoma cell line	V600D
NHM	patients	normal human melanocytes	WT
HEK293T	ATCC	embryonic kidney cells	WT
Fibroblasts	patients	fibroblasts	WT
hiPSCL1	reprogrammed from patient fibroblasts with Sendai2.0	iPSCs	WT
hiPSCL2	reprogrammed from patient fibroblasts with Sendai2.0	iPSCs	WT

Table 4: All siRNAs used in this thesis

Product	Company	Catalog No.
AllStars Neg. siRNA AF 488 (siControl)	Qiagen	1027280
Hs_ADCK2_5 FlexiTube siRNA	Qiagen	SI00287952
Hs_ARAF_2 FlexiTube siRNA	Qiagen	SI05096266
Hs_DBF4_12 FlexiTube siRNA	Qiagen	SI04900203
Hs_EPHA4_11 FlexiTube siRNA	Qiagen	SI04435025
Hs_MYL6_3 FlexiTube siRNA	Qiagen	SI00653009
Hs_TYK2_13 FlexiTube siRNA	Qiagen	SI05059264
siGENOME siRNA Human MAP2K3	Thermo Fisher Dharmacon	D-003509-05

Table 5: All plasmids used in this thesis

Name	Source
pCMV-dR8.91 (Packaging)	Konrad Hochedlinger (Harvard, Boston, USA)
pCMV-VSV-G (Packaging)	Addgene #8454
ADCK2 OE	Vector Builder
	pLV[Exp]-Puro-EF1A>hADCK2[NM_052853.4] (Vector ID: VB900090-4328zyg)
ADCK2 EV	Cloned by Dr. Daniel Novak, DKFZ by removing the ADCK2 ORF from the ADCK2 OE construct

Table 6: All qPCR primers used in this thesis

Amplification target	Forward sequence	Reverse sequence
18S	GAGGATGAGGTGGAACGTGT	TCTTCAGTCGCTCCAGGTCT
ADCK2	TCTCGCAGACCAGTCGGTTG	GCAACACTTTCACTGCCACG
ARAF	CCTGGCGTTCTGTGACTTCTG	CGGTTGGTACTCATGTCAACAC
Cxcr4	CTGAGAAGCATGACGGACAA	GACGCCAACATAGACCACCT
DBF4	GGGCAAAAGAGTTGGTAGTGG	ACTTATCGCCATCTGTTTGGATT
endo Nanog	CAGTCTGGACACTGGCTGAA	CTCGCTGATTAGGCTCCAAC
EPHA4	TTCGCCCTATTTTCGTGTCTC	TGGTAGGTTCGGATTGGTGTAT
FoxD3	CATCCGCCACAACCTCTC	CATATGAGCGCCGTCTG
MAP2K3	CCAGTCCAAAGAGAGGCTGGT	CCACAAACTCGGGGGAGAAA
MITF	AGTGTTGATAGTTTATGGC	ACTTGGTGGGGTTTTCGAGG
MYL6	GAAGACCAGACCGCAGAGTTC	TCCAGCACCTTCACATTCATC
p75	CGACAACCTCATCCCTGTCT	GCTCTTCAACCTCTTGAAGG
Pax3	CTGTGCCCAGGATGATGCG	GATCTTGTGGCGGATGTGGT
RAB2A	CGTTCCATCACAAGGTCGTATT	CTTAGCAGACGTTTCCATGAAGA
Sox10	AGCCCAGGTGAAGACAGAGA	ATAGGGTCCTGAGGGCTG
Sox2	GCGTACCGGGTTTTCTCCATGCT	GTGAGGGCCGGACAGCGAAC
Sox5	CAGCCAGAGTTAGCACAATAGG	CTGTTGTTCCCGTCGGAGTT
total Oct4	GCTTGGGCTCGAGAAGGATGTGG	GGCCCTGGGGCCAGAGGAAA
TRP1	AGCAGTAGTTGGCGCTTTGT	TCAGTGAGGAGAGGCTGTTT
TYK2	GGAGGAGGGTTCTAGTGGCA	ATGTCCCGGAAGTCACAGAAG
TYR	TTGTACTGCCTGCTGTGGAG	CAGGAACCTCTGCCTGAAAG

Table 7: All antibodies used in this thesis

Specificity	Source	Company	Catalog No.	Dilution factor	Diluent	Size of antigen [kDa]
Anti-ADCK2	rabbit	abcam or LS Bio	#ab235312	1:1.000	5% BSA	69
Anti-GAPDH	rabbit	cell signaling	#2118S	1:10.000	5% Milk	37
Anti-MYL6	rabbit	Invitrogen	PA5-106803	1:1.000	5% BSA	17
Alexa Fluor 488 goat anti-mouse IgG (H+L)	goat	Invitrogen	A11029	1:10.000	5% BSA or FACS buffer	
anti-rb IgG HRP-linked antibody	/	cell signaling	7074S	1:10.000	5% BSA or Milk	
Anti-Sox10 (D5V9L)	rabbit	cell signaling	#89356	1:1.000	5% BSA	
Monoclonal Anti-HNK-1/N-CAM (CD57)	mouse	Sigma Aldrich	C6680-50TST	5µL/sample	FACS buffer	
PE-Cy7 Mouse Anti-Human CD271	mouse	BD Pharmigen	562122	5µL/sample	FACS buffer	

Table 8: Solutions and buffers used in this thesis

Buffer/solution	ingredients
Blocking buffer	5% skim milk powder or 5% BSA, 1xTBS-T
Cell freezing medium (for melanoma and HEK cells)	80% FCS, 20% DMSO 1:2 mixed with MEF medium
Cell lysis buffer for protein isolation	Ripa buffer, 1x PhosphoStop, 1x Complete mini protease inhibitor cocktail
FACS buffer	PBS, 5%BSA, 1:1000 0.5M EDTA pH8.0
LB medium	20g LB-Medium, 1L H2O
MEF medium	DMEM+GlutaMAXX, 10% FCS, 1% penicillin/streptomycin, 1% non-essential Amino acids, 0.1 mM ß-Mercaptoethanol
Running buffer (pH 8.3)	25 mM Glycine, 190 mM Tris, 0.1% SDS, dH2O
Stem cell medium	StemFit A+B, 100ng/mL bFGF, 1:1000 Normocin
TBS 10X (pH 7.6)	150 mM NaCl, 50 mM Tris, dH2O
Transfer buffer (pH 8.3)	25 mM Glycine, 190 mM Tris, 20% SDS, dH2O
Washing buffer (TBS-T)	1xTBS, 0.02% Tween 20

Table 9: Differentiation media and coating substances for NCC differentiation

Differentiation media			
Dr. Kasia Weina (Weina, 2015)		end concentration	
	Basic medium		
	insulin	5	µg/mL
	hydrocortison	0,5	µg/mL
	cholera toxin	1,00E-10	M
	triiodothyronine	1,37	ng/mL
	adenin	24	µg/mL
	EGF	10	ng/mL
	sodium pyruvate	1	mM
	ascorbic acid	0,3	mM
	BMP4	20	pM
Basic medium:	Pen/Strep	100	x
	DMEM	225,00	mL
	DMEM + HAM/F12 (1:1)	225,00	mL
	FCS	10	%
Larribère et al., 2015		end concentration	
	FAD		
	insulin	5	µg/mL
	hydrocortison	0,5	µg/mL
	cholera toxin	1,00E-10	M
	triiodothyronine	1,37	ng/mL
	adenin	24	µg/mL
	EGF	10	ng/mL
	ascorbic acid	0,3	mM
	BMP4	20	pM
	Wnt3A	200	ng/mL
FAD:	DMEM	0,67	mL
	DMEM + HAM/F12 (1:1)	0,33	mL
	FCS	10	%

Nissan et al., 2011

		end concentration	
	FAD		
	insulin	5	µg/mL
	hydrocortison	0,5	µg/mL
	cholera toxin	1,00E-10	M
	triiodothyronine	1,37	ng/mL
	adenin	24	µg/mL
	EGF	10	ng/mL
	ascorbic acid	0,3	mM
	BMP4	20	pM
FAD:	DMEM	0,67	mL
	DMEM + HAM/F12 (1:1)	0,33	mL
	FCS	10	%

Dr. Katrin Schrenk-Siemens (Schrenk-Siemens et al., 2015)

		end concentration	
basal sphere medium	DMEM/F12	50	%
	Neurobasal medium	50	%
	B27	0,5	x
	N2	0,5	x
	insulin	2,5	µg/mL
	glutamine	1	x
added freshly onto each plate	EGF	10	ng/mL
	bFGF	10	ng/mL

Callahan et al., 2016

		end concentration	
KSR-differentiation media:			
	knockout-DMEM	820	mL
	KSR	150	mL
	L-glutamine	10	mL
	Pen/Strep	10	mL
	MEM (NEAA)	10	mL
	β-mercaptoethanol	1	mL
N2-differentiation medium:			
	DMEM/F-12 powder	12,00	g
	distilled water		
	glucose	1,55	g
	sodium bicarbonate	2,00	g
	human apotransferrin	100,00	mg
	insulin	0,025	mg/mL
	putrescine dihydrochloride	100,00	µM
	sodium selenite	30,00	nM
	progesterone	20,00	nM
Melanocyte differentiation medium:			
	Neurobasal medium	50	%
	low-glucose DMEM	30	%
	MCDB201	20	%
	ITS+	0,8	%
	L-glutamine	250	nM
	ascorbic acid	100	µM

cholera toxin	50	ng/mL
stem cell factor	50	ng/mL
dexamethasone	0,05	µM
EDN3	100	nM
FGF2	4	ng/mL
B27 supplement	2	%
BMP4	25	ng/mL
CHIR 99021	3	µM
cAMP	500	µM

Coating for NCC cultivation

Dr. Katrin Schrenk-Siemens (Schrenk-Siemens et al., 2015)

	end concentration	
polyornithine	15	µg/mL
laminin	10	µg/mL
fibronectin	10	µg/mL

Callahan et al., 2016

	end concentration	
polyornithine	15	µg/mL
laminin-I	1	µg/mL
fibronectin	2	µg/mL

Table 10: Consumables and Devices used in this thesis

Product	Company
12 Well Multiwell Plates	Greiner Bio-One
24 Well Multiwell Plates	Greiner Bio-One
48 Well Multiwell Plates	Greiner Bio-One
6 Well Multiwell Plates	Greiner Bio-One
96 Well Multiwell Plates	Greiner Bio-One
AB 7500 Real-Time PCR Machine	Applied Biosystems
Affymetrix Clariom S human Chip	Affymetrix
CELLSTAR Cell Culture Flasks	Greiner Bio-One
ChemiDoc Touch Imaging System	BioRAD
Culture-inserts 2 Well	Ibidi
FacsCanto II	BD Biosciences
glas coverslips (round, 14mm)	neolab
Haemocytometer	Neubauer
Leica DM LS light microscope	Leica
MicroAmp Optical 96well Plate qPCR	Thermo Fisher Scientific
microscope slide (SuperFrost Plus)	R. Langenbrinck GmbH
Nanodrop Spectophotometer ND-1000	peqlab Biotechnologie GmbH
Nikon Eclipse Ti Microscope	Nikon
Nunc Cell Culture Cryogenic Tubes	Thermo Fisher Scientific
Rotilabo-syringe filters, 0.22µm and 0.45 µm	Carl Roth
Tecan Infinite F200 PRO	Tecan
Zeiss LSM 700	Zeiss

Table 11: Software used for analysis in this thesis

Software name	Source
7500 Software v2.0.5	Applied Biosystems
FlowJo 7.2.2	FlowJo License
GraphPad PRISM 8	GraphPad License
i control 1.10	TECAN
Image Lab 6.0.1	Bio-Rad
ImageJ	NIH
Mendeley	Mendeley
NIS-Elements	Nikon
Tscratch	CSElab
ZEN	Zeiss

3.2 Methods

3.2.1 Cell culture

Melanoma cells, fibroblasts and HEK293T cells were cultured in MEF medium (DMEM+GlutaMAXX (Gibco) supplemented with 10% FCS (Biochrom), 1% penicillin/streptomycin (Sigma-Aldrich), 1% non-essential amino acids (Sigma-Aldrich) and 0.1 mM ß-mercaptoethanol (Gibco)) at 37°C and 5% CO_2. They were split regularly when reaching about 90-100% confluency with 0.05% Trypsin-EDTA (Gibco). Stocks of these cell lines were stored in freezing medium (20% DMSO in FCS 1:2 MEF medium) in liquid nitrogen.

Stem cells were cultured in stem cell medium (StemFit medium (A+B) (Nippon genetics)) supplemented with 100ng/mL bFGF (Peprotech) and 1:1000 Normocin (Invitrogen) on Matrigel (Corning) coated plates. For coating, Matrigel was thawed on ice overnight, aliquoted according to the manufacturer´s protocol and frozen. Before use, one aliquot was suspended in 25 mL DMEM/F-12 medium (Gibco) and 1mL was added per well of a 6-well plate or 6mL to a 10cm diameter cell culture dish. The solution was equally distributed on the surface by tapping the plate. After incubation for at least 1h at RT, excess medium was removed and stem cell medium was immediately added, to prevent the coating from drying out. For long term storage, the solution used for coating was not removed and the plates were wrapped with parafilm to prevent them from drying out. Plates could be stored at 4°C for up to 4 weeks. When hiPSCs reached about 80% confluency, they were split with StemPro Accutase (Gibco) onto fresh Matrigel-coated plates and incubated in Stem cell medium containing 1:1000 Rock inhibitor for 24h. Cells were maintained under optimal conditions at 37°C and 5% CO_2. Medium was changed every other day. Stocks of stem cells were stored in Bambanker freezing medium (Nippon genetics) in liquid nitrogen.

All cells were tested on a regular basis for contamination with mycoplasma (by PCR) and other microorganisms (by eye) and only used when they were free of any contamination.

3.2.2 Reprogramming of somatic cells

For reprogramming fibroblasts, the Sendai 2.0 Kit from Invitrogen was used according to the manufacturer´s protocol. hiPSCL1 and hiPSCL2 were both reprogrammed from fibroblasts by ectopically overexpressing the reprogramming factors Nanog, Oct4, c-Myc

and Klf4 when fibroblasts reached a confluency of about 70%. After 48h cells were washed 3 times with PBS to remove excess virus and were further cultured in normal MEF medium. When they reached about 100% confluency and the first cobblestone like structures appeared (after about 1 week) cells were splitted 1:3 onto freshly coated Matrigel plates. The next day medium was switched from MEF medium to stem cell medium (mTesR (Stemcell) for iPSCL1 and StemFit (Nippon genetics) for iPSCL2, both supplemented with 1:1000 Normocin). After another 2 weeks, the first hiPSC-colonies became visible and could be picked and transferred to a new Matrigel-coated plate. These hiPSCs were expanded to generate a new hiPSCL. For hiPSCL1 the cells were subcultured to achieve a stable hiPSCL grown in StemFit medium. For this, small colony pieces from the original hiPSCL1 were picked and seeded into Matrigel-coated wells of a 48-well plate. Colonies which grew nicely and did not differentiate after about 1,5 weeks were then transferred via Accutase splitting to a Matrigel-coated well of a 24-well plate. Again, cells were observed and non-differentiating, nicely growing cells were transferred to a Matrigel-coated plate of a 6-well plate by Accutase splitting. In the end, both hiPSCLs were grown in 10cm diameter cell culture plates in the above (3.2.1) mentioned media.

The validation of pluripotency for both hiPSCLs was done by a staining for alkaline phosphatase with the AP staining Kit from StemGent following the manufacturer´s instructions on a regular basis. In brief, hiPSCs were washed, permeabilized and fixed. Then, hiPSCs were stained with staining solution in the dark at RT for about 10-20min, resulting in red to purple color for AP-positive cells. Further, both hiPSCLs were tested for their mRNA expression level of the stem cell markers Nanog, Oct4 and Sox2 by qPCR (detailed protocol see at 3.2.6). Moreover, a teratoma formation assay was performed for hiPSL1. For this purpose, 1 million hiPSCs were mixed 1:2 with Matrigel and immediately subcutaneously injected into the flank of NOD-SCID mice. Mice were controlled once a week and as soon as a tumor appeared, tumor size was measured. When the tumor reached a size of 8.26*6.60 mm (after about 5 month) the mouse was sacrificed, the tumor excised, paraffin embedded, sliced into 10µM sections and stained by H&E staining. Structures of all three germ layers were then observed via light microscopy imaging.

3.2.3 Differentiation of hiPSCs to NCCs in a xeno-free environment

The protocols from Dr. Kasia Weina [76] and Larribère et al. [77] are both based on the protocol from Nissan et al. [46]. In all three protocols, hiPSCs were seeded one day before starting the differentiation in small cell clumps at different densities. In contrast to the original protocols, I seeded the hiPSCs on Matrigel-coated plates. The next day medium was changed to differentiation medium, which was changed every second day until day 10. The media compositions can be seen in Table 9. For the protocol from Dr. Katrin Schrenk-Siemens [78], hiPSCs were seeded as small clumps in a non-coated dish in stem cell medium. 24h later the medium was switched to basal sphere medium, which was changed every second day. After embryonic body (EB) formation, EBs settled down on the surface and NC-like cells grew out spontaneously from EBs and could be collected after Accutase treatment.

The differentiation protocol used for further experiments was adapted from Callahan et al. [79]. For this $4{,}8*10^5$ hiPSCs were seeded per Matrigel-coated well of a 6-well plate as single cells one day prior to the start of the differentiation. On day 0, 4mL KSR differentiation medium was added supplemented with 100nM LDN193189 and 10µM SB431542. On day 2, 2mL KSR medium supplemented with 100nM LDN193189,

10µM SB431542 and 3µM CHIR99021 was used. On day 3, LDN193189 was excluded from the medium. On day 4 and 5, a medium consisting of 2mL KSR medium, 1mL N2 medium and 3µM CHIR99021 was used. On day 6 and 7, cells were cultivated in medium consisting of 1.5mL KSR and 1.5mL N2 medium supplemented with 3µM CHIR99021, 25ng/mL BMP4 and 100nM EDN3. On day 8 and 9, the medium consisted of 1mL KSR and 3mL N2 medium supplemented as on day 6 and 7. On day 10, cells were washed with PBS, scrapped of the plate, pelleted and used for further analyses.

For replating experiments of NCCs, plates were either coated according to the protocol from Callahan et al. [79] or Dr. Katrin Schrenk-Siemens [78]. These protocols mostly differed in the concentration of laminin and fibronectin. In brief, wells were coated first with polyornithine (P/O) diluted in water ON at 37°C and 5% CO_2. The next day, excess water was removed and wells were coated with a laminin/fibronectin mixture ON at 37°C and 5%CO_2. Following the protocol of Dr. Katrin Schrenk-Siemens, P/O coated plates were dried under UV light for 30-60min prior to laminin/fibronectin coating. The following day, plates were dried completely under sterile conditions until crystalline structures could be spotted. Then, NCCs were seeded in different media and conditions. First, NCCs were detached with Accutase, using an approach with 25 or 10min. Then cells were either normally seeded in a 1:10 ratio or as small droplets to assure a high density in this spot but space for growth. For the droplet approach cells were diluted to $2*10^6$ cells/mL and 10µL droplets were applied onto the coated plates. After at least 30min at RT, 2mL of medium were gently added to the well. Furthermore, different media were used, either N2 medium supplemented with 3µM CHIR99021, 25ng/mL BMP4 and 100nM EDN3 or full melanocyte medium from the protocol of Callahan et al. [79]. All generated NCCs were cultivated under each condition, some with the addition of 1:1000 Rock inhibitor and some without.

The media compositions for all differentiation experiments as well as the coating concentrations can be seen in Table 9 and in Callahan et al. [79].

3.2.4 siRNA transfection and ectopic OE of ADCK2

To achieve a transient knockdown (KD), melanoma cells were seeded in MEF medium one day prior to transfection and were incubated ON at 37°C and 5% CO_2. The next day, cells were transfected with siControl, siADCK2 or siMYL6 using the Lipofectamine RNAi MAXX Kit from Thermo Fisher following the manufacturer´s instructions. In brief, Lipofectamine RNAi MAXX and siRNA were separately mixed with DMEM/F-12 and then pipetted gently together. To form complexes the mix was incubated for at least 5 min at RT. In the meanwhile, medium on the melanoma cells was changed to fresh MEF medium. Then, Lipofectamine RNAi MAXX - siRNA Mix was added dropwise to the cells. Afterwards, melanoma cells were incubated at 37°C and 5% CO_2 for 24, 48, 72 or 96h, pelleted or measured, depending on the experiment.

For the combined KD and differentiation of hiPSCs into NCCs, hiPSCs were seeded one day before transfection in stem cell medium containing 1:1000 Rock inhibitor and incubated at 37°C and 5% CO_2 for at least 24h. For transfection the Lipofectamine RNAi MAXX Kit from Thermo Fisher was used with slight adaptations. For all experiments the double amount of Lipofectamine RNAi MAXX as well as the double amount of siRNA was used compared with the manufacturer´s protocol. As mentioned above, both of them were first mixed separately in DMEM/F-12 and then pipetted gently together. During the 5 min incubation

at RT, medium of the stem cells was changed to the double amount of differentiation medium from day 0 compared to the original protocol [79]. Then, Lipofectamine RNAi MAXX - siRNA Mix was added dropwise to the cells and hiPSCs were incubated at 37°C and 5% CO_2 for 48h. Afterwards differentiation medium from day 2 was used and the differentiation was continued until day 10 as described before (3.2.3).

For ADCK2 OE in melanoma cells, a lentiviral ADCK2 expression construct was used. The empty vector control was generated by removing the open reading frame (ORF) of the ADCK2 gene from the plasmid. Successful cloning was confirmed by sequencing of the plasmid. ADCK2 OE and EV control plasmid were amplified in and isolated from E. coli bacteria. Virus was then produced in HEK293T cells with the XtremeGENE 9 DNA Transfection Reagent from Roche according to the manufacturer´s instructions. In brief, HEK293T cells were grown in MEF medium at 37°C and 5% CO_2 until they reached a confluency of about 70%. Then, XtremeGENE 9 DNA Transfection reagent was mixed with DMEM for 5min at RT. Afterwards, two packaging plasmids (5.5 µg pCMV-VSV G, 8.25 µg 1.5x pCMV-Δ8.9) and the ADCK2 OE or empty vector plasmid (11 µg 2x vector) were added and the mix was incubated for 30min at RT. HEK293T cells were then transduced with this complex and incubated at 37°C and 5% CO_2 ON. The next day, medium was discarded and fresh MEF medium was added to the transduced HEK293T cells. Then, every 12h virus containing medium was collected for three times, filtered and either directly used or aliquoted and frozen at -80°C for long term storage. For infection, melanoma cells were seeded in MEF medium and grown at 37°C and 5% CO_2 until they reached a confluency of 60-70%. Then they were infected with 1mL virus-containing medium per well of a 6-well plate and 6µg/mL polybrene (Sigma-Aldrich). After 24h at 37°C and 5% CO_2, the infection was repeated, but without polybrene and after another 24h incubation, melanoma cells were washed with PBS and grown in the incubator at 37°C and 5% CO_2 ON. The next day, selection was started by adding 0.5µg/mL puromycin (Carl Roth) to the cells. Selection was done for about one week or until control cells died. Puromycin-containing medium was changed every other day. Afterwards, cells were validated for their ADCK2 OE on RNA and protein level and stable ADCK2-overexpressing cell lines were used for further experiments. A stock was saved in freezing medium (20% DMSO in FCS 1:2 MEF medium) in liquid nitrogen.

3.2.5 Gene expression analysis

For gene expression analysis, RNA samples of high quality were extracted from cell pellets with the RNeasy Kit from Qiagen according to the manufacturer´s protocol. In this process both optional steps (DNA digestion with RNase-free DNase I (Qiagen) as well as fresh spinning tubes) were performed. Then, biological triplicates of following samples were sent to the Gene expression core facility at the DKFZ: hiPSCL1, hiPSCL1 siControl+NCC Differentiation Day10, hiPSCL1 siADCK2+NCC Differentiation Day10, hiPSCL2, hiPSCL2 siControl+NCC Differentiation Day10, hiPSCL2 siADCK2+NCC Differentiation Day10, MeWo siControl (24h), MeWo siADCK2 (24h), SkMel30 siControl (24h), SkMel30 siADCK2 (24h), C32 siControl (24h), C32 siADCK2 (24h). For the gene expression analysis, an Affymetrix Clariom S human Chip was used. The further analysis of the gene expression assay was done by Thomas Hielscher with the software R4.0 [80]. In brief, he used the Affymetrix CEL files, which were RMA normalized and expression values were log2-transformed. An empirical Bayes approach was used to identify differential expressed probe sets/genes [81]. This model is based on moderated

t-statistics as incorporated in the Bioconductor package limma [82]. In order to control a false discovery rate, the p-values were adjusted for multiple testing by using the Benjamini Hochberg correction.

3.2.6 qPCR

To determine mRNA expression levels, qPCR was used. For this, RNA was extracted from cell pellets with the RNeasy Kit from Qiagen as described in 3.2.5. 500ng of RNA were used for the cDNA synthesis reaction performed with the cDNA Kit from Thermo Fisher according to the manufacturer´s protocol, using OligodT Primer. The obtained cDNA was then diluted 1:10 with water and 1:100 Yellow TDB dye. For the final expression analysis, the QuantiNova SYBR Green Kit from Qiagen was used according to the manufacturer´s protocol. The amount of reagents used was adapted to the following: 5µL SYBR Green, 0.05µL ROX reference dye, 2.3µL H_2O and 0.15µL primer working solution. The qPCR data were analyzed either as relative mRNA expression level or as normalized fold change (FC) to a control. In all cases 18S was used as internal control.

3.2.7 Western blot

To validate the expression of specific markers on protein level western blot analysis was performed. Proteins were extracted from cell pellets by adding protein lysis buffer (RIPA buffer (Sigma-Aldrich) supplemented with 1x complete mini and 1x PhosSTOP (both from Roche)), incubating on ice for 30min on a shaker followed by 20min centrifugation at 4°C and maximum speed. Supernatant containing the proteins was then transferred to a fresh tube and the protein concentration was measured by Bradford assay using the pierce BCA Protein assay Kit from Thermo Fisher according to the manufacturer´s instructions. 30µg of protein were mixed with 10x reducing buffer and 4x Laemmli buffer and boiled for 10min at 70°C, spinned down and loaded to NuPAGE Bis-Tris 4-12% MiniGels (Invitrogen). Proteins were separated at 200V for about 45min, checking the running front by visible prestained Protein ladder. Afterwards proteins were transferred to an Immobilon-P membrane (Merck), which was then blocked with 5% skim milk or BSA, respectively, for at least 1h at RT. Afterwards, membranes were incubated with the according first antibody (see Table 7 for dilution factors and diluent) at 4°C ON. The next day, membranes were washed thoroughly with TBS-T and then incubated with the second antibody (see Table 7 for dilution factors and diluent) for 1h at RT. Following a thorough wash with TBS-T, proteins were detected with Immobilon Forte Western HRP substrate (Merck) at the ChemiDoc Touching Imaging System (BioRAD). The final analysis of the bands was done with Fiji software from ImageJ. GAPDH served as the loading control.

3.2.8 Flow cytometry analysis

To quantify the percentage of p75/HNK1 double-positive cells before and after the differentiation of hiPSCs into NCCs flow cytometry analysis was used. First, cells were carefully detached from the Matrigel coating (by scraping), washed with PBS and then with FACS buffer (PBS supplemented with 5% BSA and 0.5mM EDTA pH8.0). Then they were

incubated with anti-HNK1 antibody for 30min at 4°C in the dark. After several washing steps with FACS buffer, cells were incubated simultaneously with p75-PE Cy7-coupled antibody and anti-rabbit Alexa Fluor 488 antibody for 30min at 4°C in the dark. Following several washing steps with FACS buffer, labelled cells were directly measured with a FacsCANTO II machine from BD. The obtained data were analyzed with FowJo. The used antibodies are listed in table 11 and the gating strategy is depicted in **Supplementary Figure 1**. To minimize the overlapping fluorescence effect single stainings were performed and used for compensation and DAPI staining was used to distinguish dead and alive cells.

3.2.9 Cell viability assay

To investigate the cell viability of melanoma cells, cells were seeded into 96-well plates in MEF medium and were incubated at 37°C and 5% CO2. The exact cell numbers used for seeding are listed in Table 12. For all cell viability experiments, cells were seeded as quintuples per treatment/condition. After 24h, cells were either transfected with siRNA (as described in 3.2.4) or directly measured, according to the experiment. For measurement 1:10 AlamarBlue reagent (Invitrogen) was added to the cells and cells were incubated for 4h at 37°C and 5% CO_2. Afterwards, absorbance (at 535nm) and emission (at 590nm) were measured with the TECAN Infinite F200 PRO. Values were normalized to the control group in each experiment.

Table 12: Cell numbers for cell viability assay

cell line	cells per well
SkMel28 (parental, EV ADCK2, OE ADCK2)	2000
MeWo (parental, EV ADCK2, OE ADCK2)	1244
A375 (parental, EV ADCK2, OE ADCK2)	300
SkMel30 (parental, EV ADCK2, OE ADCK2)	1867

3.2.10 Migration assay

In order to quantify the migration capacity of melanoma cells, a wound assay was used. 2-chamber inserts (ibidi) were put into 12-well plates (1 insert per well). Then, cells were seeded into each chamber an incubated at 37°C at 5% CO_2 for 24h. The exact cell numbers were chosen so that the cells reached confluency at timepoint 0h and are listed in Table 13. The next day, cells were either transfected with siRNA (as described in 3.2.4) or inserts were removed. For removing, wells were filled with 1mL PBS, then inserts were carefully removed with forceps without detaching the cells. PBS was removed and wells were filled with 1mL MEF medium containing 1:1000 aphidicolin (Sigma-Aldrich) to prevent cell proliferation. Directly after removing the inserts (time point 0h), pictures were taken with a Nikon Eclipse Ti microscope. Cells were further incubated at 37°C and 5% CO_2 and pictures were taken until the gap visually closed. Regarding the siRNA transfected cells, inserts were removed 48h after transfection followed by the same procedure as described above. The analysis was done with TScratch software, resulting in the percentage of opened gap area.

Table 13: Cell numbers for migration assay

cell line	cells per chamber
A375	8000
A375 EV ADCK2	18700
A375 OE ADCK2	18700
MeWo	12500
MeWo EV ADCK2	37500
MeWo OE ADCK2	25000
SkMel28	16800
SkMel28 EV ADK2	25000
SkMel28 OE ADCK2	25000
SkMel30	18700
SkMel30 EV ADCK2	32800
SkMel30 OE ADCK2	32800

3.2.11 Invasion assay

The invasion capacity of SkMel28 cells was determined with a Transwell insert System (Cultrex Basement Membrane Extract Cell Invasion Assay, 24-well, R&D Systems) according to the manufacturer´s instructions. In brief, the top chambers were coated with 0.2x BME matrix one day prior to seeding and were incubated at 37°C and 5% CO_2 ON. The next day, excess medium was carefully removed and $2.75*10^5$ SkMel28 cells (48h after transfection with either siControl or siADCK2 or EV control or the ADCK2 expression construct, respectively) were seeded on top of the BME matrix per Transwell in FCS-free MEF medium. The bottom chamber was filled with complete MEF medium. FCS served as the chemoattractant for the cells. Then invasion assay chambers with cells were incubated for 96h including a medium change in the bottom well after 48h. Afterwards, cells in the top and the bottom chamber were washed and then cells in the bottom chamber were incubated with dissociation solution containing calcein-AM for 1h at 37°C and 5% CO_2. After incubation, top chambers were removed and the amount of invaded cells in the bottom well was measured using an excitation of 485nm and an emission of 520nm with TECAN Infinite F200 PRO. For each experiment performed, technical duplicates were used.

3.2.12 Immunofluorescence

To perform immunofluorescence staining, glass coverslips were activated by 1M hydrochloric acid treatment ON followed by treatment with 100% ethanol ON and were sterilized under UV light for about 45min. Then, coverslips were inserted into the wells of 12-well plates (1 coverslip fits to 1 Well) and SkMel28 cells were seeded on top of the coverslips in MEF medium and incubated at 37°C and 5% CO_2 ON. The next day, they were transfected with siControl or siADCK2 as described in 3.2.4 followed by an incubation at 37°C and 5% CO_2 for 48h. Afterwards, cells were scratched off several times with a 100µL pipette tip and medium was changed to MEF medium containing 1:1000 aphidicolin to induce a migratory phenotype. After about 12-14h, medium was removed, cells were washed with PBS and fixed with 4% paraformaldehyde for 15min (5min on ice, then RT). After a thorough wash with PBS, cells were permeabilized with 0.1% triton X100 in PBS for 10min at RT. Next, cells were blocked with 3% BSA in 0.3% triton X100 and PBS for at

least 1h at RT. Afterwards, cells were incubated with anti-MYL6 antibody (Invitrogen) in 1% BSA, 0.3% triton X100 and PBS at 4°C ON. The next day, cells were washed several times with PBS and then incubated with anti-rabbit Alexa Fluor 488 antibody in 1% BSA, 0.3% triton X100 and PBS for at least 1h at RT in the dark. After incubation 1:5000 DAPI and ActinRed 555 (2 drops per 1mL (Sigma-Aldrich)) were simultaneously added and cells were incubated for 20min at RT in the dark. Then cells were thoroughly washed with PBS and mounted with Fluoromount Aqueous Mounting Medium (Sigma Aldrich) on a microscope slide. After the mounting medium had dried, coverslips got sealed with transparent nailpolish and were stored at RT in the dark. Fluorescence images were taken with a Zeiss LSM 700 microscope at the DKFZ light microscopy core facility using the same settings for siControl and siADCK2 transfected cells.

3.2.13 Statistical analysis

For all experiments, except the gene expression analysis, the software GraphPad Prism was used for statistical analysis and figure preparation. The statistical analysis was always done from at least three independent biological replicates by using a paired t-test. All graphs show the mean with SEM. For the box and whisker plots whiskers were used as 5-95 percentile.

4 Results

4.1 High levels of ADCK2 in melanomas correlate with a better survival of melanoma patients

In order to get an idea if ADCK2 might play a role in melanoma, I initially determined the levels of ADCK2 in nine different melanoma cell lines and normal human melanocytes (NHM). The melanoma cell lines included wild type (MeWo), BRAF-mutated (WM266-4, A375, HT144, SkMel28, C32) and NRAS-mutated (SkMel30, SkMel103, SkMel173) ones. Regarding the different mutational statuses of these cell lines no differences in ADCK2 expression between them were observed. In general, all melanoma cell lines showed comparable or lower levels of ADCK2 mRNA compared to NHM (**Figure 8A**). Since a lower expression of ADCK2 was detected in some of the melanoma cell lines, I investigated if ADCK2 had a potential effect on the overall survival (OS) of melanoma patients. The cBioPortal database revealed for two distinct datasets that lower expression of ADCK2 was indeed connected with a lower OS of melanoma patients (**Figure 8B**).

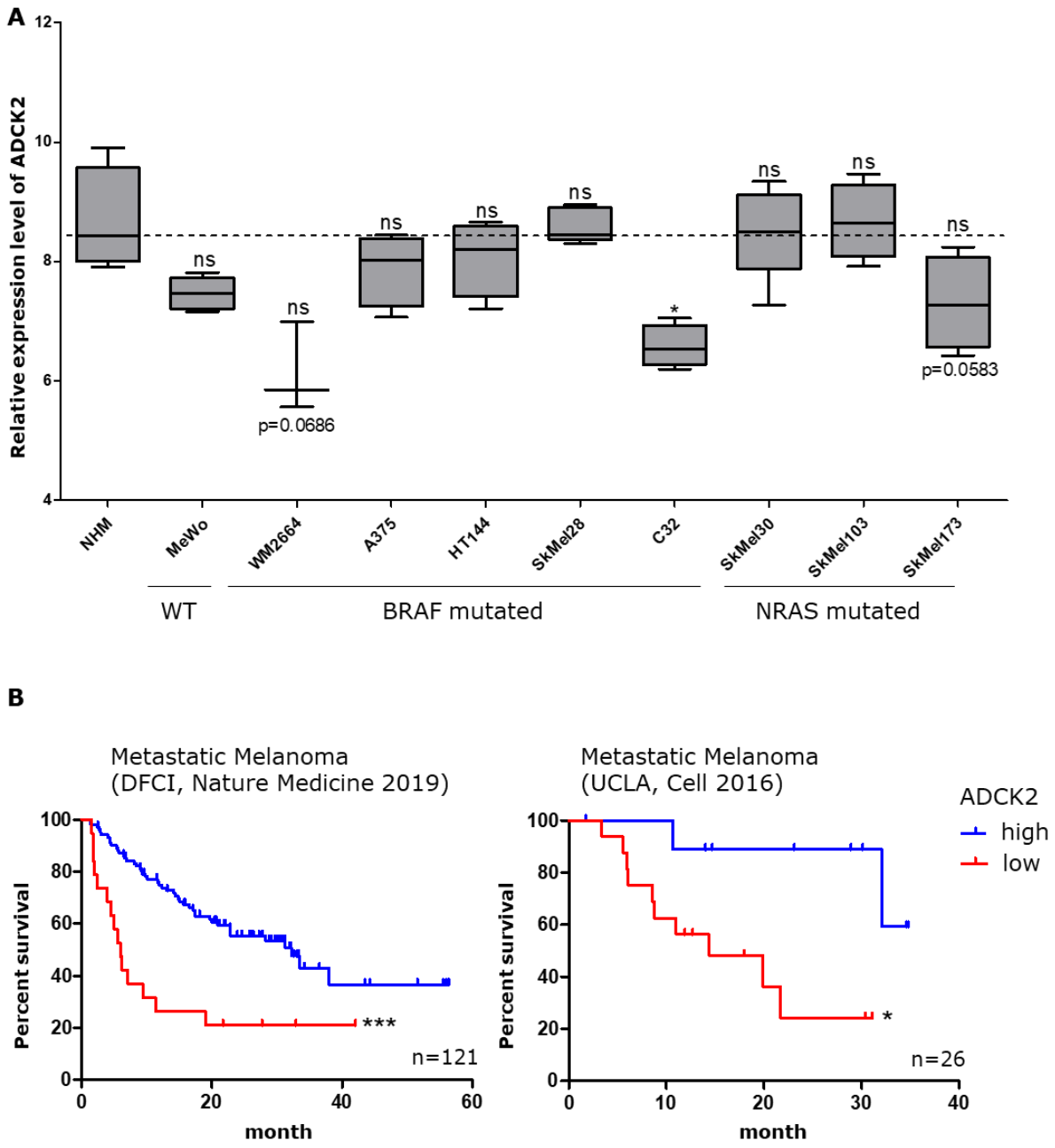

Figure 8: Higher ADCK2 levels in melanomas benefit the survival of melanoma patients
A: *Relative expression levels of ADCK2 in NHM and nine different melanoma cell lines, either WT, BRAF- or NRAS-mutated.* ***B:*** *Results from the cBioPortal database reveal for two distinct datasets a significant survival benefit for melanoma patients with tumors with higher ADCK2 levels. *p=≤0.05 **p=≤0.01 ***p=≤0.001 ns=not significant*

4.2 ADCK2 has a promoting effect on cell viability of melanoma cells

Knowing that high ADCK2 expression in melanomas positively correlated with the OS of patients, I next examined the influence of ADCK2 on cell viability of melanoma cells. For the following experiments four melanoma cell lines were used, one wild type (MeWo), two BRAF-mutated (SkMel28 and A375) and one NRAS-mutated (SkMel30). To investigate the

effect of ADCK2 on cell viability, an siRNA-mediated KD of ADCK2 as well as stable OE of ADCK2 in these cell lines was performed. The KD of ADCK2 with siRNA resulted in a reduction of ADCK2 by about 60-80% for MeWo cells, 50-60% for SkMel28 cells, 60-80% for A375 cells and 30-70% for SkMel30 cells on mRNA level at all four time points (**Figure 9A**). The KD of ADCK2 was also validated by Western blot (**Figure 9B**). To generate ADCK2-overexpressing cell lines, MeWo, SkMel28, A375 and SkMel30 cells were infected with a puromycin-selectable, lentiviral construct carrying the ADCK2 gene under the control of the constitutively active EF1α promoter or an empty vector control. After selection with puromycin, stable ADCK2-overexpressing cell lines were obtained. This ectopic OE led to an approximate 3-fold increase of ADCK2 mRNA in MeWo, SkMel28 and SkMel30 cells and a 5-fold increase in A375 cells compared to the empty vector control cells (**Figure 9C**). Additionally, the OE of ADCK2 was confirmed on protein level by Western blot (**Figure 9D**).

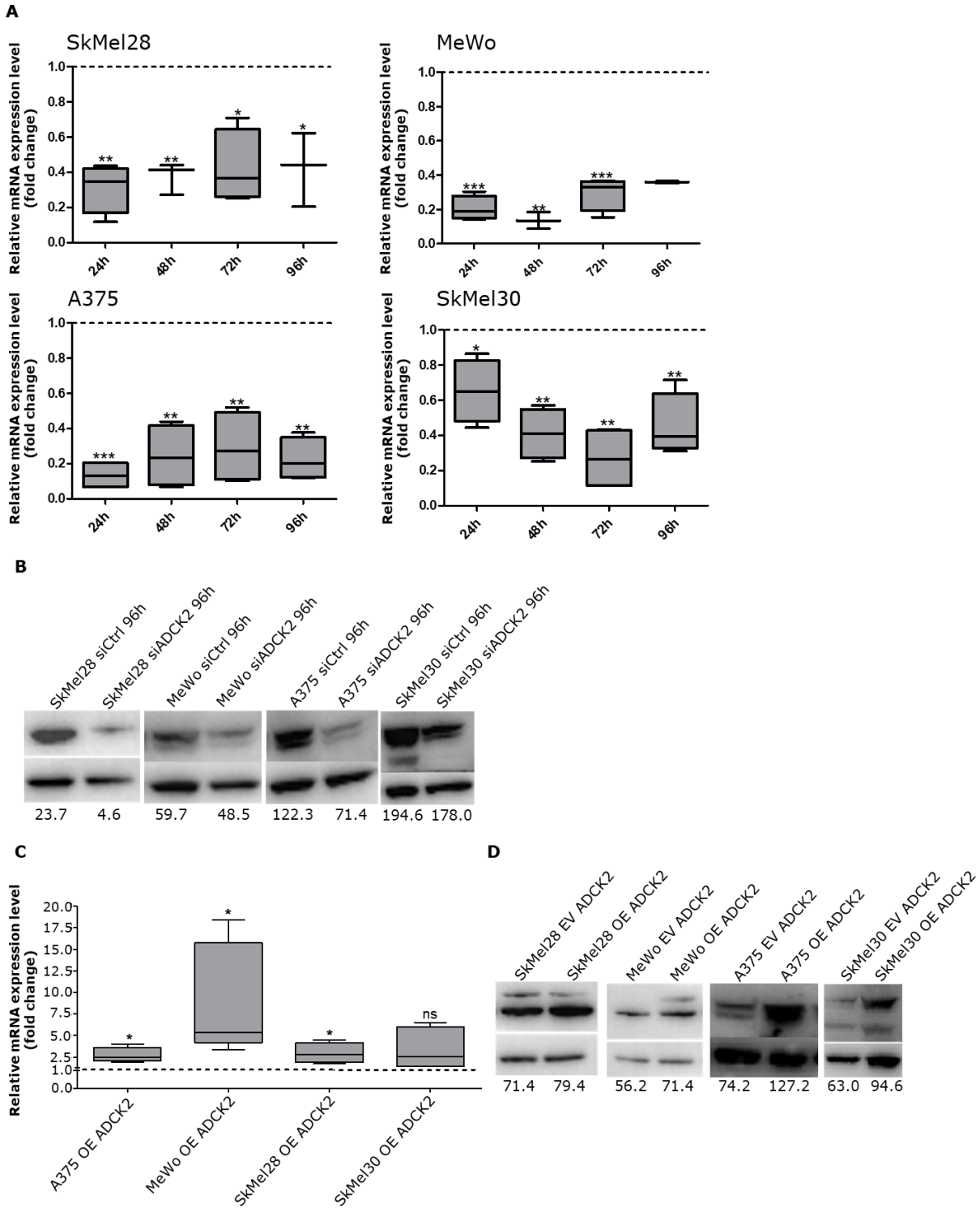

Figure 9: Validation of ADCK2 KD and OE
A: *After siRNA KD, the mRNA level of ADCK2 was reduced in all four cell lines by at least 20% at all time points.* ***B:*** *Representative images of Western blots upon ADCK2 KD. upper band: ADCK2, lower band: loading control GAPDH. Numbers indicate the normalized expression value of ADCK2.* ***C:*** *ADCK2 was overexpressed in all four cell lines by at least 2.5-fold compared to the empty vector control.* ***D:*** *Representative images of Western blots from ADCK2 OE cell lines. Upper band: ADCK2, lower band: loading control GAPDH. Numbers indicate the normalized expression value of ADCK2. n≥4 *p=≤0.05 **p=≤0.01 ***p=≤0.001 ns=not significant*

To investigate the effect of ADCK2 on cell viability the cells were seeded and for the KD approach transfected with either siControl or siADCK2. Then, the cell viability of melanoma cells was measured after 24, 48, 72 and 96h with AlamarBlue assay. Interestingly, the cell viability was reduced upon ADCK2 KD in all cell lines at all time points, except after 24h in A375 cells (**Figure 10A**). ADCK2 OE had the opposite effect in MeWo, SkMel28 and A375 cells and after 24h in SkMel30 cells, even though this effect was less pronounced as the effect upon KD of ADCK2 (**Figure 10B**). Nevertheless, these results confirmed that ADCK2 was beneficial for the cell viability of melanoma cells.

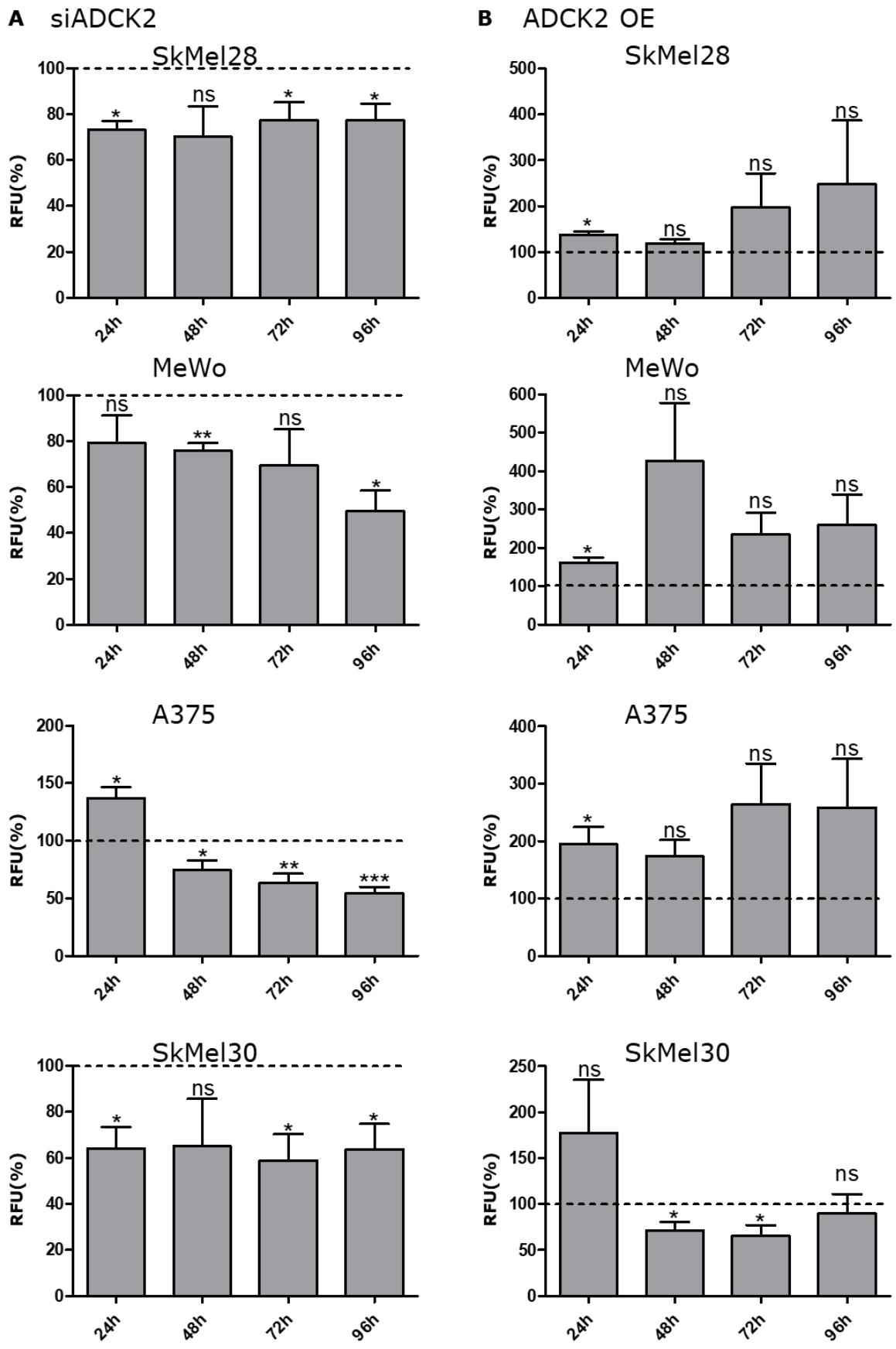

Figure 10: ADCK2 is beneficial for cell viability
A: *KD of ADCK2 led to a reduced cell viability of all cell lines latest after 48h.* ***B:*** *OE of ADCK2 led to a slightly increased cell viability of SkMel28, MeWo and A375 cells. n=6 *p=≤0.05 **p=≤0.01 ***p=≤0.001 ns=not significant*

4.3 ADCK2 suppresses migration and invasion of melanoma cells

A high migration and invasion capacity of melanoma cells is a prerequisite for their ability to metastasize, which in turn correlates with a worse outcome. As low levels of ADCK2 correlated with a worse outcome, I hence investigated the effect of ADCK2 on the migration and invasion capacity of melanoma cells. To study the migration of melanoma cells a wound healing assay with inserts was performed. For the siRNA-mediated ADCK2 KD, cells were seeded and transfected with either siControl or siADCK2. 48h later the inserts were removed and medium changed to medium with aphidicolin to stop cell proliferation. Then cell migration was quantified by measuring the area of the gap that had not been covered by cells. This quantification revealed a strikingly higher migration capacity of SkMel28 cells after 22h and 26h, of A375 cells after 11h and of SkMel30 cells after 24h. The same trend was also seen for MeWo cells after 16 and 24h (**Figure 11**, left side). Further, a wound healing assay was also done with ADCK2-overexpressing cell lines. As expected, the migration capacity was reduced, which could be seen after 11h for SkMel28 OE ADCK2 cells and as a trend after 16h for MeWo OE ADCK2 cells (**Figure 11**, right side).

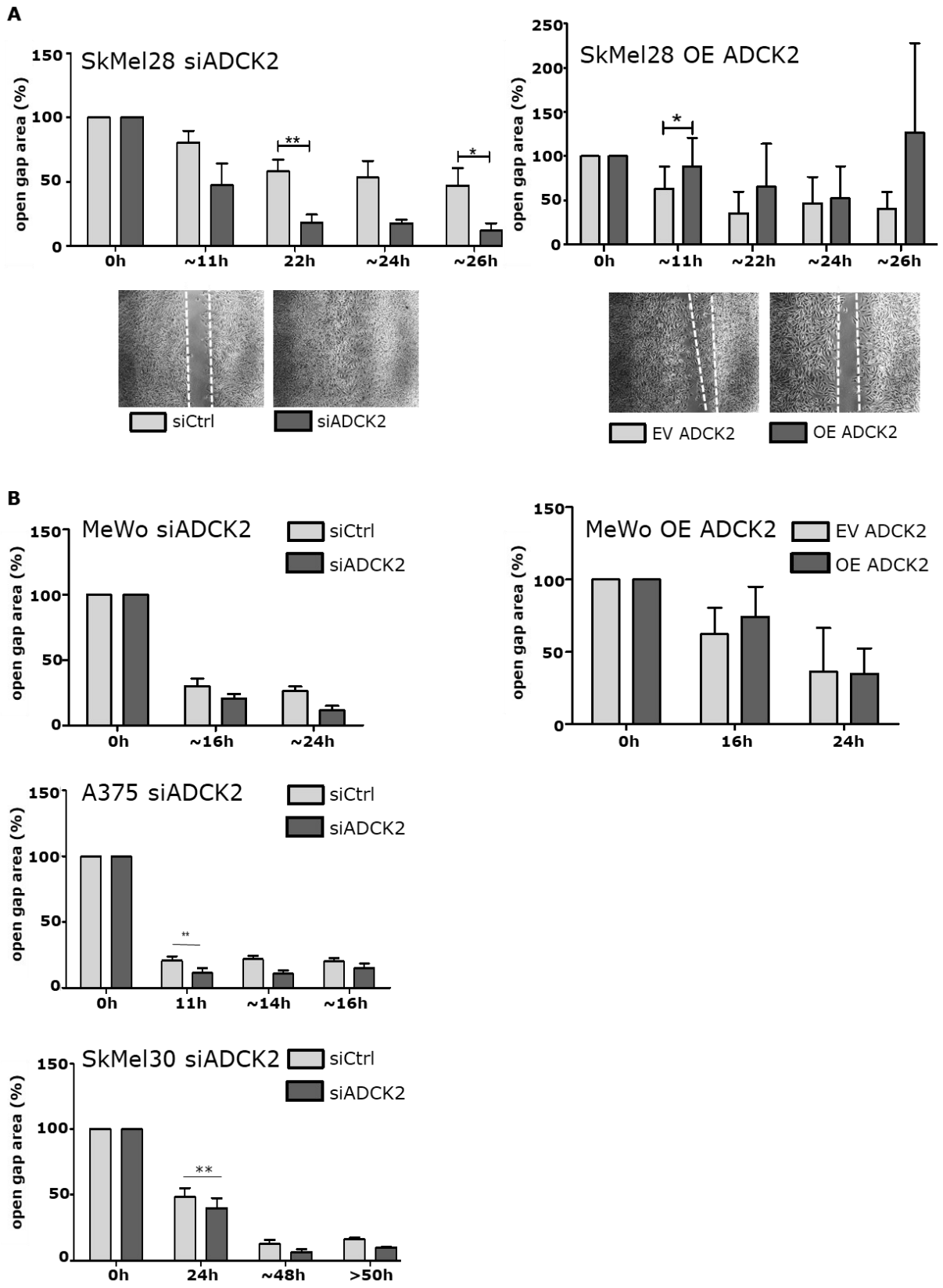

Figure 11: ADCK2 negatively affects the migration of melanoma cells
A: *A KD of ADCK2 led to an increased migration and an OE of ADCK2 led to a reduced migration of SkMel28 cells. Additionally, representative pictures of the migration assay with SkMel28 cells upon ADCK2 KD and OE, respectively, are shown.* ***B:*** *A similar trend in migrative behavior could be observed for MeWo cells. A375 and SkMel30 melanoma cells also show a significantly reduced migration upon KD with ADCK2. All bars show the percentage of the open gap. n≥4 *p=≤0.05 **p=≤0.01 ***p=≤0.001*

To further confirm the altered cell motility of ADCK2 KD and OE cells, I performed an invasion assay with SkMel28 cells. For this, a BME-coated transwell assay was used. To initiate invasion of the cells, they were seeded in serum-free medium and complete medium was used as a chemoattractant in the bottom well. A KD of ADCK2 led to a significantly enhanced invasion compared to control cells (**Figure 12A**). This effect was reversed with SkMel28 OE ADCK2 cells (**Figure 12B**).

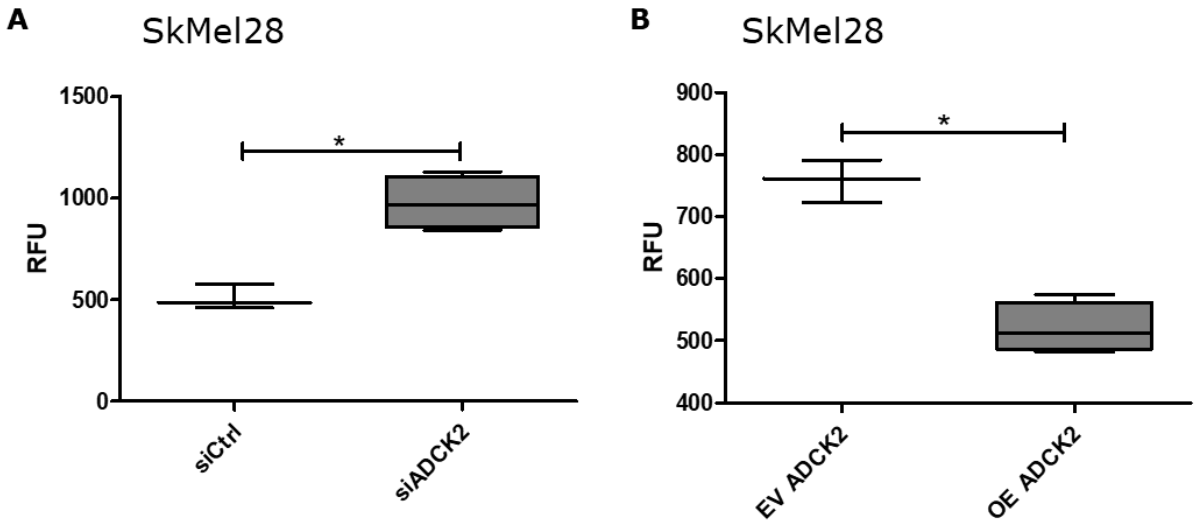

Figure 12: ADCK2 impairs the invasion of melanoma cells
A: *SkMel28 cells transfected with siADCK2 showed a significantly higher invasion rate compared to siControl transfected cells.* ***B:*** *SkMel28 OE ADCK2 cells showed a significantly lower invasion rate compared to the empty vector control n=5 *p=≤0.05*

These results show that higher levels of ADCK2 impaired the cell motility of melanoma cells suggesting that ADCK2 might function as a tumor-suppressor.

4.4 The differentiation status of melanoma cells is influenced by ADCK2

Having shown that ADCK2 had an effect on cell motility, I wanted to examine if this also went along with a phenotype switch. For this reason, I analyzed the expression of several melanocytic and NC markers and could demonstrate a decreased expression of the melanocyte markers MITF, TRP1 and TYR upon ADCK2 KD in MeWo, SkMel28 and to a lesser extent in SkMel30 cells. In A375 cells, only TRP1 expression was reduced. The reduction of melanocyte marker expression was significant 96h upon ADCK2 KD. In MeWo and SkMel30 cells this downregulation was significant for TYR 96h, for TRP1 in A375 and SkMel28 cells 72 and 96h upon ADCK2 KD (**Figure 13A**, left side). At the same time, my results revealed a tendency for a higher expression of Pax3 48, 72 and 96h upon ADCK2 KD, which however was not significant. In addition, the NCC marker p75 showed increased expression 48, 72 and 96h upon ADCK2 KD. This negative correlation was significant in SkMel28 cells 96h, in MeWo cells 48h and in SkMel30 cells at all time points upon ADCK2 KD (**Figure 13A**, right side). Furthermore, pellets of the pigmented cell line SkMel30 were

brighter upon ADCK2 KD compared to the control and darker upon ADCK2 OE (**Figure 13B**), which is in line with the previous findings.

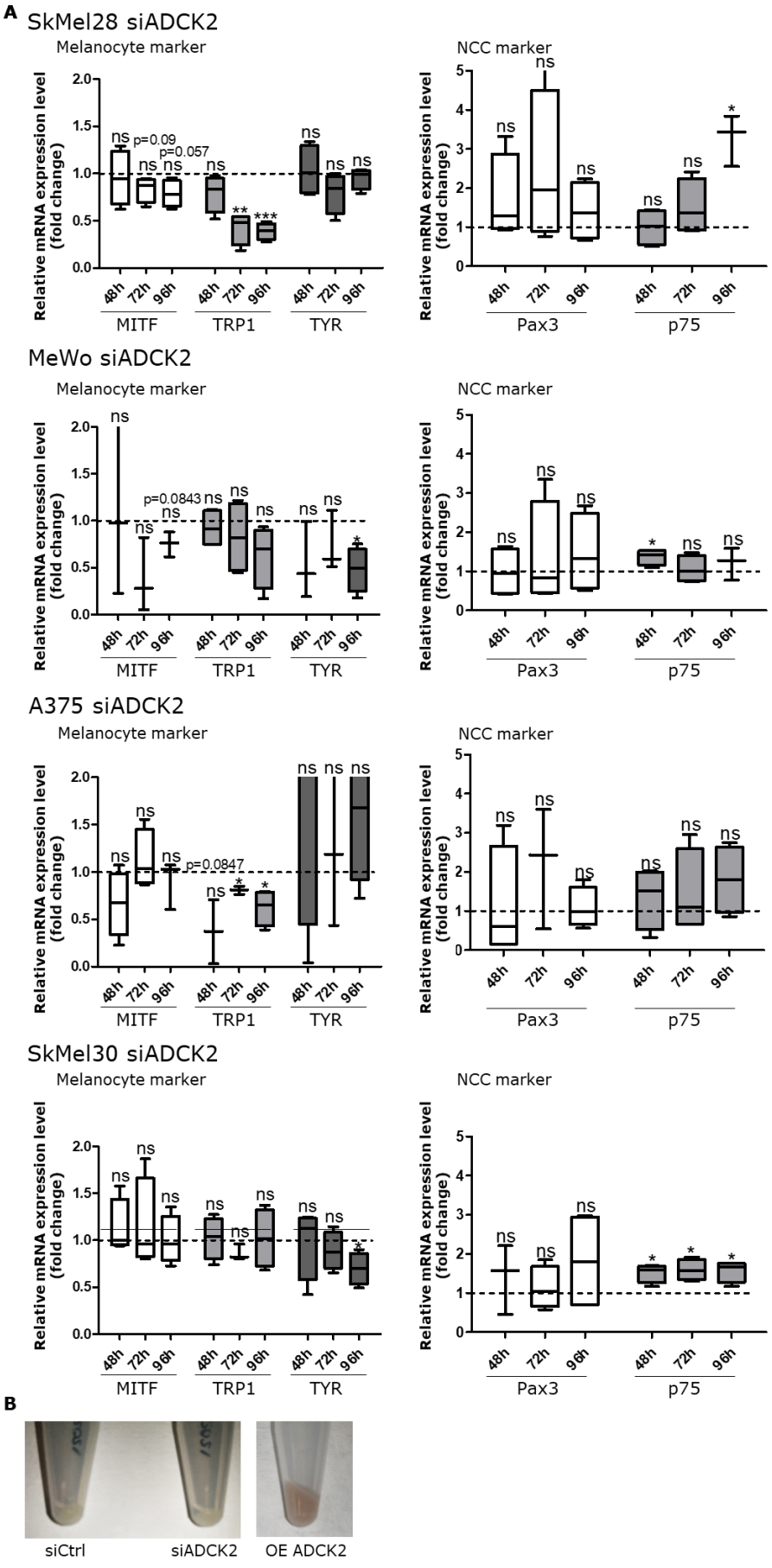

Figure 13: ADCK2 influences the differentiation status of melanoma cells
Figure legend continues on next page

A: *KD of ADCK2 led to a reduced expression of the melanocyte markers MITF, TRP1 and TYR. At the same time, the expression of the NCC markers Pax3 and p75 was slightly enhanced in all melanoma cell lines upon ADCK2 KD.* ***B:*** *The cell pellets of the pigmented melanoma cell line SkMel30 were brighter after ADCK2 KD and darker after ADCK2 OE. n=4 *p=≤0.05 **p=≤0.01 ***p=≤0.001 ns=not significant*

Further, I took a look at the expression of the transcription factors Sox5 and FoxD3, which are known to influence the differentiation of NCCs. Interestingly, the R2 database revealed a positive correlation between ADCK2 and the transcription factor Sox5 (**Figure 14A**), which was also seen in SkMel28 and SkMel30 siADCK2 samples compared to siControl samples at all four time points. MeWo and A375 siADCK2 cells show the same trend. FoxD3 is an early NC specifier gene, with lowered expression in melanoblasts. Upon ADCK2 KD reduced levels of FoxD3 could be seen in all cell lines (**Figure 14B**).

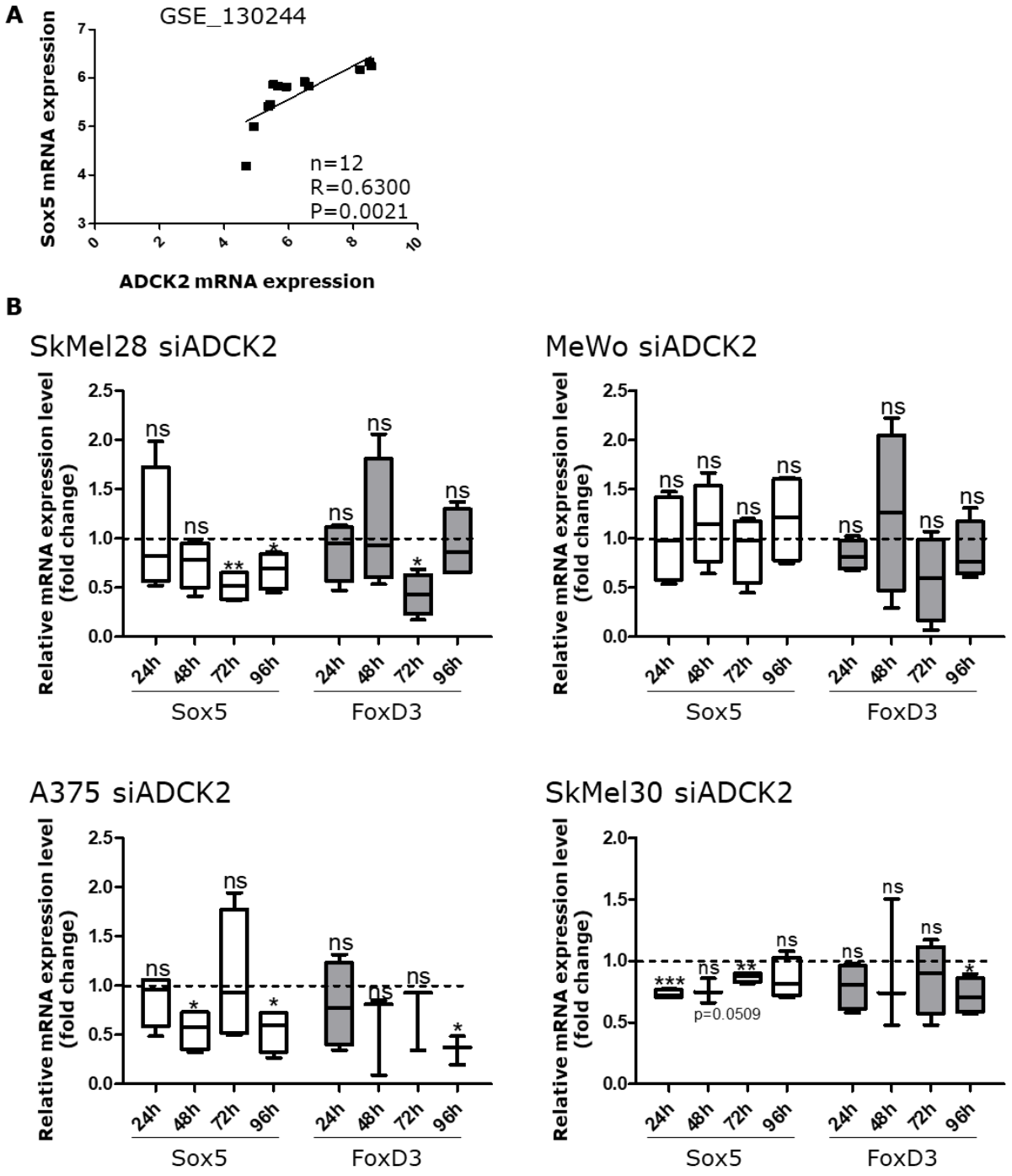

Figure 14: ADCK2 expression positively correlates with the expression of the transcription factors Sox5 and FoxD3
A: *Data from the R2 database reveal a positive correlation between ADCK2 and Sox5 expression.* ***B:*** *A KD of ADCK2 resulted in decreased levels of Sox5 and FoxD3 in all melanoma cells at all time points, especially in BRAF (SkMel28, A375) and NRAS-mutated cell lines (SkMel30). n=4 *p=≤0.05 **p=≤0.01 ***p=≤0.001 ns=not significant*

Taking these findings together, one can conclude that ADCK2 affects the differentiation status of melanoma cells because its KD pushed them to a more dedifferentiated stage.

4.5 MYL6 and RAB2A are directly affected by ADCK2

The results presented so far suggest that ADCK2 might control the phenotype switch of melanoma cells and that it regulates their motility. In order to determine the molecular mechanisms behind these processes, I wanted to identify direct up- and downstream effectors of ADCK2. For this reason, I performed a gene expression array with ADCK2 KD samples and control counterparts of three melanoma cell lines (MeWo, SkMel30 and C32). The analysis was done by Thomas Hielscher and revealed four common genes that were significantly downregulated 24h upon ADCK2 KD (**Figure 15A**). These four genes were ADCK2, RAB2A, MYL6 and ZNF275. This analysis confirmed the successful KD of ADCK2. ZNF275 is an unknown zinc finger protein, whose function has not been determined yet. RAB2A is a known oncogene which belongs to the small GTPases involved in cell trafficking. It has been studied in some cancers but not yet in melanoma. MYL6 was the most promising gene revealed by the gene expression analysis as it plays a role in cell motility. As described in paragraph 1.6, MYL6 is an essential light chain (ELC), which together with myosin heavy (MYH) and regulatory light chains (RLC) assembles to non-muscle myosin 2 (NM2). Further, a heat map of genes involved in cell migration clearly shows different gene expression patterns for cells treated with siADCK2 (light blue) or siControl (light red). These patterns are comparable in two cell lines (left: MeWo, right: SkMel30) (**Figure 15B**) and could explain the altered migration behavior of melanoma cells upon ADCK2 KD.

A

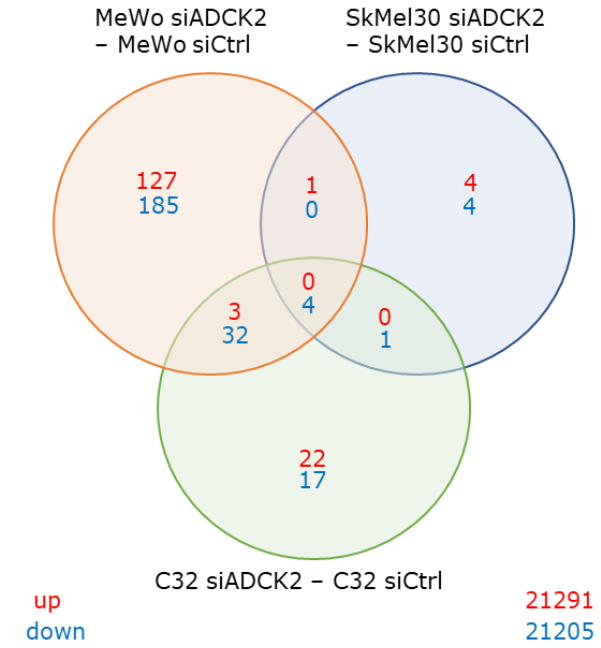

SYMBOL	GENE NAME
ADCK2	aarF domain containing kinase 2
RAB2A	RAB2A, member RAS oncogene family
ZNF275	zinc finger protein 275
MYL6	myosin light chain 6

B

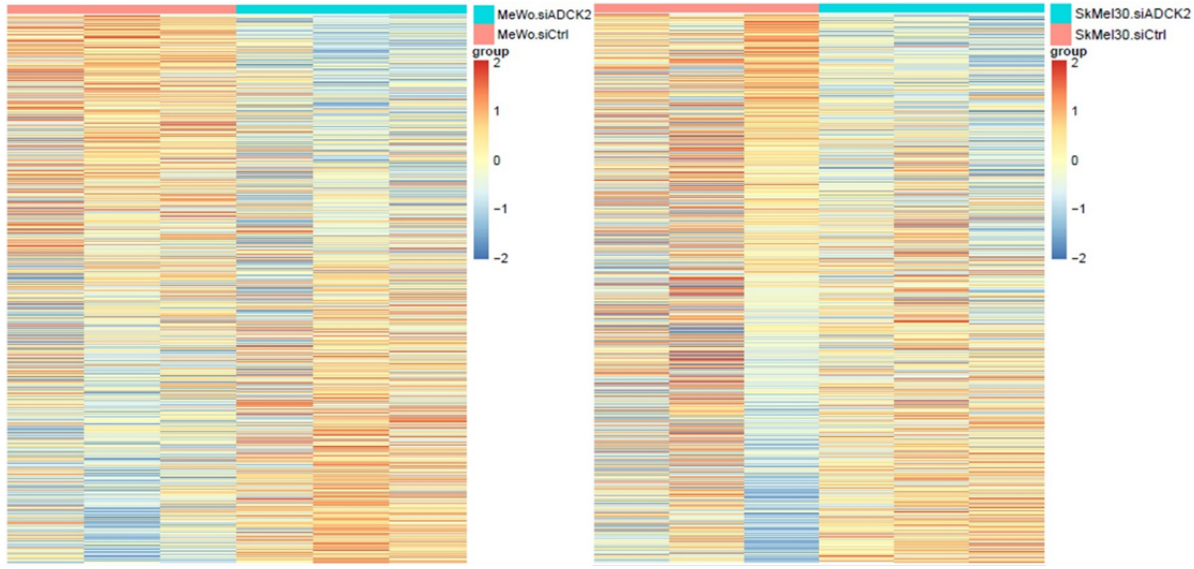

Figure 15: A gene expression array revealed four common downregulated genes upon ADCK2 KD in three melanoma cell lines
A: *Venn diagram of three cell lines, 24h upon transfection with siControl and siADCK2, respectively. Significantly upregulated genes are marked in red and significantly downregulated genes in blue. The four common downregulated genes (table on the right) are ADCK2, RAB2A, ZNF275 and MYL6.* ***B:*** *Heat map of gene expression of genes involved in cell migration upon transfection with siControl (light pink bar on top) and siADCK2 (light blue bar on top). MeWo (left side) and SkMel30 (right side) cells.*

To confirm the results of the gene expression array, the mRNA levels of MYL6 and RAB2A were quantified in siADCK2 KD cells. The expression of MYL6 was significantly lower in ADCK2 KD cells 24 and 48h after transfection with siRNA in all cell lines and also 72 and 96h after transfection in SkMel28 and SkMel30 cells. RAB2A was also found to be less expressed in ADCK2 KD cells, even though this reduction was not as strong and only significant for a few time points (**Figure 16A**). In the following, I focused on MYL6 and

assessed data from the R2 as well as the cBioPortal databases. The R2 database revealed a positive correlation between ADCK2 and MYL6 in two distinct sample sets of melanoma patients (**Figure 16B**). Moreover, in both databases a positive correlation between MYL6 and OS of melanoma patients was found (**Figure 16C**).

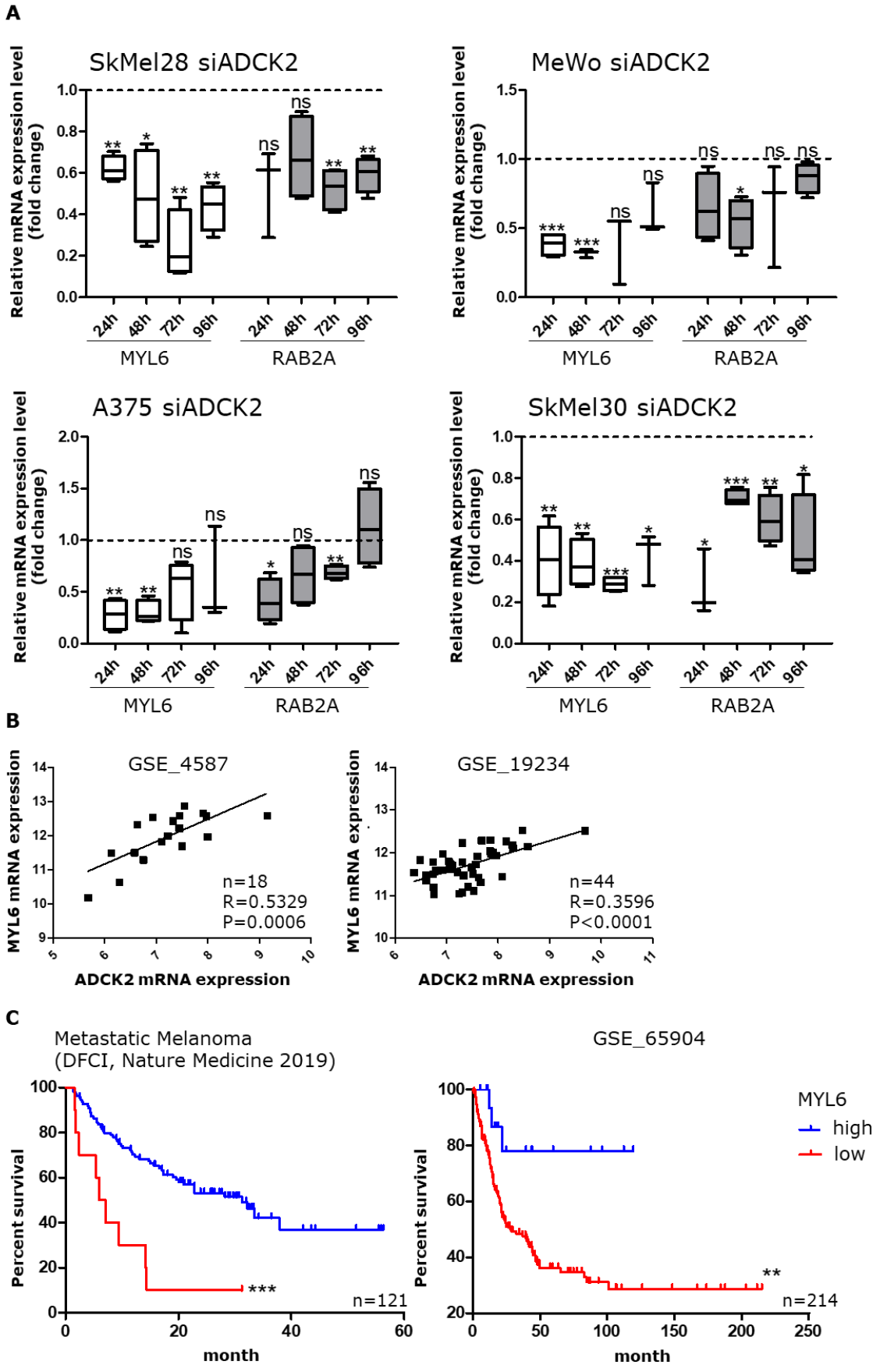

Figure 16: ADCK2 and MYL6 expression positively correlate and melanoma patients with tumors with higher levels of MYL6 show a better OS

Figure legend continues on next page

A: *Validation of MYL6 and RAB2A downregulation upon ADCK2 KD via qPCR. A lower expression of MYL6 can be seen upon ADCK2 KD in all melanoma cell lines at all time points.* ***B:*** *Analysis of data from the R2 database revealed a positive correlation between ADCK2 and MYL6 for two distinct melanoma datasets.* ***C:*** *Two distinct datasets from the R2 and cBioPortal database reveal that a higher level of MYL6 in melanoma tumors goes along with a better survival of melanoma patients. n=4 *p=≤0.05 **p=≤0.01 ***p=≤0.001 ns=not significant*

These results clearly indicate that MYL6 could be a downstream effector of ADCK2.

4.6 KD of MYL6 abrogates the effect of ADCK2 OE on melanoma cell viability and migration

To confirm that MYL6 is indeed a downstream effector of ADCK2 I performed several rescue experiments combining ADCK2 OE and MYL6 KD. First, the successful KD of MYL6 in ADCK2 OE cell lines was confirmed on RNA level for MeWo, SkMel28, A375 and SkMel30 cells. In MeWo OE ADCK2 cells the mRNA level of MYL6 was reduced by about 90% upon siRNA-mediated MYL6 KD, by 80-90% for SkMel28 OE ADCK2 and A375 OE ADCK2 cells and by 60-80% in SkMel30 OE ADCK2 cells 24, 48, 72 and 96h upon the KD (**Figure 17A**). Interestingly, the pellets of the pigmented cell line SkMel30 were brighter 96h upon knocking down MYL6 (**Figure 17B**). Next, I assessed the cell viability of OE ADCK2 melanoma cells and found that it was reduced after siMYL6 KD compared to an siControl treatment in all cell lines, even though not always significantly (**Figure 17C**). As MYL6 is known to have an effect on cell motility I performed a wound healing assay. For this purpose, SkMel28 OE ADCK2 and MeWo OE ADCK2 cells were transfected with siMYL6 or siControl, respectively. After 48h the inserts were removed and medium supplemented with aphidicolin was added to stop cell proliferation. For both cell lines a significantly increased migration rate upon MYL6 KD could be detected, most strikingly in SkMel28 OE ADCK2 cells 10 and 26h after transfection (**Figure 18**).

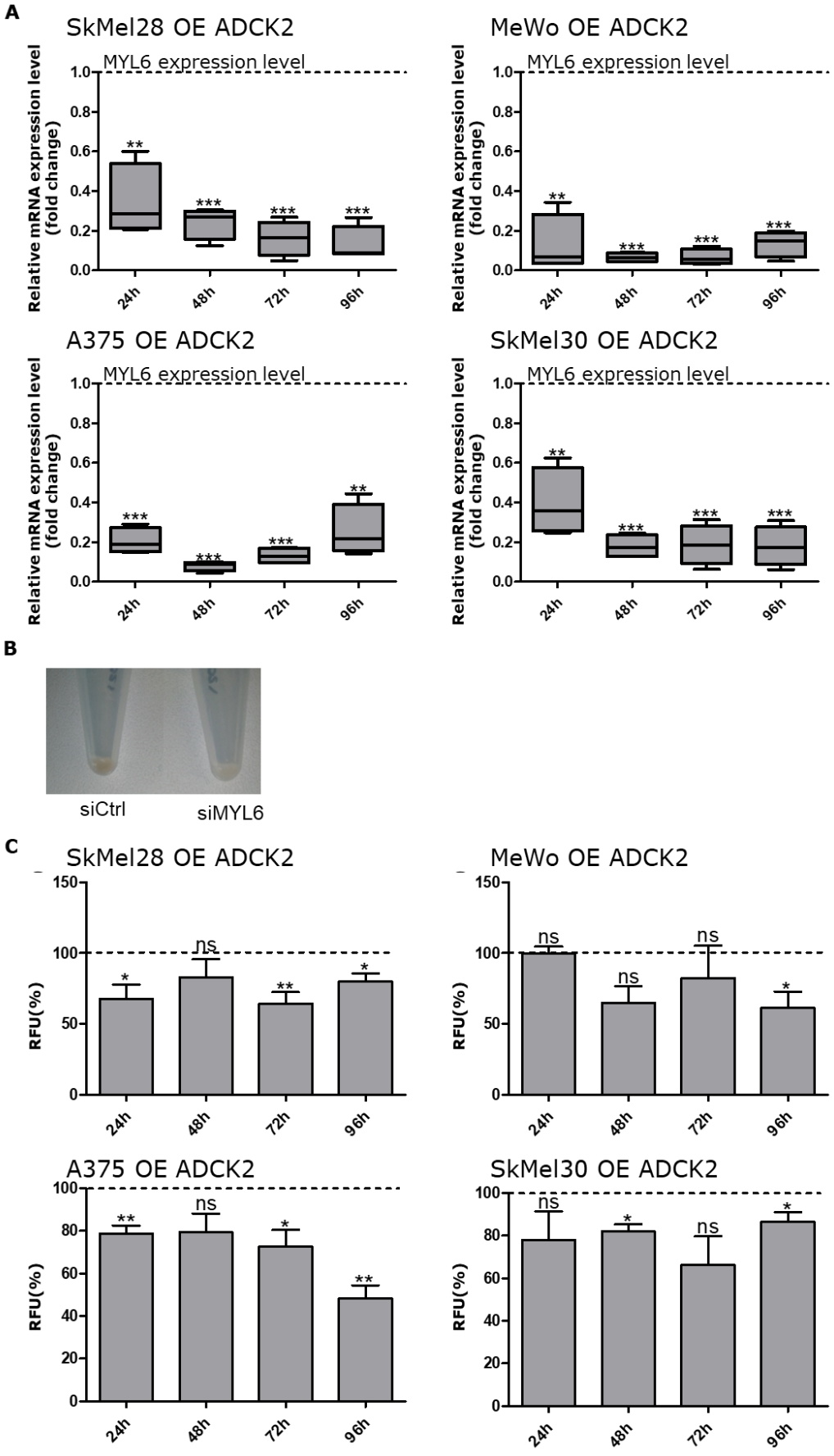

Figure 17: MYL6 KD abrogates the effect of ADCK2 OE on the cell viability of melanoma cells

Figure legend continues on next page

A: *Validation of MYL6 KD in ADCK2 OE melanoma cell lines. MYL6 expression was significantly reduced for at least 50% in all melanoma cell lines at all time points. n=4* ***B:*** *The pellet of the slightly pigmented cell line SkMel30 was brighter after MYL6 KD.* ***C:*** *The cell viability was slightly decreased in OE ADCK2 melanoma cell lines upon KD of MYL6. n=6 *p=≤0.05 **p=≤0.01 ***p=≤0.001 ns=not significant*

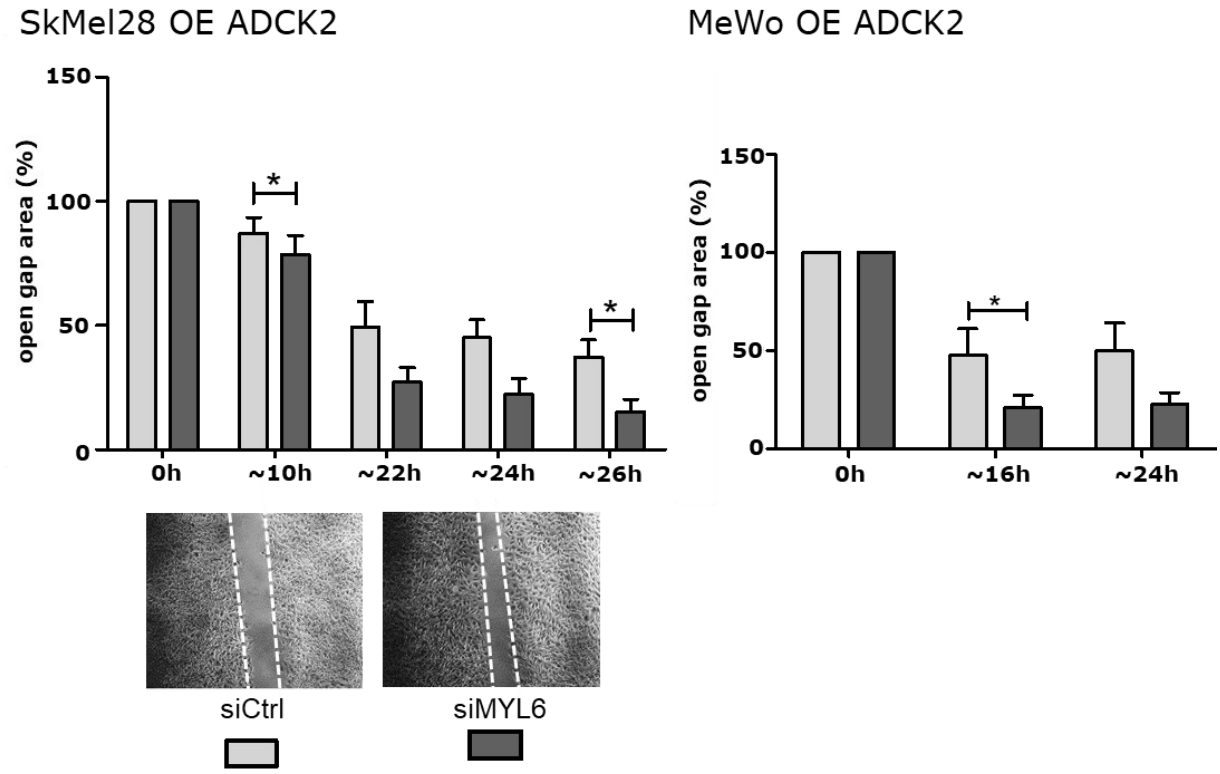

Figure 18: KD of MYL6 reverts the effect of ADCK2 OE on the migration capacity of melanoma cells
*SkMel28 OE ADCK2 and MeWo OE ADCK2 cells migrated faster upon MYL6 KD compared to siControl-treated cells. Bars present the percentage of open gap area. Representative pictures of SkMel28 OE ADCK2 cells treated with siControl or siMYL6 in the migration assay. n≥4 *p=≤0.05*

These experiments confirmed that MYL6 acted as a downstream effector of ADCK2 since the KD of MYL6 abrogated the effect of ADCK2 OE on melanoma cells.

4.7 ADCK2 alters the cell skeleton

As already mentioned earlier, I found that ADCK2 influenced cell viability and the differentiation status of melanoma cells. Additionally, I could demonstrate that ADCK2 also affected the cell motility of melanoma cells via MYL6. As described in paragraphs 1.6 and 4.5, MYL6 is a part of NM2, which binds to actin filaments to exert mechanical movement upon hydrolyzing ATP. Without myosins, actin filaments tend to disassemble. To investigate if ADCK2 also influences actin filaments an immunofluorescence staining of actin was performed. For this SkMel28 cells were seeded on glass cover slides and transfected with siADCK2 or siControl, respectively. After 48h, some cells were scratched off with a pipette tip and medium containing aphidicolin was added to stop proliferation. The next day cells were fixed and stained. I noticed that SkMel28 cells treated with siADCK2

showed less MYL6, which confirmed the successful downregulation of MYL6 on protein level. Interestingly, in both setups MYL6 was mostly localized in or close to the nucleus. The actin staining revealed a difference in the subcellular distribution between siADCK2- and siControl-treated cells. While the cells treated with siControl showed a strong actin staining along the cell membrane but also partly within the cytoplasm, the actin in siADCK2-treated cells was exclusively located and concentrated beneath the cell membrane. Moreover, the melanoma cells changed their shape from round or rectangular to more elongated and spindle-shaped (**Figure 19**).

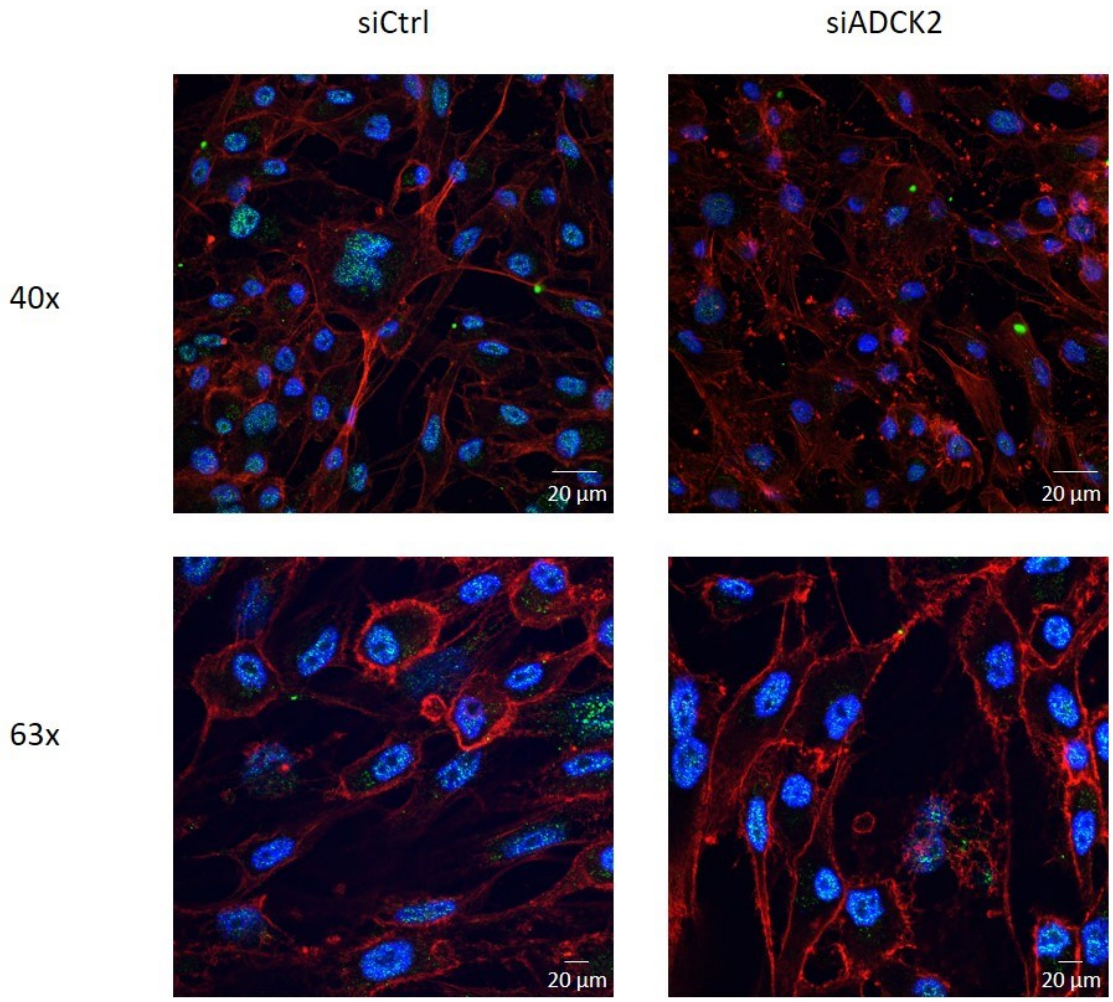

Figure 19: ADCK2 KD alters the distribution of actin filaments
Representative immunofluorescence pictures of SkMe28 cells treated with siControl or siADCK2, respectively, 48h upon transfection and cultured ON in proliferation-inhibiting medium. The MYL6 expression was clearly reduced upon ADCK2 KD. Furthermore, the cells adopted an elongated, spindle-shaped morphology and showed an altered subcellular distribution of actin upon KD with ADCK2. Green: MYL6, red: Actin, blue: DAPI

This result confirmed the reduction of MYL6 expression and an altered distribution of actin upon ADCK2 KD.

4.8 Successful reprogramming of fibroblasts to hiPSCs

The results presented so far have shown that ADCK2 was involved in controlling cell viability, motility and morphology of melanoma cells. Interestingly, alteration of the viability and motility upon KD of ADCK2 went along with a phenotype switch to a more dedifferentiated phenotype characterized by the expression of NC-specific markers. For this reason, I wanted to examine if ADCK2 might also affect the differentiation of hiPSCs to NCCs. To answer this question, I first generated hiPSCs by reprogramming patient fibroblasts with the Sendai2.0 Kit. During this process, I also established a simple method of reprogramming and cultivating hiPSCs long term in a feeder-free environment, which yielded a pure human induced pluripotent stem cell line (hiPSCL). The successful reprogramming process is depicted in **Figure 20A**. In order to have a second hiPSC line for my experiments, I subcloned an already established hiPSCL (**Figure 20B**). To confirm the pluripotency of both hiPSCLs several tests were done. The cell lines were checked on a regular basis with an AP staining kit showing strong activity of alkaline phosphatase, which is a good indicator for pluripotency. Moreover, the expression of stem cell markers was verified. I also performed a teratoma assay, where hiPSCs are injected subcutaneously into immunodeficient mice. Upon injection the hiPSCs grew to teratomas, which are tumors containing cells from all three germ layers. The formation of a teratoma is the most stringent hallmark of pluripotency, confirming that the hiPSCL I used for my experiments were indeed pluripotent. In **Figure 20C** a positive AP staining for both hiPSCLs can be seen, indicated by the purple color. Furthermore, both hiPSCLs expressed significant amounts of the stem cell markers Nanog, Oct4 and Sox2 as opposed to the original fibroblasts (**Figure 20D**). The teratoma assay with hiPSCL1 revealed a tumor with structures from all three germ layers, ectodermal keratin pearls, cartilage and muscle from the mesoderm and endodermal gut-like epithelium and glandular structures (**Figure 20E**). With these experiments, I confirmed that both hiPSCLs were pluripotent and could be used for further experiments.

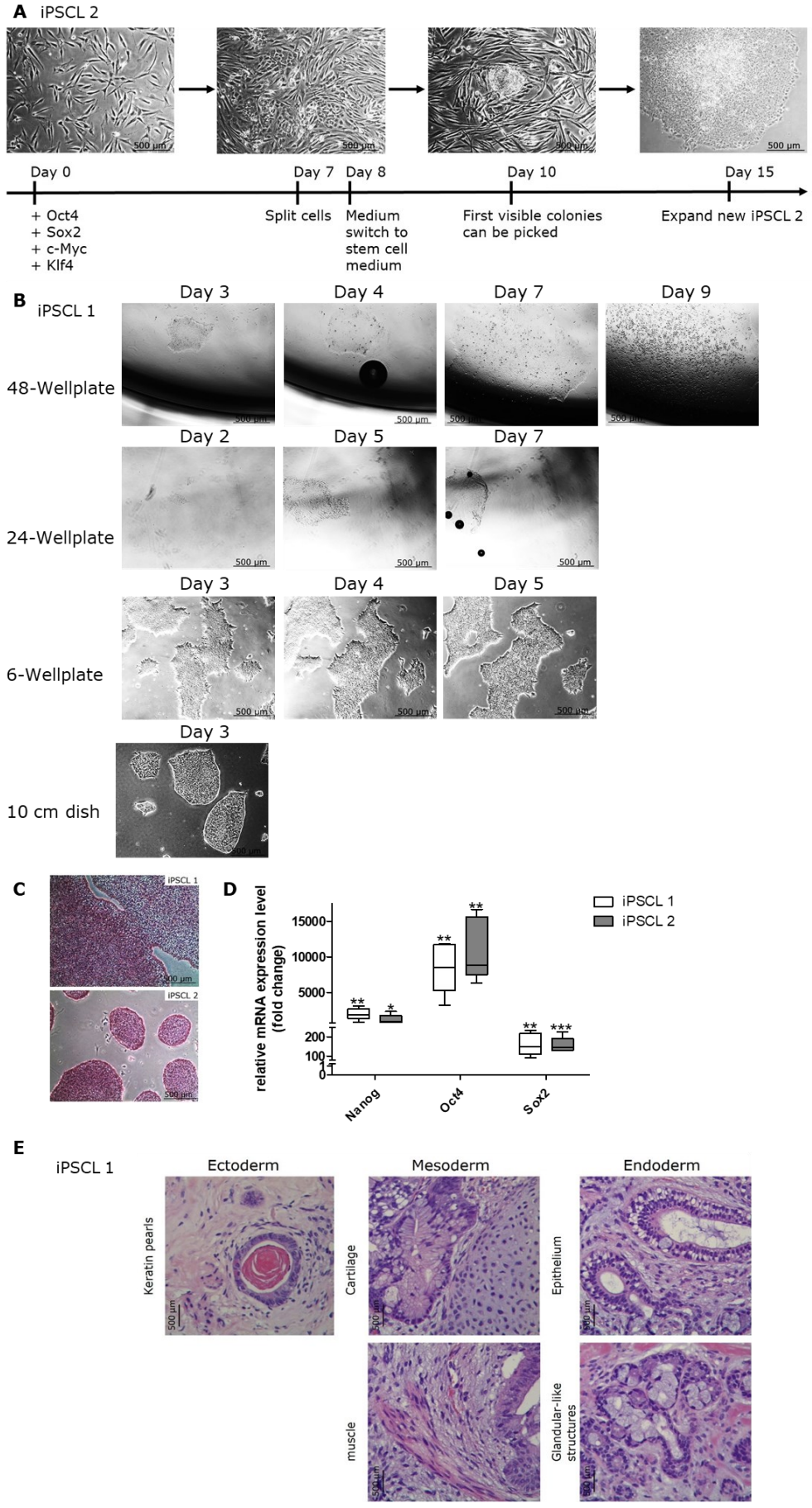

Figure 20: Successful reprogramming of fibroblasts to hiPSCs
Figure legend continues on next page

A: *Schematic overview of the reprogramming process with representative images.* ***B:*** *Display of the subcloning process of hiPSL1 with representative images.* ***C-E:*** *Pluripotency validation of hiPSCs.* ***C:*** *Positive AP staining for hiPSCL1 and hiPSCL2.* ***D:*** *The stem cell markers Nanog, Oct4 and Sox2 were expressed at significant levels in both hiPSCLs in contrast to the original fibroblasts (normalized to 1).* ***E:*** *Representative images of structures from all three germ layers derived from a teratoma formed by hiPSCL1. n=5 *p=≤0.05 **p=≤0.01 ***p=≤0.001*

4.9 Differentiation of hiPSCs to NCCs

To investigate if ADCK2 (and other kinases) affects the differentiation of hiPSCs to NCCs two different established protocols from former group members (thesis from Dr. Kasia Weina, 2015 [76], Larribere *et al*., 2015 [77]) and the protocol developed by Nissan and colleagues [46] were applied. All these protocols involve the use of feeder cells. When differentiating hiPSCs into NCCs following these protocols with using Matrigel instead of feeder cells, many cells died (**Figure 21**, top). Further, the surviving cells did not express NCC-markers. Thereafter, I tried a protocol from Dr. Katrin Schrenk-Siemens [78], which includes the formation of embryonic bodies (EBs) from the hiPSCs. When these EBs settle down eventually, NCCs are supposed to grow out from these EBs. When I applied this protocol nice EBs evolved and a small number of them also settled down, but unfortunately no NCCs grew out (**Figure 21**, bottom).

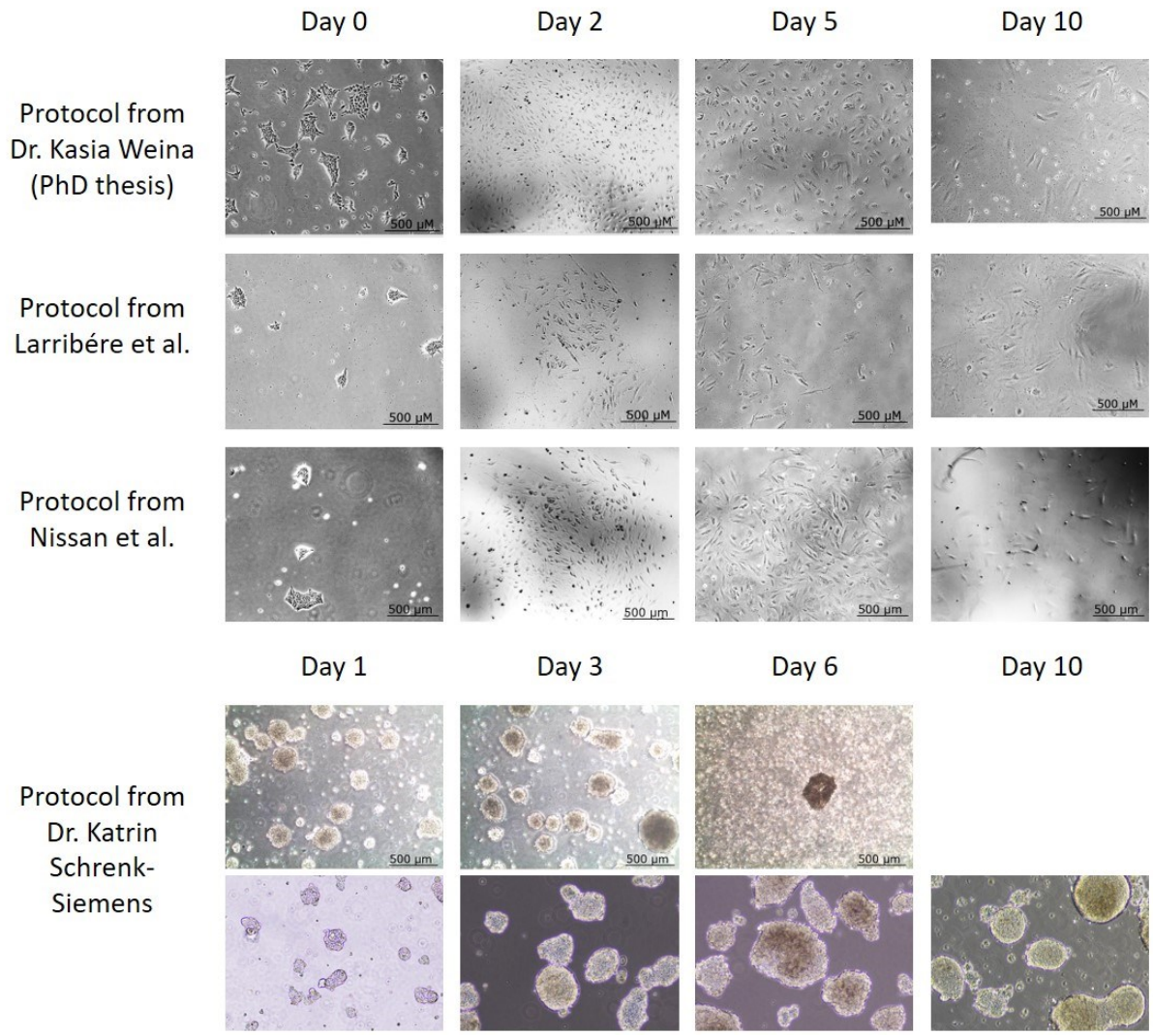

Figure 21: Differentiation of hiPSCs into NCCs
Representative images of the differentiation of hiPSCs into NCCs with the three protocols of Dr. Kasia Weina, 2015, Larribére et al, 2015 and Nisan et al., 2011 as well as the EB formation after a protocol from Dr. Katrin Schrenk-Siemens.

To finally achieve a successful differentiation of hiPSCs to NCCs the protocol from Callahan *et al*., 2016 [79] was used with slight modifications. An outline of the differentiation process can be seen in **Figure 22A**. The hiPSCs were seeded on Matrigel with half of the cell number from the original protocol. These cells then grew to a confluent monolayer of intermediate cells further differentiating to NCCs, which according to the protocol of Callahan *et* al could be found after 10 days of differentiation in the overgrown parts. Analyzing the mRNA expression of the stem cell markers Nanog and Oct4 showed a significant reduction in both hiPSCL-derived populations compared to the original hiPSCs. Additionally, in the hiPSCL1-derived cells, Sox2 expression was significantly reduced and the same trend could be observed in the hiPSCL2-derived cells. At the same time, the expression of the NCC markers p75 and Sox10 was increased in both hiPSCL-derived cell populations, Sox10 significantly in both and p75 in the hiPSCL2-derived cells (**Figure 22B-C & E-F**). Additionally, whole genome expression analyses revealed drastic differences in global gene expression between the parental hiPSCLs and the hiPSC-derived NCCs (**Figure 22D & G**). Furthermore, the functionality and efficiency of the differentiation of hiPSCs to NCCs was also confirmed on protein level by flow cytometry analysis. This revealed about

20% more p75/HNK1 double-positive and more single-positive cells after differentiation (**Figure 22H-K**).

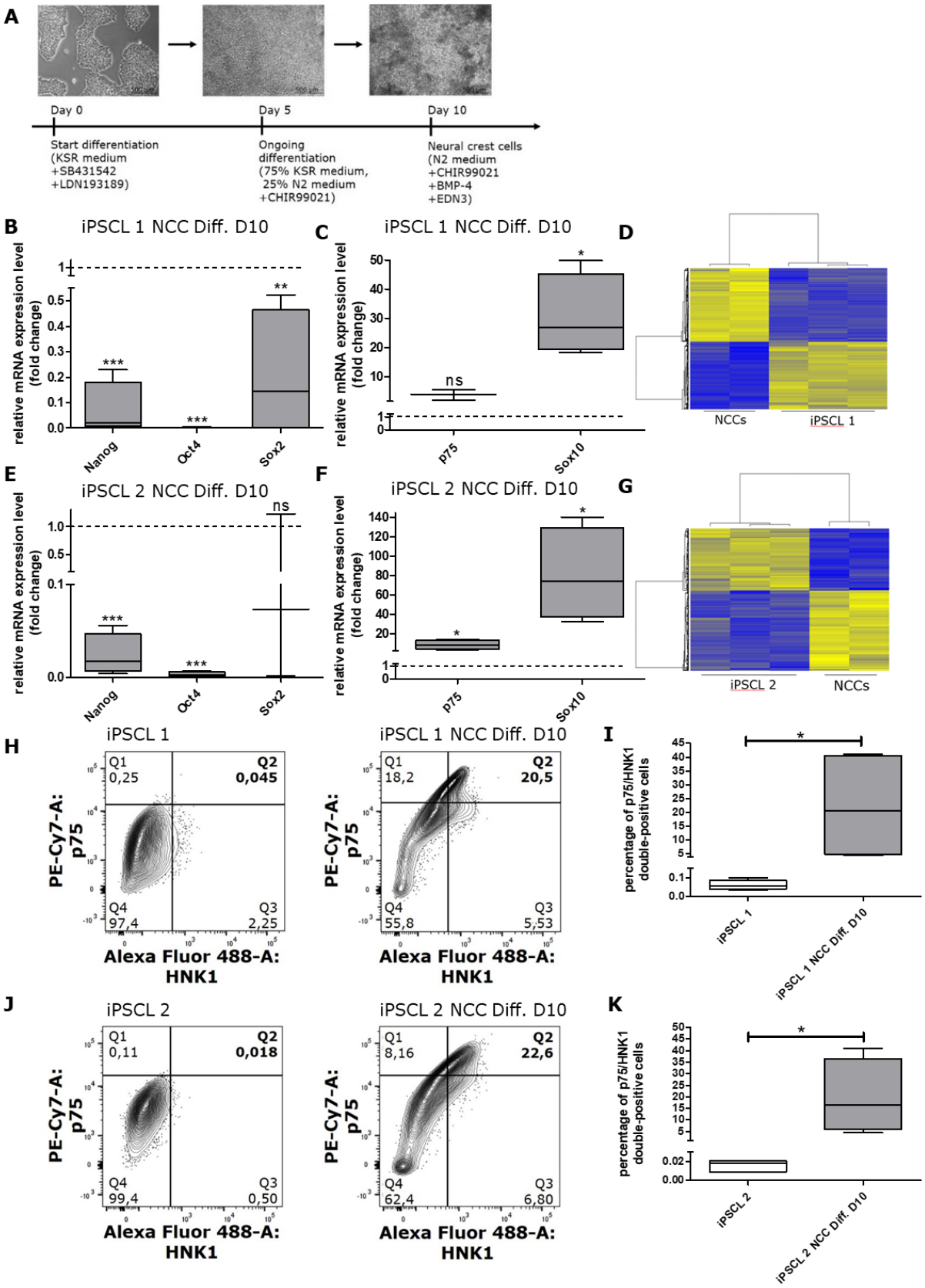

Figure 22: Differentiation of hiPSCs into NCCs

Figure legend continues on next page

***A:** Outline of the modified differentiation protocol with representative images. **B & E:** The expression of the stem cell markers Nanog, Oct4 and Sox2 decreased in both hiPSCL-derived populations after 10 days of differentiation compared with the original hiPSCs. n≥4 **C & F:** The expression of the NCC markers p75 and Sox10 increased in both hiPSCL-derived populations after 10 days of differentiation compared with the original hiPSCs. n≥4 **D & G:** Comparison of global gene expression between hiPSCLs and hiPSCL-derived NCCs after 10 days of differentiation. **H-K:** Flow cytometry analysis of hiPSCs and hiPSCL-derived NCCs after 10 days of differentiation. **H & J:** Representative images of the Contour blots. **I & K:** After 10 days of differentiation the amount of p75/HNK1 double-positive cells was increased about 20% compared to the original hiPSCs for both cell lines n≥4 *p=≤0.05 **p=≤0.01 ***p=≤0.001*

In order to research the functionality of the obtained NCCs they needed to be replated onto an ornithine/laminin/fibronectin layer. Several strategies with different coatings, reseeding approaches and different media were tried out. In general, the coating strategy of Dr. Katrin Schrenk-Siemens, seeding in melanocyte media and an addition of Rock inhibitor to the cells for 24h resulted in more cells attaching to the surface after replating. The method of replating the NCCs seemed to have no effect on the outcome. However, with every protocol the cells still died after several days or became senescent (**Figure 23**).

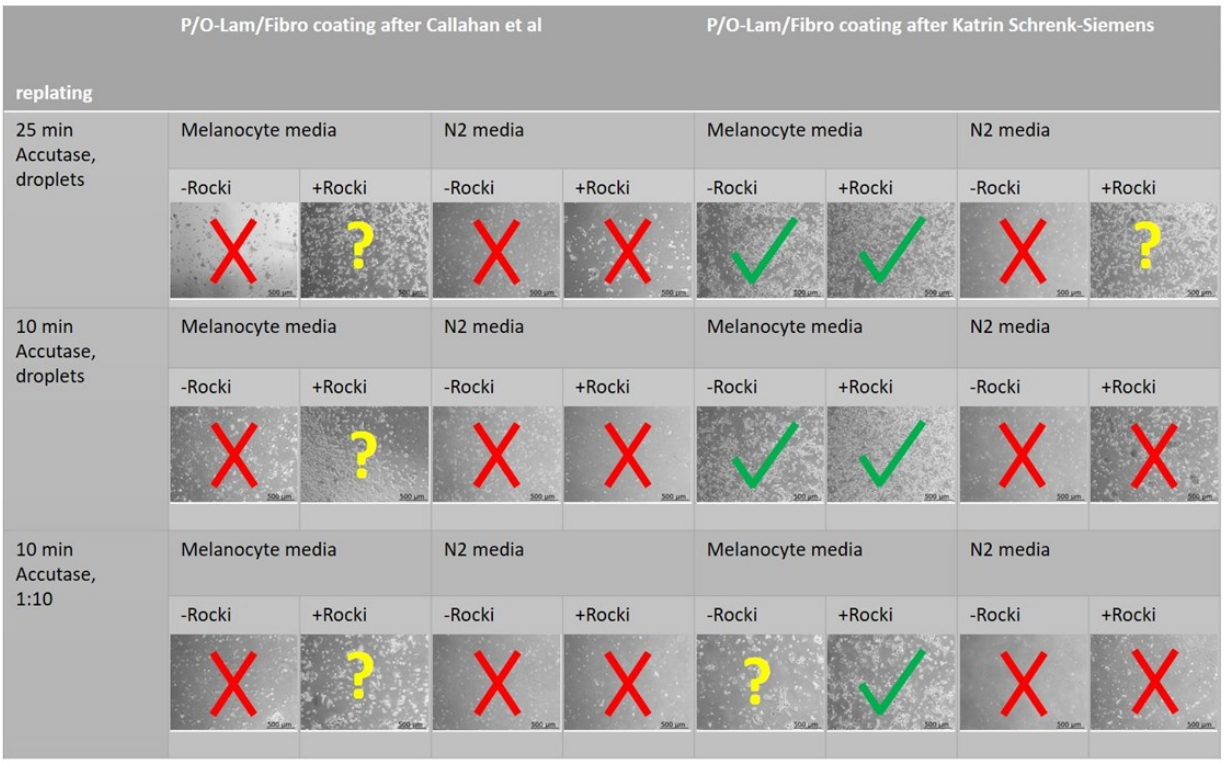

Figure 23: Replating experiments and further differentiation of NCCs into melanocytes
Representative pictures of experiments 24h after replating under different conditions. The two different coating strategies were combined each with different media and the addition of Rock inhibitor (top rows). Different replating methods are specified on the left side. The red cross marks conditions, where cells did not attach to the surface. A yellow question mark indicates conditions, where cells only partly attached to the surface and green ticks indicate conditions, where cells attached to the surface. P/O: poly-ornithine, Lam: laminin, Fibro: fibronectin

Due to these difficulties in replating NCCs, I first investigated the effect of ADCK2 (and other kinases) on the differentiation of hiPSCs to NCCs.

4.10 KD of different candidate kinases during the differentiation of hiPSCs to NCCs significantly affected the expression levels of stem cell and NCC markers

Having established a functioning protocol for the differentiation of hiPSCs to NCCs, I used this system to study the importance of several kinase candidates on the differentiation process. I combined and optimized the differentiation protocol with an siRNA KD in order to examine if the downregulation of a specific kinase impacts the differentiation of hiPSCs to NCCs. An outline of the combined siRNA KD and differentiation procedure to NCCs can be seen in **Figure 24A**. The siRNA KD resulted in a reduction of the expression of DBF4, EPHA4, TYK2. ARAF and MAP2K3 of at least 20% and in the case of ADCK2 even 50% (**Figure 24B**). A significant downregulation of ADCK2 could still be seen in hiPSCL1 96h after siRNA transfection (**Figure 24C**). Successful KD of ADCK2 on protein level was also confirmed in HEK cells (**Figure 24D**). All candidate kinases have been either shown in a previous siRNA screen to not influence the differentiation of hiPSCs to keratinocytes [83] or showed a lower expression in iPSC generated NCCs compared with iPSCs and were in the same time found as inhibitor candidates in the siRNA screen [77], [83]. To test, if these kinases influence the differentiation process of hiPSCs to NCCs, they were knocked down on day 0 of differentiation. Then, the cells were differentiated for 10 days, harvested and analyzed. Cells with a kinase KD were compared to cells, which were treated with an siControl with regard to stem cell and NCC marker expression. This analysis revealed that the KD of ADCK2 and DBF4 resulted in lower expression levels of the stem cell markers Nanog, Oct4 and Sox2 and at the same time higher levels of the NCC markers p75 and Sox10. The opposite effect was observed upon knocking down TYK2 and EPHA4, indicating that these two kinases might be necessary for efficient differentiation to NCCs. (**Figure 24E**).

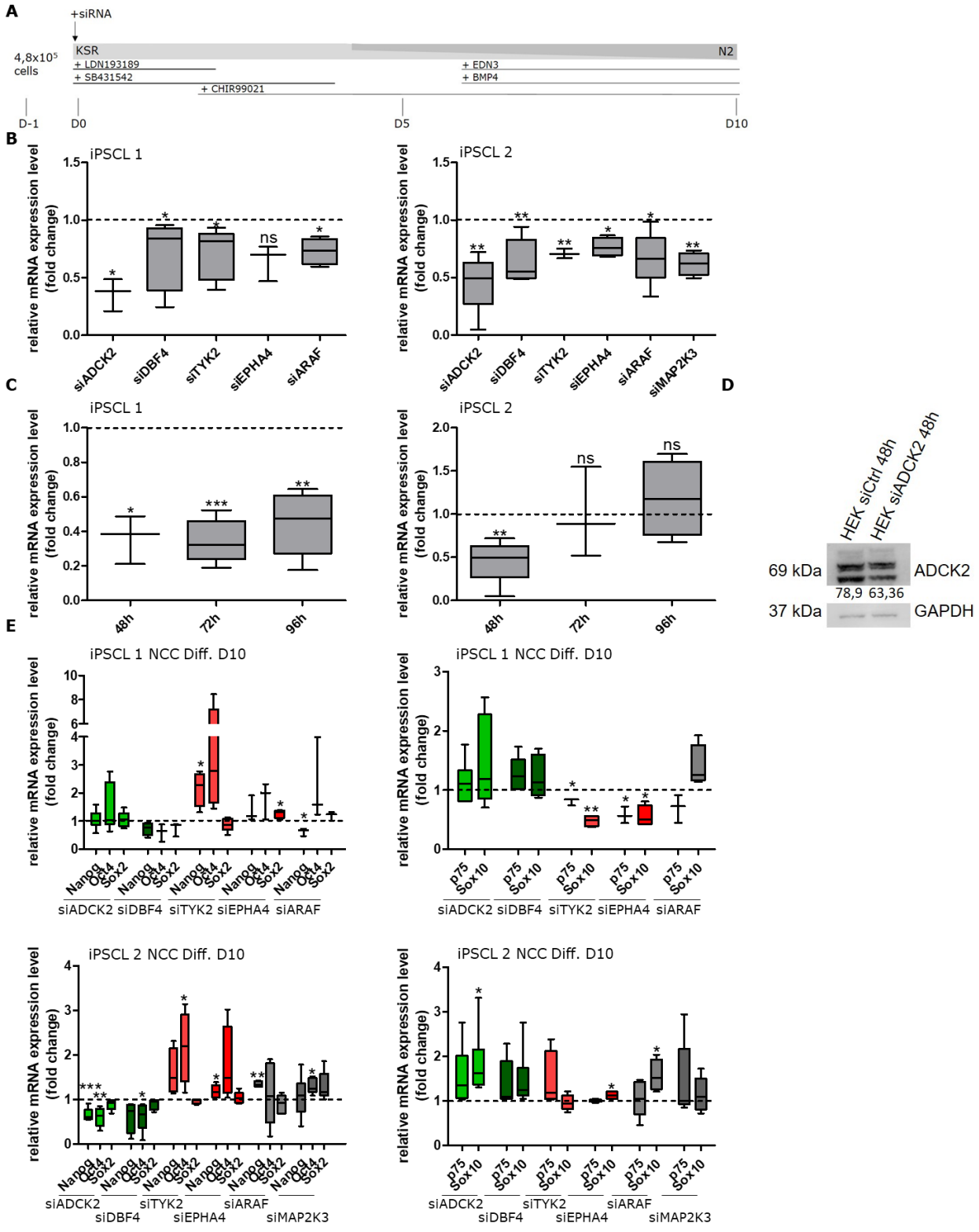

Figure 24: The effect of specific kinases on the expression of stem cell and NCC markers during the differentiation of hiPSCs into NCCs

Figure legend continues on next page.

A: *Outline of the differentiation protocol combined with an siRNA KD. hiPSCs were simultaneously treated with siRNA and cultivated in differentiation medium supplemented with a BMP4 and TGFß/Activin/Nodal pathway inhibitor one day after seeding. 48h after transfection, differentiation was continued as explained above for 10 days.* ***B:*** *Confirmation of the successful siRNA-mediated KD of all candidate kinases in hiPSCLs after 48h.* ***C:*** *ADCK2 expression was significantly reduced up to 96h upon transfection in hiPSCL1 and up to 48h in hiPSCL2.* ***D:*** *Representative Western blot image confirming ADCK2 KD on protein level in HEK cells. upper band: ADCK2, lower band: loading control GAPDH. Numbers indicate the normalized expression value of ADCK2.* ***E:*** *KD of ADCK2 or DBF4 led to a decreased expression of stem cell markers Nanog, Oct4 and Sox2 and an increased expression of the NCC markers p75 and Sox10. KD of TYK2 or EPHA4 had the opposite effect, seen by an increase in the expression of the stem cell markers Nanog, Oct4 and Sox2 and a decrease of the expression of p75 and Sox10. mRNA expression levels were normalized to hiPSCs transfected with siControl on day 0 and then differentiated for 10 days to NCCs. n≥5 *p=≤0.05 **p=≤0.01 ***p=≤0.001*

Since I could show that the KD of ADCK2 or DBF4 led to an increased expression of NC markers in hiPSCL-derived NCCs, I wanted to examine what effect a combined KD of both candidate kinases would have. I observed that the double KD altered the expression of stem cell and NCC markers in a manner comparable to the single KDs (**Figure 25A-E**).

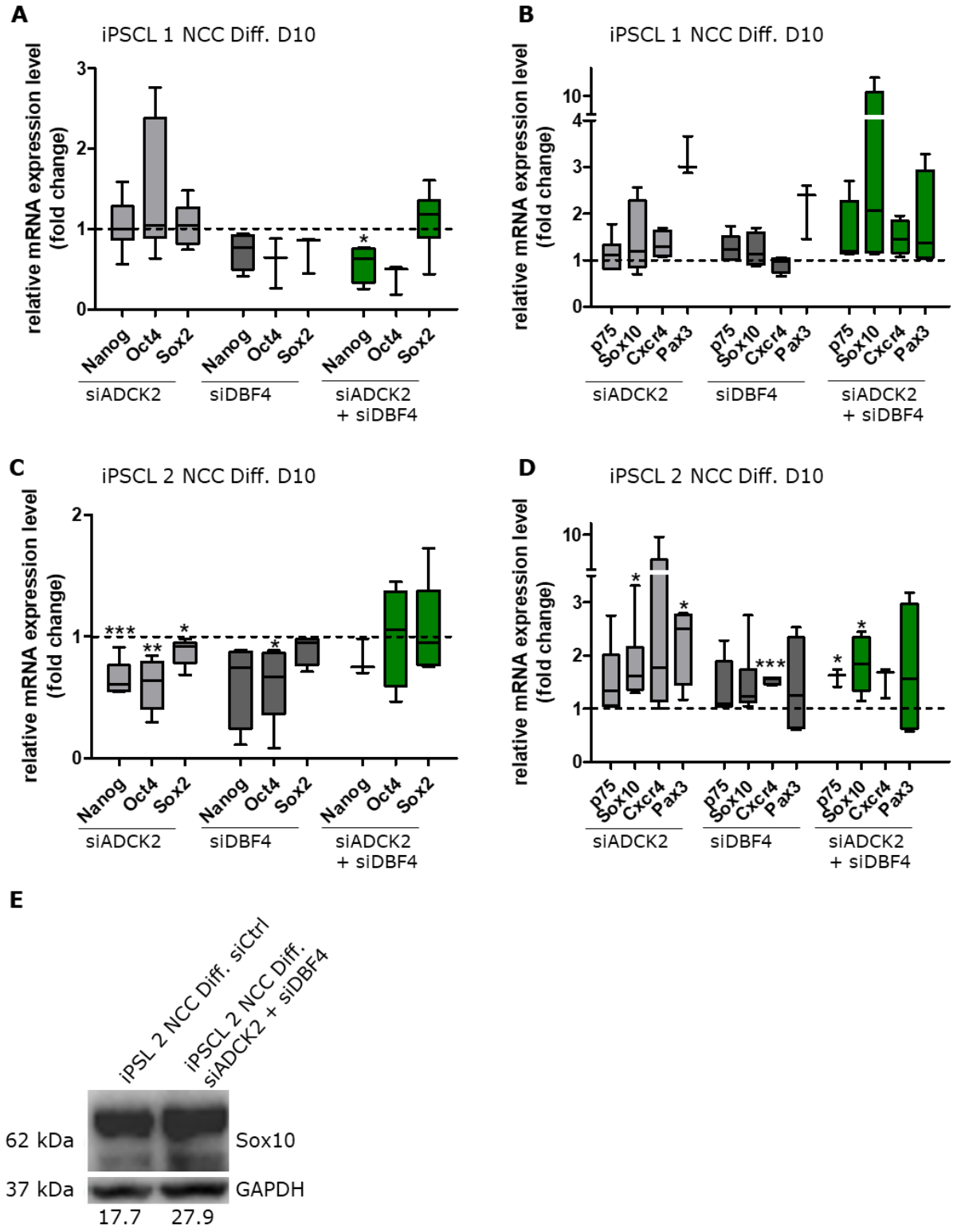

Figure 25: Comparison of the effect of single or double KD of ADCK2 and DBF4 on the expression of stem cell and NCC markers during the differentiation of hiPSCs to NCCs
A & C: *Decreased expression of the stem cell markers Nanog, Oct4 and Sox2 in hiPSCL-derived NCCs after 10 days of differentiation and KD of ADCK2, DBF4 or both at day 0.* ***B & D:*** *Increased expression of the NCC markers p75, Sox10, Cxcr4 and Pax3 in hiPSCL-derived NCCs after 10 days of differentiation and KD of ADCK2, DBF4 or both at day 0. All mRNA expression levels were normalized to hiPSCL-derived NCCs after 10 days of differentiation upon siControl transfection. n≥5* ***E:*** *Representative Western blot image confirms increased Sox10 expression on protein level in hiPSCL2-derived NCCs after 10 days of differentiation and simultaneous KD of ADCK2 and DBF4 at day 0. *p=≤0.05 **p=≤0.01 ***p=≤0.001*

Especially in iPSCL 2, a KD of ADCK2 led to a significant downregulation of stem cell and significant upregulation of NCC markers. To further characterize the NCCs generated upon ADCK2 KD, global gene expression of the original hiPSCLs and the hiPSCL-derived NCCs after 10 days of differentiation was performed. The different NCC populations showed a similar expression pattern of NCC development genes indicating high expression of many genes involved in NC development, which was clearly distinct to that of the original hiPSCLs (**Figure 26**). A full analysis of all genes related to NC development can be seen in **Supplementary Table 1** and **Supplementary Table 2**.

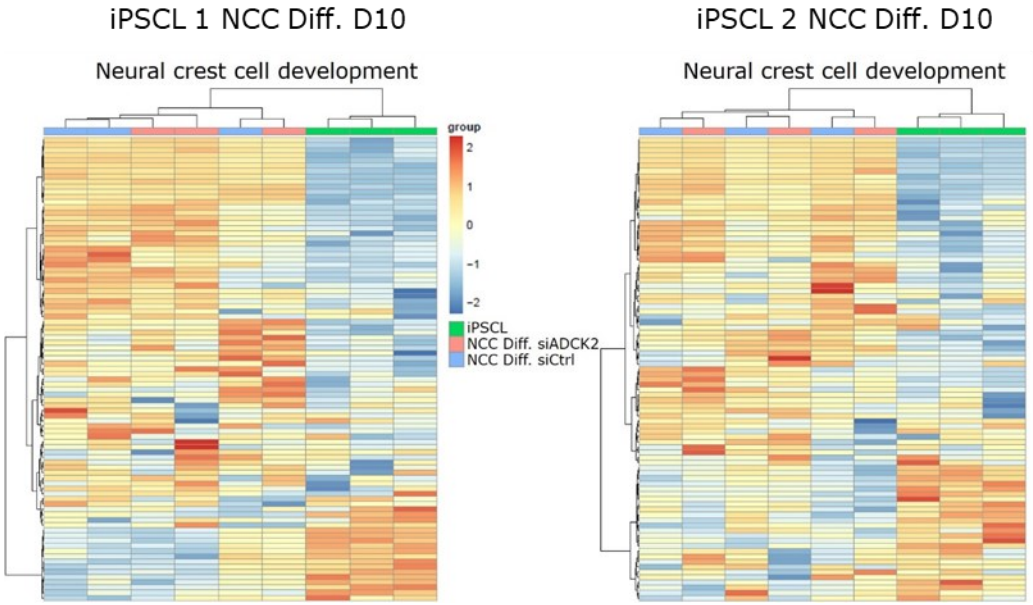

Figure 26: Gene expression profiles of the parental hiPSCLs and hiPSCL-derived NCCs with reference to genes involved in NCC development
The hiPSCLs show no expression of NC-related genes in contrast to the hiPSCL-derived NCCs after 10 days of differentiation. Green bar on top: hiPSCL, light blue bar on top: hiPSCL-derived NCCs after 10 days of differentiation and treatment with siControl at day 0, light pink bar on top: hiPSCL-derived NCCs after 10 days of differentiation and treatment with siADCK2 at day 0

4.11 Identification of genes commonly dysregulated in both melanoma cells and hiPSCL-derived NCCs upon ADCK2 KD

In order to uncover common genes in melanoma cells and hiPSCL-derived NCCs whose expression is affected by ADCK2 KD, the gene expression data of both groups was compared. Significantly dysregulated genes in comparison to the siControl were identified, revealing 10 common upregulated and 12 common downregulated genes between melanoma cells and hiPSCL-derived NCCs (**Figure 27**). Within these genes there are genes which are correlated with migration, stemness and differentiation. A full table of all genes can be found in **Supplementary Table 3** and **Supplementary Table 4**

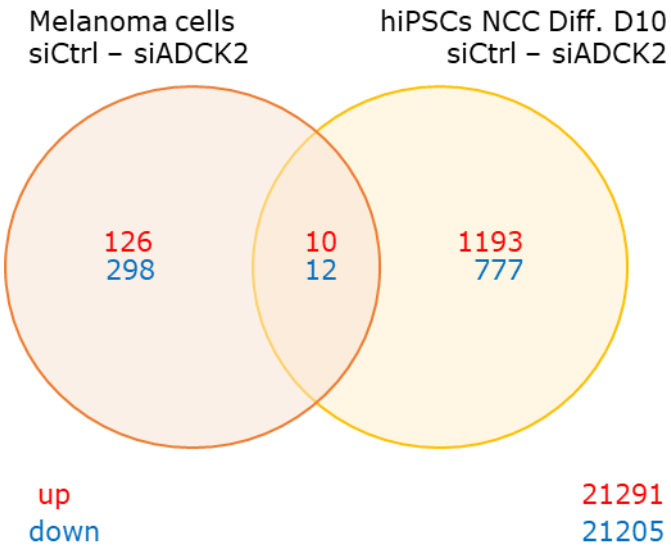

Figure 27: Venn diagram showing 10 commonly up- and 12 commonly downregulated genes in melanoma cells and hiPSCL-derived NCCs upon ADCK2 KD.
Fold-change = 1.2

5 Discussion

In this thesis, I studied the role of ADCK2 in melanoma and its influence on the differentiation of hiPSCs to NCCs. I could demonstrate that knocking down ADCK2 in melanoma cells significantly affected their viability, migration, invasion and their differentiation status. I could also show that some of these effects were mediated via MYL6, which I identified as a downstream effector of ADCK2. Analyzing the publicly available databases R2 and cBioPortal, I discovered that higher levels of ADCK2 as well as MYL6 correlated with increased overall survival of melanoma patients. From these data, one can conclude that ADCK2 might act as a tumor suppressor in melanoma. Furthermore, I reprogrammed fibroblasts successfully to hiPSCs and established a stable hiPSC culture on Matrigel layer. An efficient protocol for the differentiation of these cells in a xeno-free environment into NCCs was established and combined with an siRNA KD of different candidate kinases. Here, a KD of ADCK2 and DBF4 resulted in a higher expression of NCC markers after 10 days of differentiation compared to control cells. My research of the role of ADCK2 during tumorigenesis of melanoma cells and differentiation of hiPSCs to NCCs allows the conclusion that a knockdown of ADCK2 promotes the adoption of a NC-like phenotype in melanoma cells and leads to higher NCC marker expression in hiPSC-derived NCCs.

5.1 The influence of ADCK2 on melanoma cell behavior

I started my investigation of the role of ADCK2 in melanoma by examining the effect of altered ADCK2 expression on some basic characteristics of melanoma cells. I could show that a KD of ADCK2 decreased the cell viability of SkMel28, MeWo, A375 and SkMel30 melanoma cells by at least 20% 48h or later upon the KD. The opposite effect could be observed upon ectopic OE of ADCK2 in SkMel28, MeWo and A375 cells, even though not as pronounced. In lung, breast and cervical cancer a lower cell viability was observed upon ADCK2 KD and the same result was found for retinoblastoma [62], [65]. A better cell survival was seen in ER+ve breast cancer cells with a higher ADCK2 expression. In this case the effect is due to an interaction of ADCK2 with ERalpha (estrogen receptor), which leads to an altered estrogen signaling [54]. Furthermore, in osteosarcoma and prostate cancer cells ADCK2 has been linked to TNFα. TNFα is known to stabilize HIF1α and by this leads to a cancer cell survival benefit. Most probably this is due to an activation of a NFκB-dependent mechanism, which results in the production of reactive oxygen species [52]. In skin cancer tumor cells ADCK4 has been shown to form a complex with NUMBL, which then promotes proliferation [63]. Further, a positive regulation of ADCK4 by KLF5 has been shown, which among others, also shows functions in cell proliferation [84]. A depletion of aarF in bacteria as well as a heterozygous knockout of ADCK2 in mice resulted in slower growth compared to the respective wild type organisms [61], [85]. These studies, together with my observations, show that ADCKs affect the cell viability and proliferation of several cancers, but the exact mechanism of how ADCK2 influences cell viability and proliferation remains unknown.

In my study, I could also demonstrate that ADCK2 influenced cell motility. For all four melanoma cell lines used in my experiments (SkMel28, MeWo, A375 and SkMel30) a faster migration upon KD of ADCK2 was observed. As opposed to this, SkMel28 cells showed a reduced migration capacity upon ADCK2 OE. Additionally, a reduction of ADCK2 in SkMel28

cells led to a faster invasion and SkMel28 ADCK2 overexpressing cells showed an impaired invasion through a BME matrix compared with an according control group. Different ADCK family members have been connected to the regulation of cell motility. A KD of ADCK4 has been associated with a faster migration in epithelial cells, where also ADCK1 has shown an effect on cell motility [64]. Interestingly, a heterozygous KD of ADCK2 led to locomotor dysfunction in mice. Further, Qiu and colleagues could connect ADCK5 with lung cancer cell migration and invasion. Here, they have shown that ADCK5 phosphorylates Sox9, which then regulates PTTG1 [57]. A higher cell motility is often associated with the ability of cancer cells to form metastases. My results suggest a higher probability for melanoma with low expression of ADCK2 to metastasize. In contrast to my findings, Montagnani and colleagues have proposed that ADCK2 is metastasis-associated and demonstrated a connection between ADCK2 and metastasis, especially in BRAF-mutated melanoma [9]. Interestingly, also a BRAF-ADCK2 fusion has been found in infantile fibrosarcoma. This fusion leads to an activation of BRAF, which is known to be an oncogenic driver in melanoma, but also other tumors like thyroid carcinoma and gliomas [86].

Cell migration does not only play an important role in tumorigenesis and metastasis but also for example in tissue remodeling and development. In all these processes many different genes and pathways are involved, directly or indirectly, to cover different functions [64]. Since it is known that a more migrative and invasive phenotype of a cancer cell is often associated with an alteration of the differentiation status, I further analyzed the differentiation status of melanoma cells upon KD of ADCK2. In general, I could observe that KD of ADCK2 induced a switch to a more dedifferentiated phenotype. More precisely, the expression of the NCC markers Sox10 and p75 was increased while the expression of the melanocyte markers MITF, TRP1 and TYR was decreased in all melanoma cell lines. Additionally, the pigmented melanoma cell line SkMel30 produced less pigment upon ADCK2 KD but more pigment upon ADCK2 OE. MITF, TYR and DCT expression is usually associated with a proliferative phenotype, while Wnt5a, TGFß and FGF are markers of an invasive phenotype [6]. Furthermore, a lower MITF expression and decreased pigmentation together with expression of E-cadherin and increased expression of p75 was observed in dedifferentiated NC stem-like cells. These cells also displayed a higher migration capacity. All of these features could be observed after MSX1 OE in melanocytes, which led to the assumption that MSX1 plays a key role in melanoma phenotype switching [3]. In my study, I could see a downregulation of the transcription factor Sox5. A connection between MITF and Sox5 expression has been demonstrated in melanoma cells before, where a downregulation of Sox10 led to lower levels of MITF and Sox5. Moreover, a lower expression of Sox5 has been correlated with a worse outcome for melanoma patients and Sox5 has been shown to be overexpressed especially in BRAF and NRAS-mutated melanoma [2]. Interestingly, the KD of ADCK2 significantly reduced Sox5 expression only in BRAF- and NRAS-mutated melanoma cell lines (BRAF: SkMel38, A375 NRAS: SkMel30) and not the wild type cell line MeWo. Other factors which have been linked to MITF are Pax3 and FoxD3 [87]. Interestingly, lower MITF levels, but higher levels of Pax3 and FoxD3 have been also connected with invasion and drug resistance and FoxD3 expression is often decreased in BRAF-mutated melanoma cells [5], [50]. Further, it has been shown that FoxD3 plays a role in suppressing cell motility and by its OE leads to a reduced cell migration [45], which fits to my results showing that the expression of FoxD3 was slightly reduced and the migration enhanced in ADCK2 KD melanoma cells. The effect of FoxD3 OE on cell migration could be abrogated by the expression of TWIST1, which is a NCC marker and also known to have positive effects on cell motility in melanoma [45]. Moreover, FoxD3 suppresses MITF expression during development, which prompts NCCs to differentiate to glial cells instead of melanocytes [88]. This is in line with a study showing that FoxD3 KD during development resulted in a higher number of melanoblasts emigrating from the

neural crest [45]. Also, a misexpression of FoxD3 during early NCC development results in more NCC migration and expanded NC marker expression in the neural tube [87], [89]. With regard to my results, one could speculate that the phenotype switch of melanoma cells to more dedifferentiated cells with higher migration capacity upon KD of ADCK2 could be partially related to FoxD3 expression. To evaluate this hypothesis, further experiments are needed. Pax3 is a key regulator during melanocyte development and also a known oncogene in melanoma, which promotes metastasis by facilitating the expression of genes promoting cell motility [50], [90]. In this study, I observed that Pax3 was slightly upregulated upon ADCK2 KD. It is known that Pax3 promotes a dedifferentiated, more stem-like and more motile phenotype of melanoma cells [90], which would be in line with the switch to a more dedifferentiated phenotype with higher migrative capacity upon ADCK2 KD. Pax3 most probably mediates this switch by binding to the promoters and thereby inducing the expression of the melanoma cell adhesion molecule (MCAM) and chondroitin sulfate proteoglycan 4 (CSPG4), which are also markers for melanoma more prone to metastasize. Further, Pax3 also downregulates the anti-apoptotic factor BCL2L1 and the tumor suppressor PTEN, which gives a survival benefit to melanoma cells preventing cell cycle arrest and apoptosis. As another binding partner of Pax3, Cxcr4 is known to play a role in chemotactic migration and melanoma metastasis. Cxcr4 is regulating the "homing" of tumor cells and promotes tumor cell extravasation [4], [90]. To fully evaluate the role of Pax3 in ADCK2 KD melanoma cells further experiments are necessary.

5.2 MYL6 as a downstream effector of ADCK2

In order to learn more about the mechanism how ADCK2 influences melanoma cell behavior, whole genome expression analyses were performed. The aim was to find dysregulated genes upon ADCK2 KD. For this, global gene expression of three melanoma cell lines transfected with siADCK2 or siControl was examined. These analyses revealed four common downregulated genes upon ADCK2 KD: ADCK2, ZNF275, RAB2A and MYL6. The appearance of ADCK2 in this list underlines the efficiency of the ADCK2 KD in melanoma cells. ZNF275 is most probably a transcription factor with 11 putative zinc finger motifs. It has been shown to be conserved in eutheria, but its function is still unclear [91]. RAB2A belongs to the Ras oncogene family which is part of the superfamily of small GTPases with more than 100 members divided into the six subfamilies Ras, Rho, Rab, Sar1/Arf, Ran and others [92], [93]. All of them are highly conserved proteins, which play a key role in cell trafficking and vesicular fusion, RAB2A especially in the trafficking from the endoplasmic reticulum (ER) to the Golgi complex [93], [94]. It has been shown in several cases that an aberrant expression or function of RAB proteins can lead to various diseases, including cancer. The reason for this is the fact that several functions including for example invasion, migration and drug resistance depend on cellular trafficking. [93], [95]. Interestingly, the MITF locus is situated directly upstream of several RAB genes, including RAB27A and RAB38. RAB38 was found to have a promoting effect on invasion of melanoma cells by upregulating several MMPs. The same was seen for RAB27A and RAB2A in breast cancer cells [92]. Several RAB proteins have contrasting roles in different cancers. For example, RAB25 has promoting effects on non-small-cell lung and ovarian cancer due to its influence on integrinß1 trafficking. However, it has the opposite effect in cutaneous squamous cell carcinoma and colorectal cancer [95]. Also, RAB37 has shown inhibitory effects on the motility of lung adenocarcinoma cells via regulating MMPs [92]. A similar effect has been shown for RAB26 in breast cancer cells also via MMP downregulation [96].

Further, RAB12 and RAB31 might act as tumor suppressors as they show lower expression in metastatic melanoma cells compared to primary melanoma cells. Indeed, an upregulation of RAB31 led to a phenotype switch of breast cancer cells from an invasive to a more proliferative phenotype [92]. RAB2A has been shown to regulate the endocytic recycling of membrane type 1 metalloproteinase (MMT1-MMP) and also plays a role in the transport of E-cadherin to the Golgi complex. These functions lead to an improved invasion of breast cancer cells, which could be reversed by RAB2A and RAB28 downregulation [95], [97]. Additionally, in colon cancer a lower expression of RAB2A was correlated with less cell motility [98]. In oral squamous cell carcinoma (OSCC) RAB2A was found upregulated in the cytoplasm [93] and a KD of S100A7 resulted in a downregulation of RAB2A, which was mediated by the p38 MAPK signaling pathway [99]. Moreover, RAB2A has been predicted as a breast cancer stem cell-promoting gene which has positive effects on tumor aggressiveness and correlates with poor survival of breast cancer patients. These effects might be due to an activation of the ERK signaling pathway [100]. In contrast, RAB2A was found to function as a tumor suppressor in glioma cells where a KD led to more migration and invasion. Here, this effect was mediated via an inactivation of the AKT signaling pathway due to phosphorylation of AKT [101]. Interestingly, in prostate cancer cells, the active form of RAB2A was reduced and RAB2A was less abundant in squamous cell carcinoma or vaginal mucosa than in squamous vaginal cancer [101], [102]. Furthermore, a study in black-boned sheep revealed that there is nearly no expression of RAB2A in skin and spleen tissue, whereas it is found in muscle, heart, liver and kidney tissues [94]. The studies cited above suggest that RAB proteins seem to have contradicting roles in cancer development and metastasis depending on the type of cancer. With this in mind, it would be interesting to elucidate the role of RAB2A in melanoma cells, especially the connection with ADCK2, as a KD of ADCK2 led to a downregulation of RAB2A, but an increased migration. Interesting approaches would be to check for the expression and regulation of MMPs, especially their degradation and recycling, and to investigate the regulation of the AKT signaling pathway.

Among the four genes being downregulated MYL6 turned out to be a very interesting candidate, since its KD abrogated the effect of ADCK2 OE on melanoma cell viability and migration. Moreover, data analysis revealed that patients with tumors with low MYL6 expression levels had a reduced OS. A similar effect has been shown in neuroblastoma patient cohorts [103]. Also in a machine learning model of lung adenocarcinoma "alive without cancer" was associated with MYL6 expression [104]. Controversy to my results, MYL6 has not been seen upregulated in melanoma metastasis, but therefore in nevus nevocellularis [105]. So, MYL6 seems to be correlated with better patient outcome in several cancers and might also have an effect in precursors of cancer cells. MYL6 is an essential light chain (ELC) of non-muscle myosin 2 (NM2) which belongs to the motor proteins that are present in all cells and that are essential for migration, posterior cell retraction and cargo transport. The function of ELCs itself is still unclear, but NM2s are involved in actin binding in non-muscle cells [1], [106]. Interestingly, in UV-irradiated HeLa cells an abnormal MYL6 expression was detected [107], indicating that MYL6 could play a role in skin cancers like melanoma. There are several splicing variants of MYL6, mostly differing in the in- or exclusion of exon 6 and thereby priming them for smooth muscle or non-muscle myosin connections, respectively. A switch from one of these variants to another might also contribute to the migration behavior of breast cancer cells [72]. MYL6 has several confirmed binding partners. One of them is the nuclear transcription factor SERTAD1, which has a key role in cancer progression. Similar to the observed effect of a MYL6 KD on ADCK2 overexpressing cells also a SERTAD1 KD results in less proliferation of

melanoma cells [108]. Furthermore, PCBP1 is a binding partner of MYL6, which is involved in mRNA metabolism, RNA replication and translation but also in the regulation of muscle movement. Another one is VCL, which is a cytoskeletal protein that is often associated with cell-cell and also cell-matrix junctions, thereby also having a role in cell movement [109]. Moreover, an interaction of MYL6 and PLEKHA7 has been confirmed, which is found in adherens junctions [110]. MYL6 might also be part of the myosin regulatory light chain interacting protein complex, which plays a role in the development of the actin-myosin based contractile system [109]. Regarding the connection of MYL6 to many proteins involved in cell-cell as well as cell-matrix junctions and the newly found positive correlation of ADCK2 and MYL6 in this study, it would be interesting to investigate the effect of ADCK2 KD and OE in melanoma cells on these junctions. In prostate cancer, MYL6 has even been predicted as a potential biomarker, because of its possible involvement in the regulation of metastasis [111].

It is possible that the observed effects of MYL6 downregulation upon ADCK2 KD were connected to the contribution of MYL6 to NM2. Together with the ELCs, NM2s consist of regulatory light chains (RLC), which are MYL9, MYL12A or MYL12B and of non-muscle myosin heavy chains (NMHCs) MYH9, MYH10 or MYH14. ECLs, RLCs and the NMHC assemble to NM2s in human, where MYH9 is characteristic for NM2A, MYH10 for NM2B and MYH14 for NM2C. Interestingly MYH14 as well as MYH11 (smooth muscle myosin) are exclusively binding to MYL6 [66]. In general, all NM2s play roles in cell motility and cytoskeletal rearrangement, due to their ability to bind to actin fibers but also their contribution to substrate adhesion [70]. In NIH 3T3 fibroblasts a KD of the RLCs MYL12A and MYL12B leads to a decrease of MYH9, MYH10 and MYL6. These cells also show changes in cell morphology by abnormal arrangement of actin fibers and more and longer protrusions. Additionally, cell dynamics are changed which leads to less contractility but more migration [74]. The same effect was observed upon silencing NM2A [70] and a MYH9 KD in squamous cell carcinoma leads to increased invasion and more distant metastases as well as a lower expression of MYH9 is correlated with a lower survival chance of patients [112]. Similarly, in my study I found that the KD of ADCK2 resulted in reduced MYL6 expression, a higher migration rate, and altered actin filament assembly. To further elucidate how a lower expression of MYL6 via a KD of ADCK2 enhances the migration of melanoma cells, studies on the expression of the RLCs, MYHs as well as the full NM2s would be of great interest. The roles of NM2s can differ depending on their composition or the cell type they are expressed in. NM2A, for example, plays a key role in cell contraction and directional cell migration, whereas NM2B rather stabilizes the cytoskeleton [66]. Some lung diseases are correlated to mutations in NM2B and patients with deafness, muscle atrophy as well as cancers often show a mutation of NM2C [69]. In many cancers, aberrant expression and/or function of NM2s results in a more aggressive phenotype of the cancer cells. Inhibiting the activity of NM2s with blebbistatin reduces the migrative and invasive capacity of glioma and breast cancer cells [66]. An OE of NM2A increases the cell motility, leads to more metastatic lymph nodes and more dedifferentiated cancer cells in esophageal cancer [70]. In the skin, however, NM2A acts as a tumor suppressor by inhibiting proliferation. Here, decreased expression of NM2A or mutations that impair its function are correlated with tumorigenesis and metastasis [66], [69]. Also in head and neck squamous cell carcinoma lower levels of NM2A are associated with a worse outcome for the patients [66]. Moreover, analyzing data from publicly available databases revealed that melanomas expressing lower levels of ADCK2 as well as of MYL6 correlate with an increased patient survival. Interestingly, a lower cell proliferation has been seen in A549 lung cancer cells upon KD of MYH14, a component of the NM2C complex, due to a prolonged cytokinesis. [113]. In line with this, a splicing variant of NM2C is often localized close to the midbody in cancer cells [70]. Since MYL6 is a part of the NM2C complex, one can speculate that the

KD of MYL6 or the indirect reduction of MYL6 expression upon ADCK2 KD could directly impair the function of NM2C. Furthermore, the lower cell viability upon ADCK2 KD could be explained by abnormal cytokinesis that also occurs after knocking down a specific splicing variant of MYH14 directly [113]. Due to my observation that the distribution of actin in melanoma cells upon ADCK2 KD was altered and the fact that ELCs are necessary for stabilizing NM2s [70], I researched into the literature for connections between NM2s and actin filament arrangement. For NM2A and NM2B it has been shown that their disassembly into monomers favors cell migration and invasion. This effect might be due to an increased cytoskeletal rearrangement, which is indicated by less condensed actin structures and enhanced directional persistence during cell migration [69], [114]. In my experiments, the downregulation of ADCK2 resulted in an increased migration along with an altered distribution of actin implied by strong actin staining right below the cell membrane but less actin filaments within the cytoplasm. Enhanced NM2 filament turnover is thought to be a source of increased cell motility and angiogenesis in cancer. In B16 melanoma cells, only NM2C is expressed but no NM2B, but the cells still show a normal front-back polarization, which leads to the assumption that in these cells NM2C takes over the functions of NM2B. Usually, NM2B is responsible for the stabilization of the contractile rear by inhibiting protrusions and adhesion turnover due to vast and steady actomyosin bundles and adhesion [70]. One possible hypothesis could be, that the increased cell migration seen in ADCK2 and MYL6 KD cells could be due to a lower expression of NM2C, which could lead to a higher turnover of it and thereby an increased migration. To validate this hypothesis further experiments are needed. Together with NM2s, also other filaments can have an effect on assembling and disassembling of myosin complexes. For example, myosin-18A cannot form filaments by itself, but it can integrate into NM2 filaments, which leads to a morphology change and to altered function, sometimes necessary in a cell. However, if myosin-18A is aberrantly overexpressed, which is often the case in cancer, it will lead to the disassembly of NM2 [69]. Aside from changes of expression, also changes in phosphorylation of the NM2s, especially the RLCs, lead to altered cell function and morphology [74]. So, NM2A mutants, with constantly phosphorylated NM2A show more cell migration, focal adhesion and cell protrusions compared to wild-type NM2A cancer cells. A similar effect was seen for an NM2C mutant, which contains a longer loop region and is thereby constitutively active [70]. Thereby also experiments concerning the phosphorylation status of NM2C in ADCK2 KD melanoma cells would be of great interest.

The first part of my thesis can be summarized as follows: A KD of ADCK2 reduced the cell viability of melanoma cells, but increased their migrative capacity. These effects could be reversed by OE of ADCK2, which also led to a slower invasion of ADCK2-overexpressing SkMel28 cells. MYL6 was identified as a putative downstream factor of ADCK2 by global gene expression analysis and MYL6 KD experiments. The mechanism how the ADCK2-mediated MYL6 KD led to an increased migration and invasion of melanoma cells is still unclear and needs further investigation. However, alterations of actin distribution in SkMel28 cells upon ADCK2 KD imply that the changes of migration capacity might be due to the function of MYL6 within NM2C. Regarding the effect of MYL6 on the NM2C complex, I suggest the following hypotheses. A reduced MYL6 expression results in an altered structure of the NM2C complex, thereby leading to a constitutively active form of NM2C, which facilitates faster migration.

5.3 Generation of hiPSCs

As described in chapter 1.4 of the introduction, the molecular mechanism underlying tumorigenesis and metastasis resemble those that play a role during the development from stem cells to NCCs. In my study, I found several hints that ADCK2 affects the differentiation status of melanoma cells. For this reason, I was interested in investigating if ADCK2 might also be involved in controlling the differentiation of hiPSCs to NCCS. For this purpose, I first generated a new hiPS cell line with a non-integrating method under xeno-free conditions from fibroblasts. Additionally, I subcloned an already existing hiPSCL in order to have two different hiPSCLs to work with. The pluripotency of both cell lines was confirmed by positive AP staining and an increased expression of the pluripotency markers Nanog, Oct4 and Sox2 on mRNA level. Furthermore, a teratoma assay was performed with hiPSCL1. Both hiPSCLs where then used for differentiation experiments.

5.4 Efficient differentiation of hiPSCs into NCCs

To establish an efficient method to differentiate hiPSCs to NCCs under xeno-free conditions several protocols were tested. The differentiation procedure according to the protocols from Dr. Kasia Weina, Larribère et al. and Nissan et al. [46], [76], [77] did not yield NCCs. Most probably, this was because these protocols were established with mouse embryonic feeder cells (MEFs). Switching these protocols to xeno-free conditions (differentiation on Matrigel instead of MEFs) could result in forfeiting specific factors produced by MEFs, which are necessary for the differentiation process. It has been shown that in early development the formation of NCCs is induced by signals from and cell contact to the surface ectoderm and the underlying mesoderm [115]. Moreover, it has been shown that during melanocyte differentiation specific extrinsic factors like mast cell factor and EDN3 are necessary for a proper development [116]. These external signals are usually coming from the surrounding environment, e.g. keratinocytes [12]. Additionally, for the differentiation to NCCs, not only the availability but also the concentration of specific factors like BMP4 and Wnt3a were found to be important [14]. Although these factors were added to the medium, they probably were not present in an optimal concentration. Furthermore, some cells became senescent during the differentiation, which is due to a safeguard program preventing aberrantly growing cells from turning into cancer cells [77]. Also this might be due to missing factors in the media [25], [77]. Next, the differentiation protocol from Dr. Katrin Schrenk-Siemens was tested. This protocol involves the formation of embryonic bodies (EBs) as an intermediate step [78]. EBs are aggregates of pluripotent cells, which can differentiate into any cell type of the three germ layers, depending on the medium in which they formed [117], [118]. The hiPSCLs established by me did successfully form EBs when applying the protocol from Dr. Katrin Schrenk-Siemens, but no NCCs grew out. Possible explanations here are, that different maintenance media for the hiPSCs have been used which could have primed the hiPSCs differently. Furthermore, the hiPSCs were not counted prior to differentiation. However, the cell number has been shown to be important in differentiation procedures [118]. Also, it has been shown for ES cell differentiation into hematopoietic cells via EBs, that plating efficiency and kinetics of differentiation have to be adjusted for each cell line [119]. A switch from StemFit to E8 medium (used by Dr. Katrin Schrenk-Siemens) and seeding a defined cell number before starting the differentiation process could help to solve this problem. A modification of the protocol from Callahan, Mica and Studer [79] finally led to a successful differentiation of hiPSCs to NCCs. The modifications implemented by me mostly concern the number of cells seeded out and

the amount of medium added in the beginning. These adjustments were necessary to combine the differentiation with an siRNA-mediated KD. The NCCs obtained with this method showed a significantly lower expression of the stem cell markers Nanog, Oct4 and Sox2. At the same time, expression of the NCC markers p75 and Sox10 was elevated markedly. Furthermore, I detected an increase in the percentage of the HNK1/p75 double-positive cells of about 20%. Callahan and colleagues have shown, that after 10 days of differentiation NCCs can be mostly found in the overgrown parts and are not equally distributed on the plate [79]. Thus, I can assume that my differentiation protocol yielded a heterogeneous population of cells consisting of undifferentiated hiPSCs, NCCs and the different stages in between both. This assumption would also explain the variations between samples and that on average only about 20% of the cells were p75/HNK1 double positive. I hypothesize that during differentiation some of the cells reached a NC stem cell stage and did not further differentiate to NCCs. However, further experiments are needed to completely evaluate which stage of NCC differentiation was attained and how to optimize the protocol to generate pure populations of either NC stem cells or fully differentiated NCCs. For functional analysis of my obtained NCCs e.g., further differentiation capacity to melanocytes and migrative behavior, these NCCs need to be replated on an ornithine/laminin/fibronectin layer. In replating experiments, I observed that the coating strategy from Dr. Katrin Schrenk-Siemens in combination with adding Rock inhibitor to the medium allowed the NCCs to attach to the surface after splitting most efficiently. Moreover, most NCCs attached when maintained in melanocyte medium. However, more investigation is needed to establish an efficient replating protocol for NCCs that would allow the functional analysis of the NCCs I generated.

5.5 Investigation of the impact of kinase KD on the differentiation process of hiPSCs to NCCs

Previous studies from our research group [77], [83] led to the identification of several candidate kinases, which could have an effect on the differentiation of hiPSCs to NCCs. From these potential candidates I investigated the following six: ADCK2, DBF4, TYK2, EPHA4, ARAF and MAP2K3. In order to examine their influence on the differentiation of hiPSCs to NCCs, I knocked down each candidate kinase in hiPSCs while simultaneously differentiating these pluripotent cells to NCCs. A decreased level of stem cell along with an increased expression of NCC markers could be observed upon KD of ADCK2, DBF4 or KD of both kinases at the same time. In these NCCs, p75, Sox10, Cxcr4 and Pax3 were highly expressed. Interestingly, Sox10 and Cxcr4 are known to be mostly expressed in trunk NCCs that delaminate and/or exit the neural tube to start migration, but Sox10 is also important for the multipotent character of NC stem cells. Further, Sox10 is crucial for NCC survival and their self-renewal capacity. p75 and Pax3 are markers of NC precursors and Pax3 is also known to play a key role in melanocyte development [15], [28], [90], [120], [121]. Elevated expression of these different NCC markers supports the hypothesis, that the differentiation protocol established during my thesis yielded a heterogeneous population of NCCs, NC stem cells and intermediate links between them. In contrast, the KD of TYK2 or EPHA4 resulted in a reduced expression of the NCC markers p75 and Sox10 and an increased stem cell marker expression. The KD of ARAF or MAP2K3 led to a slightly increased expression of NCC and stem cell markers in hiPSCL2.

As of today, there is not much known about ADCK2 and its potential role in development. In one study, Vázquez-Fonseca and colleagues showed that a heterozygous knockout of ADCK2 in mice leads to locomotor dysfunctions but not to any defects in the central nervous system [61]. Other members of the ADCK family, namely ADCK1 and

ADCK4, are important for differentiation and development. ADCK1 has been shown to affect the development of Drosophila melanogaster. A homozygous KD resulted in smaller larvae compared to the WT and lethality already in the larval stage [122]. To evaluate if the KD of ADCK2 at the beginning of differentiation to NCCs results in enriched cell death an apoptosis assay needs to be done. In my studies I could observe, that a KD of ADCK2 led to a lower stem cell marker (Nanog, Oct4, Sox2) expression in NCCs obtained after 10 days of differentiation. It has been shown, that the promotor of ADCK4 binds Klf5, a stemness regulator, and further all Klf family members have been shown to play a role in cell differentiation and development [84]. In this light, it would be interesting to test the expression of Klf5 at different stages of differentiation and compare its levels between siControl and siADCK2-treated cells to investigate if ADCK2 also has a correlation to Klf5. Moreover, further experiments on the connection of ADCK2 and other stem cell markers would be of great interest. Furthermore, I could observe that a KD of ADCK2 followed by 10 days of differentiating hiPSCLs to NCCs yielded cells with an increased NCC marker expression compared to a control group without ADCK2 KD. ADCK family members have not been studied with reference to a potential role in vertebrate development. However, ADCK1 has been shown to influence the development of Drosophila melanogaster, where a loss of ADCK1 is lethal and a partial KD leads to a lower lifespan, slower development and smaller size [122]. In vertebrates, an effect of ADCK2 on muscle development has been suggested, because a haploinsufficiency of ADCK2 leads to an induction of several muscle development genes, among others. Most probably this is due to the function of ADCK2 within mitochondrial lipid oxidation and the CoQ metabolism [123]. Further, in humans a loss of ADCK2 can lead to liver dysfunction and a lipid storage myopathy [123], while a loss of ADCK3 is linked to ataxia and defects in ADCK4 can lead to steroid-resistant nephrotic syndrome [122]. Interestingly, all patients with lower levels of any ADCK family member show a CoQ deficiency [122], [123]. None of these studies have investigated the effect of ADCK family members on NCC development. For this reason, my results point to a new possible function of ADCK2 in the differentiation of hiPSCs into NCCs, which requires further investigation in order to be confirmed.

Interestingly, DBF4 (also known as ASK or MEKK5/6), ARAF and MAP2K3 (also known as MKK3, MEK3 or MAPKK3) are all components of the MAPK signaling pathway. DBF4 (Dumbell former 4 protein) is upstream of MAP2K3, which then activates the p38 pathway, which, next to other functions, is known to play a role in differentiation. p38 exists in four different isoforms (α, β, γ and δ), but MAP2K3 can only phosphorylate the α, γ and δ isoform but not p38 β [124]. Furthermore, DBF4 also plays a role in the JNK/SAPK pathway [124], which could be also the cause of the altered stem cell and NCC marker expression upon DBF4 KD in hiPSCs followed by 10 days of differentiation. Moreover, DBF4 mediates apoptosis upon stress stimuli [125]. Interestingly, DBF4 knockout mice did not show any developmental defects [125], while an inactivation of DBF4 together with the kinase Cdc7 led to cell death [126]. Further experiments are needed to investigate if the altered expression levels of stem cell and NCC markers upon DBF4 KD is due to cell death. Furthermore, DBF4 is known to share conserved motifs between different species and functions as the regulatory subunit of Cdc7 where it plays a role in controlling the activity of this cyclin-dependent kinase. Together, DBF4 and Cdc7 are involved in regulating DNA synthesis, meiosis and mitosis, among others [127]. Taking the connection of DBF4 and Cdc7 into account, a lower expression of DBF4 leading to a higher expression of NCC markers would also fit to the idea that for a successful initiation of differentiation cyclin-dependent kinase (CDKs) inhibitors might be necessary [128]. Interestingly, it has been found, that proliferation and differentiation are opposing mechanisms [129]. Differentiation is more likely to happen in G1, than in S phase of the cell cycle. Cells

emerging early in development do not have a measurable G1/G2 phase at all, in accordance with the rapid proliferation directly after fertilization. Also, naïve pluripotent cells go through a short G1 phase, which is later prolonged when differentiating. Further, it is known that different CDKs oscillate during different phases of the cell cycle. Together, this gives evidence that a short S1 phase and high CDK activity promote differentiation [129]. Interestingly, in humans, DBF4 mRNA and protein levels have been found to oscillate during the cell cycle, being highest in S phase and lowest in G2/M phase [126]. Taking these studies together, a KD of DBF4 in hiPSCs could prolong the G1/G2 phase, which in turn would lead to more differentiation. This would be in line with the increased expression of NCC markers revealed in my experiments. Moreover, it is known that lower levels of DBF4 result in a negative effect on cell proliferation, especially shown in different cancers like melanoma, gastric cancer and lung squamous cell carcinoma [130]–[132]. Further experiments are needed to evaluate the effect of DBF4 KD on proliferation of hiPSCs and during the differentiation to NCCs. Additionally, there are also some studies showing that DBF4 has an influence on development, especially of the eye and the heart. For example, in Xenopus it has been shown that DBF4 is an inhibitor of Wnt signaling [133]. Wnt signaling also plays an important role at the beginning of the differentiation from stem cells to NCCs. Studies have shown that Wnt activation is required very early in the differentiation process to get a sufficient amount of NCCs [134], [135]. In terms of the altered expression levels of stem cell and NCC markers upon DBF4 KD an investigation of the endogenous Wnt levels during differentiation would be of great interest. Furthermore, studying the role of DBF4 in ectoderm-derived cells, might yield new insights into NCC development and differentiation.

ARAF is involved in ERK signaling [124], which plays an important role in NCC development. ERK2 signaling is mandatory for the formation of NC-derived craniofacial structures [136]. Since a KD of ARAF in my experiments led to an increased stem cell and NCC marker expression in hiPSCL2, it would be of great interest to investigate ERK signaling during the differentiation of hiPSCs to NCCs.

EPHA4 and TYK2 both belong to the tyrosine kinase family. These kinases have been shown to play a major role in embryogenesis [137]. Smith and colleagues have shown that EPHA4 is essential for the correct migration of third arch NCCs to the third branchial arch during embryonic development and thereby directs these NCCs to their final destination [138]. In my study, I could show that EPHA4 KD during the differentiation of hiPSCs to NCCs led to an increase of stem cell along with a decrease of NCC marker expression. These observations indicate that EPHA4 is not only necessary for NCC migration as known from the literature, but might also be necessary for NCC development. Further experiments are needed to verify this hypothesis. Members of the TYK2 family have been shown to influence early embryogenesis by the activation of transcription factors and signaling cascades, some through associations with cytokine receptors [137], [139]. In my thesis, I could show that a KD of TYK2 altered the expression levels of stem cell and NCC markers during differentiation of hiPSCs to NCCs. The mechanism how TYK2 is influencing these marker expressions needs to be explored in more detail. Furthermore, it has been shown that the process of NCC development and tumorigenesis are similar in many respects [140] and that some cancers show an increased signaling as well as a high TYK2 immunoreactivity [141]. Taking these results together with the fact that tyrosine kinases are important for embryogenesis, one could speculate that TYK2 plays a role in NCC development by influencing the expression levels of stem cell and NCC markers.

Besides investigating the mechanism by which a KD of ADCK2, DBF4, TYK2 and EPHA4 alters the stem cell and NCC marker expression upon 10 days of differentiation, it would be also interesting to get further insights into the derived NCCs. It still remains questionable if these cells can further differentiate into cells like melanocytes or neurons.

Furthermore, it would be compelling to determine, if the KD also has an influence on this further development.

To sum up the second part of my thesis, I have successfully generated a new human induced pluripotent stem cell line from fibroblasts (hiPSCL2) and subcloned an already existing one (hiPSCL1) for further experiments. With these cells, I established a successful differentiation protocol for the generation of NCCs. This protocol yielded about 20% of p75/HNK1 double-positive cells. Furthermore, I have found, that a KD of ADCK2 and DBF4 at the beginning of differentiation decreased stem cell and increased NCC marker expression, whereas a KD of TYK2 and EPHA4 had the opposite effect.

6 Conclusion

In my thesis, I have shown that ADCK2 influences melanoma cell behavior. In detail, a KD of ADCK2 resulted in a lower cell viability and increased motility of melanoma cells. Moreover, the melanoma cells adopted a more dedifferentiated state upon ADCK2 KD indicated by a decrease of melanocyte marker and an increase of NCC marker expression. Ectopic OE of ADCK2 had the opposite effect on cell viability and motility of melanoma cells. ADCK2 most likely altered the cell motility via MYL6 since knocking down MYL6 could abolish the effect of ADCK2 OE on melanoma cells. One can speculate that MYL6 exerts its influence due to its function within NM2 and thus its contribution to the organization of actin filaments. Furthermore, by analyzing data from different online databases, I could reveal that high ADCK2 and MYL6 expression in the tumors of melanoma patients correlate with a better overall survival. Based on my results, I hypothesize that ADCK2 functions as a tumor suppressor in melanoma cells, preventing cancer cells from metastasizing. In this regard, ADCK2 and its downstream factor MYL6 might qualify as prognostic markers. Additionally, further studies will show if the knowledge about the molecular mechanisms influenced by ADCK2 and MYL6 might open up new possibilities for the development of therapeutic options for the treatment of melanoma.

As tumorigenesis and development share many similarities, the influence of ADCK2 (and other kinases) on the differentiation of hiPSCs to NCCs was investigated. For this purpose, I first generated two hiPSCLs that could be stably maintained on Matrigel, one by reprogramming fibroblasts and one by subcloning an existing cell line. Next, I established an efficient protocol for the differentiation of hiPSCs to NCCs in a xeno-free environment. This differentiation protocol was combined with siRNA KD of different candidate kinases. Here, I found that a KD of ADCK2 led to a lower stem cell along with a higher NCC marker expression. The same effect could be observed after knocking down DBF4 and also after simultaneous KD of ADCK2 and DBF4. However, the resemblance to naturally occurring NCCs in terms of functionality still needs to be validated. Furthermore, I could also show that a KD of TYK2 and EPHA4 led to higher stem cell along with lower NCC marker expression. So, one could speculate that TYK2 and EPHA4 might be essential for the development of NCCs. Additional experiments are needed to clarify this hypothesis.

In summary, I have shown that a KD of ADCK2 resulted in cells with more pronounced NCC-like character, either by dedifferentiating melanoma cells or by leading to a higher NCC marker expression upon differentiation of hiPSCs to NCCs. Based on these findings, one could speculate that ADCK2 counteracts NCC development and also acts as a tumor suppressor in melanoma. Since it has been shown in previous studies that ADCK2 also does not promote the differentiation of keratinocytes [83], it might be interesting to investigate the role of ADCK2 in mesoderm or endoderm-derived tissues. Furthermore, it would be interesting to study in more detail how ADCK2 and MYL6 control melanoma cell proliferation and motility in order to understand the mechanism behind metastasis. This knowledge might open up new possibilities for diagnostic and therapeutic applications for melanoma treatment.

7 References

[1] M. Z. Sun *et al.*,"Responding proteins for hacat cells against 2,4-dinitrobenzene sulfonic acid stimulation-A proteomic study," *The Journal of Animal & Plant Sciences*, vol. 26, no. 1, pp. 233–241, 2016

[2] T. Kordaß *et al.*, "SOX5 is involved in balanced MITF regulation in human melanoma cells," *BMC Medical Genomics*, vol. 9, no. 10, 2016

[3] A. Wessely *et al.*, "How neural crest transcription factors contribute to melanoma heterogeneity, cellular plasticity, and treatment resistance," *International Journal of Molecular Sciences*, vol. 22, no. 11, 2021

[4] J. D. Kubic *et al.*, "PAX3 and FOXD3 promote CXCR4 expression in melanoma," *The Journal of Biological Chemistry*, vol. 290, no. 36, pp. 21901–21914, 2015

[5] A. K. Bosserhoff, "Melanoma Development, Molecular Biology, Genetics and Clinical Application", 2nd edition, *Springer International Publishing AG,* 2017.

[6] P. F. Cheng *et al.*, "Methylation-dependent SOX9 expression mediates invasion in human melanoma cells and is a negative prognostic factor in advanced melanoma," *Genome Biology*, vol. 16, no. 42, 2015

[7] M. Rathore *et al.*, "Cancer cell-derived long pentraxin 3 (PTX3) promotes melanoma migration through a toll-like receptor 4 (TLR4)/NF-κB signaling pathway," *Oncogene*, vol. 38, no. 30, pp. 5873–5889, 2019

[8] R. M. Bakos *et al.*, "Nestin and SOX9 and SOX10 transcription factors are coexpressed in melanoma," *Experimental Dermatology*, vol. 19, no. 8, pp. e89-e94, 2010

[9] V. Montagnani *et al.*, "Thin and thick primary cutaneous melanomas reveal distinct patterns of somatic copy number alterations," *Oncotarget*, vol. 7, no. 21, pp. 30365–30378, 2016

[10] D. Fang *et al.*, "A tumorigenic subpopulation with stem cell properties in melanomas," *Cancer Res.*, vol. 65, no. 20, pp. 9328–9337, 2005

[11] S. E. Zabierowski and M. Herlyn, "Melanoma stem cells: The dark seed of melanoma," *Journal of Clinical Oncology*, vol. 26, no. 17, pp. 2890–2894, 2008

[12] T. Hirobe, "How are proliferation and differentiation of melanocytes regulated?," *Pigment Cell & Melanoma Research*, vol. 24, no. 3, pp. 462–478, 2011

[13] R. Mayor and E. Theveneau, "The neural crest," *Development*, vol. 140, no.11, pp. 2247-2251, 2013

[14] L. Larribere and J. Utikal, "De- and re-differentiation of the melanocytic lineage," *European Journal of Cell Biology*, vol. 93, no. 1-2, pp. 30–35, 2014

[15] O. Shakhova and L. Sommer, "Neural crest-derived stem cells ∗," *StemBook, ed. The Stem Cell Research Community, StemBook*, 2010

[16] M. P. O'Connell and A. T. Weeraratna, "Change is in the air: The hypoxic induction of phenotype switching in melanoma," *Journal of Investigatiove Dermatology*, vol. 133, no. 10, pp. 2316–2317, 2013

[17] J. E. Kim *et al*., "Heterogeneity of expression of epithelial-mesenchymal transition markers in melanocytes and melanoma cell lines," *frontiers in Genetics*, vol. 4, no. 97, 2013

[18] N. Knappe *et al.*, "Directed Dedifferentiation Using Partial Reprogramming Induces Invasive Phenotype in Melanoma Cells," *Stem Cells*, vol. 34, no. 4, pp. 832–846, 2016

[19] I. J. Bettum *et al.*, "Metabolic reprogramming supports the invasive phenotype in malignant melanoma," *Cancer Letters*, vol. 366, no. 1, pp. 71–83, 2015

[20] T. Kawakami *et al.*, "Approach for the Derivation of Melanocytes from Induced Pluripotent Stem Cells," *Journal of Investigative Dermatology*, vol. 138, no. 1, pp. 150–158, 2018

[21] N. Vandamme and G. Berx, "Melanoma cells revive an embryonic transcriptional network to dictate phenotypic heterogeneity," *frontiers in Oncology*, vol. 4, no. 352, pp. 1–6, 2014

[22] D. S. Widmer *et al.*, "Hypoxia contributes to melanoma heterogeneity by triggering HIF1α-dependent phenotype switching," *Journal of Investigative Dermatology*, vol. 133, no. 10, pp. 2436–2443, 2013

[23] M. E. Bronner and N. M. LeDouarin, "Development and evolution of the neural crest: An overview," *Developmental Biology*, vol. 366, no. 1, pp. 2–9, 2012

[24] M. Fukuta *et al.*, "Derivation of Mesenchymal Stromal Cells from Pluripotent Stem Cells through a Neural Crest Lineage using Small Molecule Compounds with Defined Media," *PLoS One*, vol. 9, no. 12, 2014

[25] M. Cichorek *et al.*, "Skin melanocytes: Biology and development," *Postepy Dermatologii i Alergologii*, vol. 30, no. 1, pp. 30–41, 2013

[26] A. Tomokiyo *et al.*, "Generation of Neural Crest-Like Cells From Human Periodontal Ligament Cell-Derived Induced Pluripotent Stem Cells," *Journal of Cellular Physiology*, vol. 232, no.2, pp. 402–416, 2016

[27] G. Lee *et al.*, "Isolation and directed differentiation of neural crest stem cells derived from human embryonic stem cells," *nature biotechnology*, vol. 25, no. 12, pp. 1468–1475, 2007

[28] C. L. Curchoe *et al.*, "Early Acquisition of Neural Crest Competence During hESCs Neuralization," *PLoS One*, vol. 5, no. 11, pp. 1-17, 2010

[29] Wissensschau.de, "Was sind Stammzellen?" 2021 Retrieved from: https://www.wissensschau.de/stammzellen/stammzellen_entwicklung_teilung Retrieved at: 09/2021

[30] Deutsches Referenzzentrum für Ethik in den Biowissenschaften, "Im Blickpunkt: Forschung mit humanen embryonalen Stammzellen," 2020. Retrieved from: http://www.drze.de/im-blickpunkt/stammzellen Retrieved at: 09/2021

[31] G. Q. Daley, "Stem cells and the evolving notion of cellular identity," *Philosophcal Transactions B Royal Society Publishing*, vol. 370, no. 1680, 2015

[32] J. L. Mignone *et al.*, "Neural potential of a stem cell population in the hair follicle," *Cell Cycle*, vol. 6, no. 17, pp. 2161–2170, 2007

[33] Y. Atlasi and H. G. Stunnenberg, "The interplay of epigenetic marks during stem cell differentiation and development," *Nature Reviews Genetics*, vol. 18, no. 11, pp. 643–658, 2017

[34] C. Jopling, S. Boue, and J. C. I. Belmonte, "Dedifferentiation, transdifferentiation and reprogramming: Three routes to regeneration," *Nature Reviews Molecular Cell Biology*, vol. 12, pp. 79–89, no. 2, 2011

[35] S. He *et al.*, "Passive DNA demethylation preferentially up-regulates pluripotency-related genes and facilitates the generation of induced pluripotent stem cells," *Journal of Biological Chemistry*, vol. 292, no. 45, pp. 18542–18555, 2017

[36] M. Vierthaler *et al.*, "Stammzellen - Das Rezept der Unsterblichkeit," in *Unsterblichkeit - Traum oder Trauma*, H. Kümper and W. Rosendahl, Eds. Nünnerich-Asmus, 2020

[37] K. Ohbo and S. Tomizawa, "Epigenetic regulation in stem cell development , cell fate conversion , and reprogramming," *De Gruyter, BioMol Concepts*, vol. 6, no. 1, pp. 1–9, 2015

[38] K. Takahashi and S. Yamanaka, "Induction of Pluripotent Stem Cells from Mouse Embryonic and Adult Fibroblast Cultures by Defined Factors," *Cell*, vol. 126, no. 4, pp. 663–676, 2006

[39] M. Galach and J. Utikal, "From skin to the treatment of diseases - the possibilities of iPS cell research in dermatology," *Experimental Dermatology*, vol. 20, no. 6, pp. 523–528, 2011

[40] N. Malik and M. S. Rao, "A review of the methods for human iPSC derivation," *Methods in Molecular Biology*, vol. 997, pp. 23–33, 2013

[41] J. Utikal *et al*., "Sox2 is dispensable for the reprogramming of melanocytes and melanoma cells into induced pluripotent stem cells," *Journal of Cell Science*, vol. 122, no. 19, pp. 3502-3510, 2009

[42] K. M. Kim *et al.*, "High–efficiency generation of induced pluripotent stem cells from human foreskin fibroblast cells using the Sagunja-tang herbal formula," *BMC Complementary and Alternative Medicine*, vol. 17, no. 1, 2017

[43] U. Martin, "Therapeutic Application of Pluripotent Stem Cells : Challenges and Risks," *frontiers in Medicine*, vol. 4, 2017

[44] C. M. Bailey, J. A. Morrison, and P. M. Kulesa, "Melanoma revives an embryonic migration program to promote plasticity and invasion," *Pigment Cell & Melanoma Research*, vol. 25, no. 5, pp. 573–583, 2012

[45] M. B. Weiss *et al.*, "FOXD3 Modulates Migration through Direct Transcriptional Repression of TWIST1 in Melanoma," *Molecular Cancer Research*, vol. 12, no. 9, pp. 1314–1323, 2014

[46] X. Nissan *et al.*, "Functional melanocytes derived from human pluripotent stem cells engraft into pluristratified epidermis," *Proceedings of the National Academy of Sciences*, vol. 108, no. 36, pp. 14861–14866, 2011

[47] J. Yang *et al.*, "BMP4 is required for the initial expression of MITF in melanocyte precursor differentiation from embryonic stem cells," *Experimental Cell Research*, vol. 320, no. 1, pp. 54–61, 2014

[48] T. Rothhammer *et al*., "Bone Morphogenic Proteins Are Overexpressed in Malignant Melanoma and Promote Cell Invasion and Migration," *Cancer Research*, vol. 65, no. 2, pp. 448–457, 2005

[49] M. Avitabile *et al.*, "Neural crest derived tumors neuroblastoma and melanoma share 1p13.2 as susceptibility locus that shows a long-range interaction with the *SLC16A1* gene," *Carcinogenesis*, vol. 41, no. 3, pp. 284-295, 2020

[50] J. D. Kubic *et al*., "FOXD3 promotes PAX3 expression in melanoma cells," *Journal of Cell Biochemistry*, vol. 117, no. 2, pp. 533–541, 2016

[51] M. Bernhardt *et al*., "Mediators of induced pluripotency and their role in cancer cells - current scientific knowledge and future perspectives," *Biotechnology Journal*, vol. 7, no. 6, pp. 810-821, 2012

[52] A. Schoolmeesters, D. D. Brown, and Y. Fedorov, "Kinome-Wide Functional Genomics Screen Reveals a Novel Mechanism of TNFa-Induced Nuclear Accumulation of the HIF-1a Transcription Factor in Cancer Cells," *PLoS One*, vol. 7, no. 2, 2012

[53] Y. Nakashima *et al*., "Atorvastatin Inhibits the HIF1α-PPAR Axis, Which Is Essential for Maintaining the Function of Human Induced Pluripotent Stem Cells," *Molecular Therapy*, vol. 26, no. 7, pp. 1715–1734, 2018

[54] R. Brough *et al.*, "Functional Viability Profiles of Breast Cancer," *Cancer Discovery*, vol. 1, no. 3, pp. 260–273, 2011

[55] C. J. Leonard, L. Aravind, and E. V. Koonin, "Novel families of putative protein kinases in bacteria and archaea: Evolution of the 'eukaryotic' protein kinase superfamily," *Genome Research*, vol. 8, no. 10, pp. 1038–1047, 1998

[56] C. Lagier-Tourenne *et al.*, "ADCK3 , an Ancestral Kinase , Is Mutated in a Form of Recessive Ataxia Associated with Coenzyme Q 10 Deficiency," *The American Journal of Human Genetics,* vol. 82, no. 3, pp. 661–672, 2008

[57] M. Qiu *et al.*, "aarF domain containing kinase 5 gene promotes invasion and migration of lung cancer cells through ADCK5-SOX9-PTTG1 pathway," *Experimental Cell Research*, vol. 392, no.1, 2020

[58] T. Kakiuchi *et al*., "Association between Crohn ' s disease and AarF domain-containing kinase 4 glomerulopathy," *Clinical Journal of Gastroenterology*, vol. 12, no. 3, pp. 263–268, 2019

[59] L. Goto *et al*., "Therapeutic predictors of neoadjuvant endocrine therapy response in estrogen receptor-positive breast cancer with reference to optimal gene expression profiling," *Breast Cancer Research and Treatment*, vol. 172, no. 2, pp. 353–362, 2018

[60] B. Wheeler and Z. Jia, "Preparation and characterization of human ADCK3 , a putative atypical kinase," *Protein Expression and Purification*, vol. 108, pp. 13–17, 2015

[61] L. Vázquez-Fonseca *et al.*, "ADCK2 Haploinsufficiency Reduces Mitochondrial Lipid Oxidation and Causes Myopathy Associated with CoQ Deficiency," *Journal of Clinical Medicine*, vol. 8, no. 9, 2019

[62] E. Iorns *et al.*, "Integrated functional, gene expression and genomic analysis for the identification of cancer targets," *PLoS One*, vol. 4, no. 4, 2009

[63] S. Egashira *et al.*, "Recurrent Fusion Gene ADCK4-NUMBL in Cutaneous Squamous Cell Carcinoma Mediates Cell Proliferation," *Journal of Investigative Dermatology*, vol. 139, no. 4, pp. 954–957, 2019

[64] K. J. Simpson *et al.*, "Identification of genes that regulate epithelial cell migration using an siRNA screening approach," *Nature Cell Biology,* vol. 10, no. 9, pp. 1027–1038, 2008

[65] W. R. Wiedemeyer *et al.*, "Pattern of retinoblastoma pathway inactivation dictates response to CDK4/6 inhibition in GBM," *Proceedings of the National Academy of Sciences of the United States of America*, vol. 107, no. 25, pp. 11501–11506, 2010

[66] C. Brito and S. Sousa, "Non-Muscle Myosin 2A (NM2A): Structure, Regulation and Function," *Cells*, vol. 9, no. 7, 2020

[67] V. Betapudi, "Life without double-headed non-muscle myosin II motor proteins," *frontiers in Chemistry*, vol. 2, pp. 1–13, 2014

[68] Y. R. Li and W. X. Yang, "Myosins as fundamental components during tumorigenesis: diverse and indispensable," *Oncotarget*, vol. 7, no. 29, pp. 46785–46812, 2016

[69] J. R. Sellers and S. M. Heissler, "Nonmuscle myosin-2 isoforms," *Current Biology*, vol. 29, no. 8, pp. R265-R279, 2019

[70] S. M. Heissler and D. J. Manstein, "Nonmuscle myosin-2: Mix and match," *Cellular and Molecular Life Sciences*, vol. 70, no. 1, pp. 1–21, 2013

[71] N. Hundt *et al*., "Load-dependent modulation of non-muscle myosin-2A function by tropomyosin 4.2," *Scientific Reports*, vol. 6, 2016

[72] C. Li *et al*., "Cell type and culture condition-dependent alternative splicing in human breast cancer cells revealed by splicing-sensitive microarrays," *Cancer Research*, vol. 66, no. 4, pp. 1990–1999, 2006

[73] M. F. Halstead *et al.*, "An unusual transduction pathway in human tonic smooth muscle myosin," *Biophysical Journal*, vol. 93, no. 10, pp. 3555–3566, 2007

[74] I. Park *et al.*, "Myosin regulatory light chains are required to maintain the stability of myosin II and cellular integrity," *Biochemical Journal*, vol. 434, no. 1, pp. 171–180, 2011

[75] E. Golomb *et al.*, "Identification and Characterization of Nonmuscle Myosin II-C, a New Member of the Myosin II Family," *The Journal of Biological Chemistry*, vol. 279, no. 4, pp. 2800–2808, 2004

[76] K. Weina, "Functional analysis of SOX2 in melanocyte development and melanoma pathogenesis," doctoral thesis, Ruperto-Carola University of Heidelberg, Germany, 2015

[77] L. Larribere *et al.*, "NF1 loss induces senescence during human melanocyte differentiation in an iPSC-based model," *Pigment Cell & Melanoma Research*, vol. 28, no. 4, pp. 407–416, 2015

[78] K. Schrenk-Siemens *et al.*, "PIEZO2 is required for mechanotransduction in human stem cell-derived touch receptors," *Nature Neuroscience*, vol. 18, no. 1, pp. 10–16, 2015

[79] S. J. Callahan, Y. Mica, and L. Studer, "Feeder-free Derivation of Melanocytes from Human Pluripotent Stem Cells," *Journal of Visualized Experiments*, no. 109, 2016

[80] R Core Team, "R: A language and environment for statistical computing". *R Foundation for Statistical Computing.* 2019, [Online]. Available: https://www.r-project.org/

[81] G. K. Smyth, "Linear models and empirical bayes methods for assessing differential expression in microarray experiments," *Statistical Applications in Genetics and Molecular Biology,* vol. 3, 2004

[82] J. W. Gordon *et al*., "Limma: linear models for microarray data"*. Bioinformatics and Computational Biology Solutions using R and Bioconductor.* New York: Springer, 2005

[83] L. Larribère *et al.*, "An RNAi Screen Reveals an Essential Role for HIPK4 in Human Skin Epithelial Differentiation from iPSCs," *Stem Cell Reports*, vol. 9, no. 4, pp. 1234–1245, 2017

[84] X. Chen *et al*., "Transcription factor Kruppel-like factor 5 positively regulates the expression of AarF domain containing kinase 4," *Molecular Biology Reports.*, vol. 47, no. 11, pp. 8419-8427, 2020

[85] D. R. Macinga *et al.*, "Identification and characterization of *aarF*, a locus required for production of ubiquinone in *Providencia stuartii* and *Escherichia coli* and for expression of 2′-N-acetyltransferase in *P. stuartii*," *Journal of Bacteriology*, vol. 180, no. 1, pp. 128–135, 1998

[86] A. J. Penning *et al.*, "Novel *BRAF* gene fusions and activating point mutations in spindle cell sarcomas with histologic overlap with infantile fibrosarcoma," *Modern Pathology*, vol. 34, no. 8, pp. 1530-1540, 2021

[87] L. Sommer, "Generation of melanocytes from neural crest cells," *Pigment Cell & Melanoma Research*, vol. 24, no. 3, pp. 411–421, 2011

[88] A. J. Thomas and C. A. Erickson, "FOXD3 regulates the lineage switch between neural crest derived glial cells and pigment cells by repressing MITF through a non-canonical mechanism," *Development*, vol. 136, no. 11, pp. 1849–1858, 2009

[89] R. Kos *et al*., "The winged-helix transcription factor FoxD3 is important for establishing the neural crest lineage and repressing melanogenesis in avian embryos" *Development*, vol. 128, no. 8, pp. 1467–1479, 2001

[90] S. Medic, H. Rizos, and M. Ziman, "Differential PAX3 functions in normal skin melanocytes and melanoma cells," *Biochemical and Biophysial Research Communications*, vol. 411, no. 4, pp. 832–837, 2011

[91] A. M. Mallon *et al.*, "Comparative genome sequence analysis of the *Bpa/Str* region in mouse and man," *Genome Research*, vol. 10, no. 6, pp. 758–775, 2000

[92] M. Huang, T. F. Qi, L. Li, G. Zhang, and Y. Wang, "A targeted quantitative proteomic approach assesses the reprogramming of small GTPases during melanoma metastasis," *Cancer Research*, vol. 78, no. 18, pp. 5431–5445, 2018

[93] K. K. Dey *et al.*, "Identification of RAB2A and PRDX1 as the potential biomarkers for oral squamous cell carcinoma using mass spectrometry-based comparative proteomic approach," *Tumor Biology*, vol. 36, no.12, pp. 9829–9837, 2015

[94] Y. D. He *et al.*, "Isolation, sequence identification and expression profile of three novel genes *Rab2A*, *Rab3A* and *Rab7A* from black-boned sheep (*Ovis aries*)," *Molecular Biology*, vol. 44, no. 1, pp. 14–22, 2010

[95] H. Jin *et al.*, "Rab GTPases: Central Coordinators of Membrane Trafficking in Cancer," *frontiers in Cell and Developmental Biology*, vol. 9, 2021

[96] H. Liu *et al.*, "Rab26 suppresses migration and invasion of breast cancer cells through mediating autophagic degradation of phosphorylated Src," *Cell Death and Disease*, vol. 12, no. 4, 2021

[97] H. Kajiho *et al.*, "RAB2A controls MT1-MMP endocytic and E-cadherin polarized Golgi trafficking to promote invasive breast cancer programs," *EMBO Reports*, vol. 17, no. 7, pp. 1061–1080, 2016

[98] X. F. Zheng *et al*., "MicroRNA-192 acts as a tumor suppressor in colon cancer and simvastatin activates miR-192 to inhibit cancer cell growth," *Molecular Medicine Reports*, vol. 19, no. 3, pp. 1753–1760, 2019

[99] K. K. Dey *et al.*, "S100A7 has an oncogenic role in oral squamous cell carcinoma by activating p38/MAPK and RAB2A signaling pathway," *Cancer Gene Therapy*, vol. 23, no. 11, pp. 382-391, 2016

[100] M. L. Luo *et al.*, "The Rab2A GTPase promotes breast cancer stem cells and tumorigenesis via erk signaling activation," *Cell Reports*, vol. 11, no. 1, pp. 111–124, 2015

[101] L. Wang *et al.*, "Over-expression of Rap2a inhibits glioma migration and invasion by down-regulating p-AKT," *Cell Biology International,* vol. 38, no. 3, pp. 326–334, 2014

[102] M. I. Lomnytska *et al.*, "Diagnostic protein marker patterns in squamous cervical cancer," *Proteomics - Clinical Applications,* vol. 4, no. 1, pp. 17–31, 2010

[103] J. Middelbeek *et al.*, "The TRPM7 interactome defines a cytoskeletal complex linked to neuroblastoma progression," *European Journal of Cell Biology*, vol. 95, no. 11, pp. 465–474, 2016

[104] F. Deng *et al.*, "Classify multicategory outcome in patients with lung adenocarcinoma using clinical, transcriptomic and clinico-transcriptomic data: machine learning versus multinomial models.," *American Journal of Cancer Research*, vol. 10, no. 12, pp. 4624–4639, 2020

[105] N. J. W. De Wit *et al.*, "Analysis of differential gene expression in human melanocytic tumour lesions by custom made oligonucleotide arrays," *British Journal of Cancer*, vol. 92, no. 12, pp. 2249–2261, 2005

[106] A. V. Timofeeva *et al.*, "miRNAs and their gene targets—a clue to differentiate pregnancies with small for gestational age newborns, intrauterine growth restriction, and preeclampsia," *Diagnostics*, vol. 11, no. 4, 2021

[107] E. D. Decker *et al.*, "Proteomic analysis of differential protein expression induced by ultraviolet light radiation in HeLa cells," *Proteomics*, vol. 3, no. 10, pp. 2019–2027, 2003

[108] R. K. Mongre, S. Jung, C. B. Mishra, B. S. Lee, S. Kumari, and M. S. Lee, "Prognostic and clinicopathological significance of sertad1 in various types of cancer risk: A systematic review and retrospective analysis," *Cancers*, vol. 11, no. 3, 2019

[109] L. Huo *et al.*, "Identification of novel partner proteins of PCBP1," *Journal of Peking University (Health Sciences)*, vol. 41, no. 4, pp. 402–408, 2009

[110] A. Kourtidis and P. Z. Anastasiadis, "PLEKHA7 defines an apical junctional complex with cytoskeletal associations and miRNA-mediated growth implications," *Cell Cycle*, vol. 15, no. 4, pp. 498–505, 2016

[111] K. Cao *et al.*, "Quantitative Analysis of Seven New Prostate Cancer Biomarkers and the Potential Future of the 'Biomarker Laboratory,'" *Diagnostics*, vol. 8, no. 3, 2018

[112] D. Schramek *et al.*, "Direct in vivo RNAi screen unveils myosin IIa as a tumor suppressor of squamous cell carcinomas," *Science*, vol. 343, no. 6168, pp. 309–313, 2014

[113] S. S. Jana, S. Kawamoto, and R. S. Adelstein, "A Specific Isoform of Nonmuscle Myosin II-C Is Required for Cytokinesis in a Tumor Cell Line," *The Journal of Biological Chemistry*, vol. 281, no. 34, pp. 24662–24670, 2006

[114] M. S. Shutova and T. M. Svitkina, "Common and Specific Functions of Nonmuscle Myosin II Paralogs in Cells," *Biochemistry*, vol. 83, no. 12, pp. 1459–1468, 2018

[115] S. Bhatt *et al.*, "Signals and Switches in Mammalian Neural Crest Cell Differentiation Signals and Switches in Mammalian Neural Crest Cell Differentiation," *Cold Spring Harbor Perspectives in Biology*, vol. 5, no. 2, 2013

[116] K. Opdecamp *et al.*, "Melanocyte development in vivo and in neural crest cell cultures: crucial dependence on the Mitf basic-helix-loop-helix-zipper transcription factor.," *Development*, vol. 124, no. 12, pp. 2377–2386, 1997

[117] J. Itskovitz-Eldor *et al.*, "Differentiation of human embryonic stem cells into embryoid bodies compromising the three embryonic germ layers.," *Molecular Medicine*, vol. 6, no. 2, pp. 88-95, 2000

[118] G. Höpfl, M. Gassmann, and I. Desbaillets, "Differentiating Embryonic Stem Cells into Embryoid Bodies," *Methods in Molecular Biology*, vol. 254, pp. 79-98, 2004

[119] M. V. Wiles and G. Keller, "Multiple hematopoietic lineages develop from embryonic stem (ES) cells in culture," *Development*, vol. 111, no. 2, pp. 259–267, 1991

[120] A. Baggiolini *et al.*, "Premigratory and migratory neural crest cells are multipotent in vivo," *Cell Stem Cell*, vol. 16, no. 3, pp. 314–322, 2015

[121] L. Dyson *et al.*, "A chemotactic model of trunk neural crest cell migration," *Genesis*, vol. 56, no. 9, 2018

[122] D. R. Wisidagama *et al*., "Functional analysis of Aarf domain-containing kinase 1 in Drosophila melanogaster," *Developmental Dynamics*, vol. 248, no. 9, pp. 762–770, 2019

[123] Vázquez-Fonseca *et al.*, "ADCK2 Haploinsufficiency Reduces Mitochondrial Lipid Oxidation and Causes Myopathy Associated with CoQ Deficiency," *Journal of Clinical Medicine*, vol. 8, no. 9, 2019

[124] Z. Wei and H. T. Liu, "MAPK signal pathways in the regulation of cell proliferation in mammalian cells," *Cell Research*, vol. 12, no. 1, pp. 9–18, 2002

[125] E. A. Craig *et al.*, "MAP3Ks as central regulators of cell fate during development," *Developmental Dynamics*, vol. 237, no. 11, pp. 3102–3114, 2008

[126] J. M. Kim, M. Yamada, and H. Masai, "Functions of mammalian Cdc7 kinase in initiation / monitoring of DNA replication and development," *Mutation Research*, vol. 532, no. 1-2, pp. 29–40, 2003

[127] L. A. Matthews and A. Guarné, "Dbf4 - The whole is greater than the sum of its parts," *Cell Cycle*, vol. 12, no. 8, pp. 1180–1188, 2013

[128] G. Brown, P. J. Hughes, and R. H. Michell, "Cell differentiation and proliferation - Simultaneous but independent?," *Experimental Cell Research*, vol. 291, no. 2, pp. 282–288, 2003

[129] S. Ruijtenberg and S. van den Heuvel, "Coordinating cell proliferation and differentiation: Antagonism between cell cycle regulators and cell type-specific gene expression," *Cell Cycle*, vol. 15, no. 2, pp. 196–212, 2016

[130] S. Nambiar *et al.*, "Identification and functional characterization of *ASK/Dbf4*, a novel cell survival gene in cutaneous melanoma with prognostic relevance," *Carcinogenesis*, vol. 28, no. 12, pp. 2501–2510, 2007

[131] Y. Qi, Y. Hou, and L. Qi, "miR-30d-5p represses the proliferation, migration, and invasion of lung squamous cell carcinoma via targeting DBF4," *Journal of Environmental Science and Health, Part C*, vol. 39, no. 3, pp. 251-268, 2021

[132] T. Wang *et al.*, "Lactate Induces Aberration in the miR-30a-DBF4 Axis to Promote the Development of Gastric Cancer and Weakens the Sensitivity to 5-Fu," *Cancer Cell International*, In Review, 2021

[133] B. K. Brott and S. Y. Sokol, "A Vertebrate Homolog of the Cell Cycle Regulator Dbf4 Is an Inhibitor of Wnt Signaling Required for Heart Development," *Developmental Cell*, vol. 8, no. 5, pp. 703–715, 2005

[134] Y. Mica *et al*., "Modeling Neural Crest Induction, Melanocyte Specification, and Disease-Related Pigmentation Defects in hESCs and Patient-Specific iPSCs," *Cell Reports*, vol. 3, no. 4, pp. 1140–1152, 2013

[135] M. I. García-Castro, C. Marcelle, and M. Bronner-Fraser, "Ectodermal Wnt function as a neural crest inducer.," *Science*, vol. 297, no. 5582, pp. 848–51, 2002

[136] J. Newbern *et al.*, "Mouse and human phenotypes indicate a critical conserved role for ERK2 signaling in neural crest development," *Proceedings of the National Academy of Sciences of the United States of America*, vol. 105, no. 44, pp. 17115–17120, 2008

[137] A. W. Brändli and M. W. Kirschner, "Molecular cloning of tyrosine kinases in the early *Xenopus* embryo: Identification of Eck-related genes expressed in cranial neural crest cells of the second (Hyoid) Arch," *Developmental Dynamics*, vol. 203, no. 2, pp. 119–140, 1995

[138] A. Smith *et al*., "The EphA4 and EphB1 receptor tyrosine kinases and ephrin-B2 ligand regulate targeted migration of branchial neural crest cells," *Current Biology*, vol. 7, no. 8, pp. 561-570, 1997

[139] B. A. Witthuhn *et al.*, "JAK2 associates with the erythropoietin receptor and is tyrosine phosphorylated and activated following stimulation with erythropoietin," *Cell*, vol. 74, no. 2, pp. 227–236, 1993

[140] M. Avitabile *et al.*, "Neural crest-derived tumor neuroblastoma and melanoma share 1p13.2 as susceptibility locus that shows a long-range interaction with the *SLC16A1* gene," *Carcinogenesis*, vol. 41, no. 3, pp. 284–295, 2020

[141] A. C. Hirbe *et al.*, "Clinical genomic profiling identifies *TYK2* mutation and overexpression in patients with neurofibromatosis type 1-associated malignant peripheral nerve sheath tumors," *Cancer*, vol. 123, no. 7, pp. 1194–1201, 2017

8 Supplemental material

8.1 Supplementary Figures

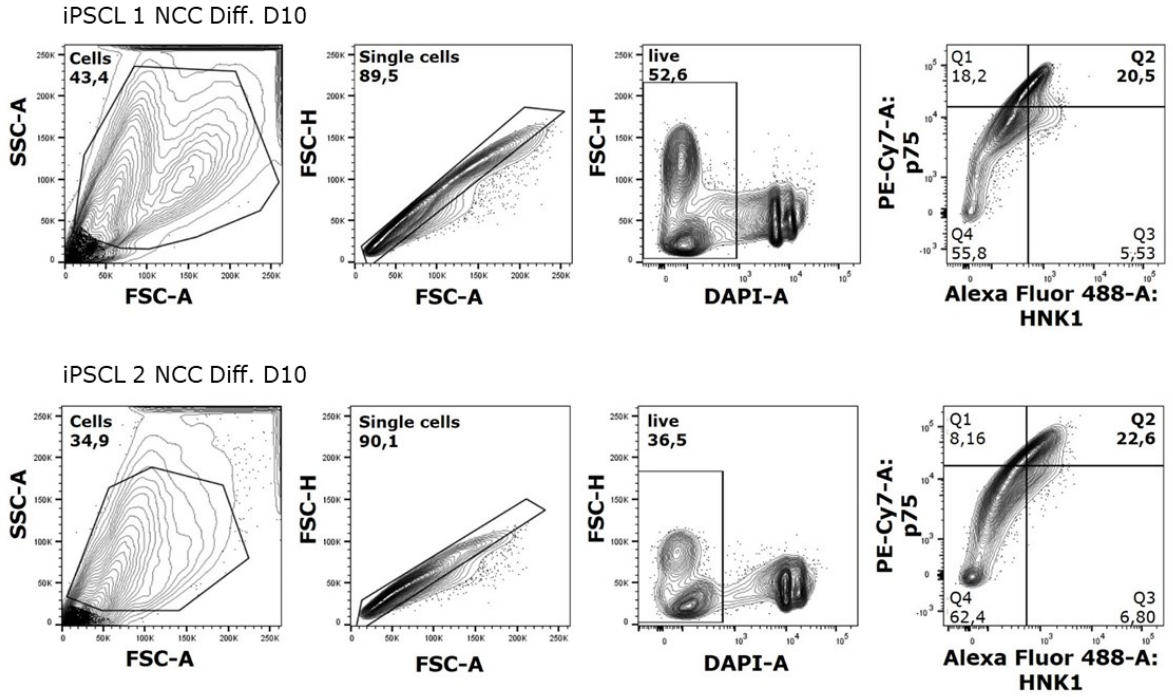

Supplementary Figure 1: Gating strategy
The used gating strategy for flow cytometry analysis with representative pictures. Top panels: hiPSCL1, bottom panels: hiPSCL2

8.2 Supplementary Tables

Supplementary Table 1: *Gene expression analysis results: NCC development genes of 10 days differentiated hiPSL1 cells transfected with siADCK2 vs. siControl*

This table shows the ID as well as the symbol of all NCC development genes (GO:0014032) together with logFC and further data. Cells of hiPSCL1 were transfected with siADCK2 and differentiated into NCCs for 10 days. These were then compared to siControl transfected and differentiated cells.

ID	SYMBOL	logFC	AveExpr	t	P.Value	adj.P.Val	B
NM_183374	CYP26C1	-1,203	6,568	-4,492	0,000	0,115	0,485
NM_001159995	NRG1	-1,187	5,954	-2,740	0,013	0,281	-2,864
NM_003966	SEMA5A	-0,993	9,172	-3,405	0,003	0,186	-1,611
NM_152754	SEMA3D	-0,939	6,528	-2,991	0,008	0,238	-2,399
NM_172037	RDH10	-0,921	6,868	-2,582	0,019	0,301	-3,150
NM_003108	SOX11	-0,553	9,345	-2,710	0,014	0,286	-2,919
SEMA3A.gAug10-unspliced	SEMA3A	-0,528	5,098	-1,441	0,167	0,588	-4,923
NM_000115	EDNRB	-0,505	8,733	-3,006	0,008	0,237	-2,371
NM_001163417	FAM172A	-0,426	7,590	-1,633	0,120	0,533	-4,672
NM_001198999	SEMA6D	-0,413	7,527	-1,418	0,173	0,594	-4,952
NM_004429	EFNB1	-0,406	9,208	-1,746	0,098	0,504	-4,513
NM_003068	SNAI2	-0,346	8,855	-1,086	0,292	0,697	-5,322

NM_001202	BMP4	-0,336	9,969	-1,373	0,186	0,608	-5,006
NM_001719	BMP7	-0,335	9,464	-1,303	0,209	0,631	-5,089
NM_012392	PEF1	-0,282	6,815	-1,379	0,185	0,607	-5,000
NM_001271661	SEMA4F	-0,268	6,860	-1,352	0,193	0,614	-5,032
NM_005507	CFL1	-0,264	11,390	-2,056	0,055	0,418	-4,043
NM_006379	SEMA3C	-0,239	9,048	-0,853	0,405	0,772	-5,530
ISL1.cAug10-unspliced	ISL1	-0,223	6,466	-1,025	0,319	0,718	-5,381
NM_032505	KBTBD8	-0,218	6,369	-0,808	0,429	0,786	-5,565
NM_014587	SOX8	-0,215	7,683	-1,188	0,250	0,667	-5,217
NM_001155	ANXA6	-0,209	9,597	-1,312	0,206	0,628	-5,079
ENST00000525710	CFL1	-0,203	7,117	-0,765	0,454	0,800	-5,596
NM_001031702	SEMA5B	-0,198	7,879	-1,226	0,236	0,652	-5,176
NM_004329	BMPR1A	-0,186	11,151	-1,333	0,199	0,621	-5,055
NM_003872	NRP2	-0,170	10,678	-0,625	0,540	0,842	-5,689
NM_004558	NRTN	-0,169	8,112	-0,991	0,335	0,730	-5,412
NM_000899	KITLG	-0,137	7,617	-0,351	0,730	0,917	-5,817
NM_001206897	ALDH1A2	-0,123	6,623	-0,699	0,494	0,821	-5,643
ENST00000471474	SEMA3A	-0,117	3,642	-0,303	0,765	0,929	-5,832
NM_005524	HES1	-0,115	8,818	-0,519	0,610	0,872	-5,747
ERBB4.jAug10-unspliced	ERBB4	-0,107	3,186	-0,585	0,566	0,853	-5,712
NM_005631	SMO	-0,103	8,849	-0,778	0,447	0,796	-5,587
NM_001146029	SEMA7A	-0,099	8,289	-0,581	0,568	0,854	-5,714
NM_002202	ISL1	-0,084	5,746	-0,314	0,757	0,927	-5,829
NM_005560	LAMA5	-0,075	9,134	-0,311	0,760	0,928	-5,830
NM_153365	TAPT1	-0,073	7,592	-0,374	0,713	0,910	-5,809
NM_000193	SHH	-0,070	6,283	-0,351	0,729	0,917	-5,817
NM_001142287	SEMA4D	-0,062	8,888	-0,334	0,742	0,922	-5,823
NM_032108	SEMA6B	-0,060	8,334	-0,275	0,786	0,935	-5,840
NM_002745	MAPK1	-0,046	10,322	-0,407	0,689	0,902	-5,797
NM_001048183	PHACTR4	-0,042	9,064	-0,294	0,772	0,931	-5,835
NM_020210	SEMA4B	-0,041	8,557	-0,252	0,804	0,940	-5,846
NM_003924	PHOX2B	-0,039	8,022	-0,251	0,804	0,940	-5,846
NM_020163	SEMA3G	-0,034	7,659	-0,185	0,855	0,958	-5,860
NM_001453	FOXC1	-0,024	7,765	-0,112	0,912	0,975	-5,871
NM_001243084	HIF1A	-0,015	10,947	-0,109	0,914	0,975	-5,871
NM_000325	PITX2	0,001	9,632	0,003	0,997	0,999	-5,877
NM_001024628	NRP1	0,010	7,947	0,045	0,964	0,992	-5,876
NM_001193300	SEMA4A	0,011	7,615	0,058	0,955	0,988	-5,875
NM_001105237	CORO1C	0,022	10,726	0,159	0,875	0,963	-5,864
NM_001040056	MAPK3	0,029	10,129	0,243	0,811	0,943	-5,848
NM_001178061	SEMA6C	0,031	8,735	0,109	0,914	0,975	-5,871
NM_006080	SEMA3A	0,034	10,348	0,117	0,908	0,974	-5,870
NM_000867	HTR2B	0,044	4,158	0,171	0,866	0,962	-5,863
NM_000356	TCOF1	0,056	9,314	0,327	0,748	0,923	-5,825
NM_001171653	ZEB2	0,059	8,910	0,256	0,801	0,939	-5,845
NM_001284388	NOLC1	0,075	10,537	0,505	0,620	0,877	-5,754
NM_006982	ALX1	0,083	5,634	0,218	0,830	0,949	-5,854

NM_001005914	SEMA3B	0,084	7,338	0,446	0,661	0,892	-5,781
NM_005251	FOXC2	0,086	6,372	0,468	0,646	0,886	-5,771
NM_001306129	FN1	0,092	11,194	0,375	0,712	0,910	-5,809
NM_001303051	KLHL12	0,107	8,607	0,750	0,463	0,804	-5,607
NM_001267556	PDCD6	0,108	7,897	0,763	0,456	0,800	-5,598
NM_001166055	EDNRA	0,109	9,769	0,517	0,611	0,873	-5,748
NM_017789	SEMA4C	0,113	8,765	0,802	0,433	0,788	-5,569
NM_000514	GDNF	0,117	7,612	0,589	0,563	0,852	-5,709
NM_001302455	EDN3	0,121	6,059	0,942	0,359	0,741	-5,456
NM_020630	RET	0,136	7,482	0,933	0,363	0,743	-5,464
NM_001203244	SEMA4G	0,136	5,815	0,593	0,560	0,851	-5,707
NM_005117	FGF19	0,140	7,861	0,911	0,374	0,751	-5,482
NM_001168319	EDN1	0,172	7,723	0,625	0,540	0,842	-5,689
NM_021973	HAND2	0,173	6,990	1,254	0,226	0,643	-5,145
hsa_circ_0001872	SEMA4D	0,176	7,927	0,945	0,357	0,740	-5,453
ENST00000530157	CFL1	0,180	3,839	0,751	0,462	0,804	-5,607
NM_000346	SOX9	0,189	8,941	0,914	0,373	0,750	-5,480
NRP1.vdAug10-unspliced	NRP1	0,203	3,910	0,862	0,400	0,769	-5,523
NM_000214	JAG1	0,249	10,179	1,355	0,192	0,613	-5,028
NM_005992	TBX1	0,253	8,122	0,927	0,366	0,745	-5,469
NM_001105	ACVR1	0,254	8,174	1,068	0,300	0,704	-5,340
NM_001042599	ERBB4	0,270	7,803	1,338	0,198	0,620	-5,049
NM_001300780	SEMA6A	0,304	12,171	1,558	0,136	0,552	-4,773
NM_004186	SEMA3F	0,313	8,036	1,667	0,113	0,526	-4,626
NM_006941	SOX10	0,385	7,889	1,690	0,108	0,520	-4,593
NM_000474	TWIST1	0,414	7,669	2,015	0,059	0,426	-4,108
NM_001303461	OVOL2	0,444	6,820	1,536	0,142	0,558	-4,802
NM_000802	FOLR1	0,451	6,475	1,546	0,139	0,555	-4,789
NM_001301687	GBX2	0,513	7,265	1,881	0,076	0,464	-4,315
NM_001178129	SEMA3E	0,840	8,255	2,529	0,021	0,310	-3,245

Supplementary Table 2: *Gene expression analysis results: NCC development genes of 10 days differentiated hiPSL2 cells transfected with siADCK2 vs. siControl*

This table shows the ID as well as the symbol of all NCC development genes (GO:0014032) together with logFC and further data. Cells of hiPSCL2 were transfected with siADCK2 and differentiated into NCCs for 10 days. These were then compared to siControl transfected and differentiated cells.

ID	SYMBOL	logFC	AveExpr	t	P.Value	adj.P.Val	B
NM_032108	SEMA6B	-0,500	8,334	-2,285	0,035	1,000	-3,689
NM_001303461	OVOL2	-0,486	6,820	-1,670	0,112	1,000	-4,257
ISL1.cAug10-unspliced	ISL1	-0,473	6,466	-2,156	0,045	1,000	-3,815
NM_000346	SOX9	-0,428	8,941	-2,061	0,054	1,000	-3,906
NM_012392	PEF1	-0,372	6,815	-1,811	0,087	1,000	-4,135
NM_002202	ISL1	-0,341	5,746	-1,269	0,221	1,000	-4,569
NM_004186	SEMA3F	-0,334	8,036	-1,764	0,095	1,000	-4,177
NM_032505	KBTBD8	-0,316	6,369	-1,165	0,259	1,000	-4,639
NM_001146029	SEMA7A	-0,284	8,289	-1,660	0,114	1,000	-4,266
hsa_circ_0001872	SEMA4D	-0,261	7,927	-1,393	0,180	1,000	-4,479

NM_001719	BMP7	-0,248	9,464	-0,959	0,350	1,000	-4,764
NM_001202	BMP4	-0,234	9,969	-0,953	0,353	1,000	-4,767
NM_020210	SEMA4B	-0,215	8,557	-1,327	0,201	1,000	-4,527
NM_001178061	SEMA6C	-0,204	8,735	-0,726	0,477	1,000	-4,880
NM_005117	FGF19	-0,197	7,861	-1,277	0,218	1,000	-4,563
NM_001142287	SEMA4D	-0,169	8,888	-0,912	0,374	1,000	-4,789
ENST00000530157	CFL1	-0,136	3,839	-0,564	0,580	1,000	-4,942
NM_006941	SOX10	-0,128	7,889	-0,558	0,584	1,000	-4,944
NM_004429	EFNB1	-0,125	9,208	-0,536	0,598	1,000	-4,952
NM_000474	TWIST1	-0,125	7,669	-0,607	0,551	1,000	-4,927
NM_001048183	PHACTR4	-0,123	9,064	-0,850	0,406	1,000	-4,822
NM_001178129	SEMA3E	-0,119	8,255	-0,357	0,725	1,000	-5,001
NM_000115	EDNRB	-0,111	8,733	-0,654	0,521	1,000	-4,909
NM_021973	HAND2	-0,108	6,990	-0,779	0,446	1,000	-4,856
NM_003108	SOX11	-0,106	9,345	-0,518	0,611	1,000	-4,958
NM_001301687	GBX2	-0,101	7,265	-0,367	0,718	1,000	-4,998
NM_005992	TBX1	-0,099	8,122	-0,359	0,723	1,000	-5,000
NM_020630	RET	-0,091	7,482	-0,620	0,543	1,000	-4,922
NM_001168319	EDN1	-0,086	7,723	-0,310	0,760	1,000	-5,010
NM_001303051	KLHL12	-0,086	8,607	-0,597	0,558	1,000	-4,931
NM_001155	ANXA6	-0,084	9,597	-0,522	0,608	1,000	-4,956
NM_005524	HES1	-0,067	8,818	-0,298	0,769	1,000	-5,013
NM_002745	MAPK1	-0,062	10,322	-0,544	0,593	1,000	-4,949
NM_001300780	SEMA6A	-0,060	12,171	-0,304	0,764	1,000	-5,011
NM_001193300	SEMA4A	-0,052	7,615	-0,268	0,791	1,000	-5,018
NM_001243084	HIF1A	-0,050	10,947	-0,361	0,722	1,000	-5,000
NM_005507	CFL1	-0,049	11,390	-0,380	0,709	1,000	-4,996
NM_000356	TCOF1	-0,046	9,314	-0,271	0,789	1,000	-5,017
NM_001105237	CORO1C	-0,042	10,726	-0,295	0,771	1,000	-5,013
ENST00000525710	CFL1	-0,036	7,117	-0,134	0,895	1,000	-5,035
NM_004329	BMPR1A	-0,033	11,151	-0,238	0,815	1,000	-5,023
NM_001284388	NOLC1	-0,030	10,537	-0,199	0,845	1,000	-5,028
NM_001203244	SEMA4G	-0,015	5,815	-0,065	0,949	1,000	-5,039
NM_000214	JAG1	0,010	10,179	0,053	0,959	1,000	-5,039
NM_001453	FOXC1	0,016	7,765	0,078	0,939	1,000	-5,038
NM_000193	SHH	0,017	6,283	0,087	0,932	1,000	-5,038
NM_001040056	MAPK3	0,023	10,129	0,192	0,850	1,000	-5,029
NM_020163	SEMA3G	0,025	7,659	0,140	0,890	1,000	-5,034
NM_014587	SOX8	0,030	7,683	0,165	0,871	1,000	-5,032
NM_001306129	FN1	0,031	11,194	0,127	0,900	1,000	-5,035
NRP1.vdAug10-unspliced	NRP1	0,032	3,910	0,136	0,893	1,000	-5,034
ERBB4.jAug10-unspliced	ERBB4	0,035	3,186	0,192	0,850	1,000	-5,029
NM_001267556	PDCD6	0,036	7,897	0,250	0,805	1,000	-5,021
NM_006080	SEMA3A	0,048	10,348	0,165	0,871	1,000	-5,032
NM_001005914	SEMA3B	0,050	7,338	0,264	0,795	1,000	-5,018
NM_001031702	SEMA5B	0,053	7,879	0,327	0,747	1,000	-5,007
NM_183374	CYP26C1	0,055	6,568	0,203	0,842	1,000	-5,027

NM_001159995	NRG1	0,069	5,954	0,158	0,876	1,000	-5,032
NM_003924	PHOX2B	0,071	8,022	0,450	0,658	1,000	-4,978
NM_005560	LAMA5	0,078	9,134	0,325	0,749	1,000	-5,007
NM_001271661	SEMA4F	0,083	6,860	0,416	0,682	1,000	-4,987
NM_005251	FOXC2	0,099	6,372	0,532	0,601	1,000	-4,953
NM_001171653	ZEB2	0,101	8,910	0,437	0,668	1,000	-4,981
NM_003872	NRP2	0,102	10,678	0,372	0,714	1,000	-4,997
NM_000802	FOLR1	0,103	6,475	0,351	0,730	1,000	-5,002
NM_003068	SNAI2	0,105	8,855	0,327	0,748	1,000	-5,007
NM_000899	KITLG	0,110	7,617	0,279	0,783	1,000	-5,016
NM_001302455	EDN3	0,112	6,059	0,870	0,396	1,000	-4,811
NM_000514	GDNF	0,115	7,612	0,576	0,572	1,000	-4,938
NM_004558	NRTN	0,117	8,112	0,679	0,506	1,000	-4,899
NM_001042599	ERBB4	0,135	7,803	0,667	0,513	1,000	-4,904
NM_001198999	SEMA6D	0,138	7,527	0,473	0,642	1,000	-4,971
NM_153365	TAPT1	0,141	7,592	0,722	0,480	1,000	-4,881
NM_001105	ACVR1	0,189	8,174	0,793	0,438	1,000	-4,849
NM_006379	SEMA3C	0,205	9,048	0,730	0,475	1,000	-4,878
NM_005631	SMO	0,207	8,849	1,556	0,137	1,000	-4,352
NM_006982	ALX1	0,228	5,634	0,594	0,560	1,000	-4,932
NM_017789	SEMA4C	0,229	8,765	1,612	0,124	1,000	-4,306
NM_001024628	NRP1	0,231	7,947	0,996	0,333	1,000	-4,743
NM_000325	PITX2	0,259	9,632	0,757	0,459	1,000	-4,866
NM_003966	SEMA5A	0,263	9,172	0,896	0,382	1,000	-4,798
NM_172037	RDH10	0,265	6,868	0,738	0,470	1,000	-4,874
NM_001166055	EDNRA	0,274	9,769	1,295	0,212	1,000	-4,551
NM_001206897	ALDH1A2	0,298	6,623	1,684	0,109	1,000	-4,246
NM_001163417	FAM172A	0,303	7,590	1,157	0,262	1,000	-4,644
NM_000867	HTR2B	0,326	4,158	1,271	0,220	1,000	-4,567
NM_152754	SEMA3D	0,330	6,528	1,046	0,310	1,000	-4,714
SEMA3A.gAug10-unspliced	SEMA3A	0,502	5,098	1,361	0,190	1,000	-4,503
ENST00000471474	SEMA3A	0,520	3,642	1,340	0,197	1,000	-4,518

Supplementary Table 3: *Gene expression analysis results: common deregulated genes by ADCK2 KD in melanoma and differentiated hiPSCs. Results for siADCK2 vs. siControl transfected melanoma cells*

For this analysis all melanoma ADCK2 KD samples (Mewo, SkMel30, C32) were pooled and compared to the pooled siControl melanoma samples. In the same way siADCK2 tranfected and 10 days differentiated hiPSCs were pooled and compared to siControl transfected and differentiated hiPSCs. Now, these two sample sets were compared for similar deregulated genes upon ADCK2 KD. This analysis resulted in 22 commonly deregulated genes, which are listed below together with the respective logFC and further data values for melanoma cells. The FC value of this analysis was 1.2.

ID	SYMBOL	logFC	AveExpr	t	P.Value	adj.P.Val	B
NM_001199814	ZNF812P	-0,435	6,065	-4,812	0,000	0,014	1,306
NM_001040153	SLAIN1	-0,269	6,628	-2,970	0,008	0,199	-2,658
ENST00000628319	SURF4	-0,361	9,689	-4,996	0,000	0,010	1,704
NM_001243093	FYB	-0,266	7,170	-1,695	0,106	0,554	-4,977
NM_152510	HORMAD2	0,281	3,290	3,995	0,001	0,052	-0,469

NM_001100874	SLC9B1	0,298	4,009	3,209	0,005	0,151	-2,161
NM_004869	VPS4B	0,323	9,540	4,872	0,000	0,012	1,435
NM_001282695	FAM107B	-0,364	5,080	-3,410	0,003	0,119	-1,735
NM_001009984	C20orf194	0,316	7,506	4,094	0,001	0,045	-0,254
NM_003713	PLPP3	-0,314	8,563	-3,878	0,001	0,063	-0,724
ENST00000632025	FMN1	-0,326	5,968	-2,133	0,046	0,404	-4,264
NM_005073	SLC15A1	0,348	4,412	3,805	0,001	0,069	-0,883
NM_001278204	KCNN2	0,324	6,120	2,524	0,020	0,295	-3,546
NM_001293298	CEMIP	-0,311	6,917	-1,931	0,068	0,477	-4,607
NM_001005288	OR51I1	-0,438	4,405	-3,360	0,003	0,125	-1,842
FMN1.qAug10-unspliced	FMN1	0,269	5,932	2,493	0,022	0,302	-3,605
NM_001080425	BEX4	-0,279	5,607	-2,212	0,039	0,382	-4,124
NM_032160	DSEL	-0,309	5,627	-2,827	0,011	0,224	-2,949
NM_001291992	SPATA19	0,372	4,052	3,892	0,001	0,061	-0,695
NM_001079910	LRRIQ1	0,483	4,850	3,745	0,001	0,073	-1,013
NM_001034836	RDM1	-0,490	5,422	-3,462	0,003	0,112	-1,624
NM_001177969	VIT	0,272	3,085	3,956	0,001	0,055	-0,556

Supplementary Table 4: *Gene expression analysis results: common deregulated genes by ADCK2 KD in melanoma and differentiated hiPSCs. Results for siADCK2 vs. siControl transfected and differentiated hiPS cells.*

For this analysis all melanoma ADCK2 KD samples (Mewo, SkMel30, C32) were pooled and compared to the pooled siControl melanoma samples. In the same way siADCK2 transfected and 10 days differentiated hiPSCs were pooled and compared to siControl transfected and differentiated hiPSCs. Now, these two sample sets were compared for similar deregulated genes upon ADCK2 KD. This analysis resulted in 22 commonly deregulated genes, which are listed below together with the respective logFC and further data values for hiPS cells. The FC value of this analysis was 1.2.

ID	SYMBOL	logFC	AveExpr	t	P.Value	adj.P.Val	B
NM_001199814	ZNF812P	-0,382	5,918	-2,907	0,011	0,724	-2,943
NM_001040153	SLAIN1	-0,575	5,881	-2,837	0,013	0,729	-3,022
ENST00000628319	SURF4	-0,278	9,316	-2,757	0,015	0,754	-3,111
NM_001243093	FYB	-0,373	4,881	-2,540	0,023	0,754	-3,352
NM_152510	HORMAD2	0,305	3,569	2,317	0,036	0,767	-3,597
NM_001100874	SLC9B1	0,412	5,121	2,173	0,047	0,776	-3,753
NM_004869	VPS4B	0,288	8,590	2,001	0,065	0,792	-3,934
NM_001282695	FAM107B	-0,320	5,537	-1,974	0,068	0,802	-3,961
NM_001009984	C20orf194	0,266	7,971	1,833	0,087	0,819	-4,105
NM_003713	PLPP3	-0,274	10,315	-1,788	0,095	0,827	-4,149
ENST00000632025	FMN1	-0,326	4,556	-1,760	0,099	0,834	-4,177
NM_005073	SLC15A1	0,306	4,638	1,681	0,114	0,846	-4,253
NM_001278204	KCNN2	0,323	5,482	1,594	0,132	0,858	-4,335
NM_001293298	CEMIP	-0,297	4,204	-1,586	0,134	0,860	-4,342
NM_001005288	OR51I1	-0,267	3,574	-1,575	0,137	0,861	-4,353
FMN1.qAug10-unspliced	FMN1	0,283	6,359	1,554	0,142	0,861	-4,371
NM_001080425	BEX4	-0,357	8,237	-1,513	0,152	0,866	-4,409
NM_032160	DSEL	-0,285	7,295	-1,457	0,166	0,870	-4,458
NM_001291992	SPATA19	0,276	4,092	1,422	0,176	0,873	-4,488
NM_001079910	LRRIQ1	0,272	6,011	1,416	0,178	0,873	-4,494

NM_001034836	RDM1	-0,264	6,610	-1,366	0,193	0,881	-4,536
NM_001177969	VIT	0,285	4,708	0,563	0,582	0,951	-5,043

9 Acknowledgements

During my four years as a PhD student, I have experienced many hurdles on the one side but also many fantastic days on the other side. All of these experiences, participated to my professional and personal growth and I do not want to miss a single step of it. But it is to 100 percent clear that I would not have made this journey without the help of others. So, it is now time to acknowledge all this people for their amazing help.

First of all, my deepest gratitude goes to **Prof. Dr. Jochen Utikal** for the opportunity to conduct my PhD in his laboratory at the DKFZ and letting me dig deeper into very interesting and pioneering research in the fields of melanoma and induced pluripotent stem cells. Further, I am very thankful that he always believed in my capabilities and always pushed me further, but in the same time leaving me space to discover my own working skills. Also, his ideas and advices were always very kind and helpful.

Next, I want to thank **Prof. Dr. Viktor Umansky** for his scientific contribution to my research projects. His knowledge and experience resulted in meaningful feedback and suggestions, which always led my project further. Also, I want to thank him to be my first examiner and also one of my TAC members.

I am very grateful to **Dr. Michael Milsom** and **Dr. Katrin Schrenk-Siemens** to be my TAC members and for their fruitful discussions regarding my project, which always led to new and subsequent ideas. Moreover, I want to express my gratitude to Dr. Katrin Schrenk-Siemens for her guidance and the opportunity to conduct some research investigations in her laboratory at the University of Heidelberg.

Additionally, to getting all these kind support, I had the chance to meet amazing people during my PhD studies, starting with all my laboratory colleagues with whom I spent many hours a day in the last couple of years.

Here, I first want to thank **Dr. Qian Sun (Sunee)** for her great help during experiments, especially for data analysis and her scientific support. Also, I want to thank her for always having kind words and a smile for me, which made every day better and work easier. Further, I like to express my gratitude to **Dr. Daniel Novak (Schnobert)** for his excellent scientific advice and proofreading of all my texts. Your corrections were always amazing and welcomed, it made sound all my content way nicer. Also, I like to thank him, for always be up to a joke and thereby enhancing a great working atmosphere. Next, I like to thank **Juliane Poelchen**, **Tamara Steinfass** and **Yiman Wang** for their support. All of you always had an open ear for me and my problems, supported me scientifically and privately throughout my PhD and always believed in me. Also, you were always ready to assist me during my experiments if I needed some help. Further I like to thank all my previous and current lab members **Dr. Karol Granados Blanco**, **Dr. Aniello Federico**, **Dr. Laura Hüser**, **Dr. Lionel Larribére**, **Özge Sener** and **Nina Wang** for making the laboratory life fun. We have spent many nice and funny moments together, which I would have missed without you. And thanks to all my laboratory members we also survived the COVID-19 pandemic with not only negative thoughts. Belonging to the laboratory I also like to thank the technicians **Marlene Pach**, **Jennifer Dworacek** and **Sayran Arif-Said** for their kind assistance during all these years, followed by the help of all our Bufdis in the daily laboratory life.

Moreover, I kindly thank **Thomas Hielscher** for his support in analyzing the gene expression data. He did all the bioinformatics analysis of this experiment providing me with informative graphs and tables to work with.

Also, I want to thank my ZIM project partners from trenzyme and the University of Hannover (**Reinhold Horlacher**. **Stefanie Traub**, **Ellinor Ade**, **Cornelia Lee-Thedieck**, **Hamidreza Pirmahboub**) for their fruitful discussion on hiPSCs and the nice interchange at our meetings.

Further I like to thank the institutions of the University of Heidelberg, the UMM, the DKFZ with the core facilities for light microscopy and gene expression as well as its graduate school HIGS and its career service for accepting me as a PhD student and giving support whenever needed.

Last but not least I want to give a huge thank you to all my **family and friends** for believing in me and supporting me during all these years of studies. Especially, I like to thank my mam for raising me to an independent and intelligent woman. Also, to my family for giving me the opportunity and freedom to choose my own way and always supporting me on this trac. A special thanks goes to all my friends who listened to all my complains and stories, for getting me back on trac if I lost it and for their understanding of changing plans due to my PhD studies. A very special thank goes to **Philip**, who more than everybody else was coping with all my fluctuating moods, supporting me during every step of my PhD, celebrating every success with me and help me stand up whenever I was down. You were my tower of strength during all these years.

A huge thank you again to all of you. Without you the last four years would not have been the same!